

Raúl García Hernández

Multilevel Sampling System for Gas Analyser in Circulating Fluidized Bed Gasification

Espoo, 04.10.2016

Thesis Supervisor:

Professor Mika Järvinen

Thesis Advisors:

D.Sc. Loay Saeed

M.Sc. Jonatan Skagersten

Author: Raúl García Hernández

Title: Multilevel Sampling System for Gas Analyser in Circulating Fluidized Bed Gasification

Date: 04.10.2016

Language: English

Number of pages: 78

Department of Mechanical Engineering

Professorship: Energy Engineering (MEN.thes)

Supervisor: Professor Mika Järvinen

Advisors: D.Sc. Loay Saeed, M.Sc. Jonatan Skagersten

The main topic of this Master's Thesis is the development of a multilevel sampling system for gas analysers, in which a single gas analyser can measure the gas composition from gasification or combustion, in three different levels in a riser of a circulating fluidized bed reactor. The two analysers used in this work were the Dx-4000 GASMET gas analyser and the Siemens ULTRAMAT 23 gas analysers.

The multilevel sampling system consist of three levels, which are connected to the reactor by steel pipes. There is a computer controlled solenoid valves that controls which level is sampled. In addition, there is an oil scrubber in each level to protect the system from unwanted and dangerous substances such as tar.

Heat transfer equations have been used in the process of designing the multilevel system in order to not surpass the maximum allowable temperature of some components. The residence time has also been considered in designing the system, as it is an important parameter, since it had to be as short as possible to avoid some changes in the composition of the gas sampled as well as increasing the acquired amount of reliable measurement data from each test.

Finally, the transitional and steady time (residence time) for reliable measurements were calculated for both analysers, obtaining 60 seconds of reliable measurements for GASMET analyser and 40 seconds for ULTRAMAT analyser. One combustion test was done in order to check that the system worked correctly, whose the results were satisfactory.

Keywords: multilevel, gasification, combustion, reactor, analyser, residence time, tar, scrubber, solenoid.

Autor: Raúl García Hernández

Título: Sistema Multinivel de Muestras para Analizador de Gases en Gasificación Circulante de Lecho Fluido

Fecha: 04.10.2016

Idioma: Inglés

Número de páginas: 78

Departamento de Ingeniería Mecánica

Profesión: Ingeniería Energética (MEN.thes)

Director: Profesor Mika Järvinen

Supervisores: D.Sc. Loay Saeed, M.Sc. Jonatan Skagersten

El tópico principal del Trabajo de Fin de Master es el desarrollo de un sistema multinivel de muestras para analizadores de gases, en el que un analizador puede medir la composición del gas producido en gasificación o combustión, en tres diferentes niveles de un reactor de lecho fluidizado circulante. En este trabajo se usaron dos analizadores que fueron el Dx-4000 GASMET analizador de gas y Siemens ULTRAMAT 23 analizador de gas.

El sistema multinivel de muestras consiste de tres niveles diferentes, los cuales son conectados al reactor por tuberías de acero. Además, hay válvulas solenoides que con un control automático, que controlan que nivel es medido. Por si no fuera poco, en cada nivel hay un depurador de aceite para proteger al sistema de sustancias indeseadas y peligrosas como por ejemplo el tar.

Ecuaciones de transferencia de calor han sido usadas para no sobrepasar la temperatura máxima permitida de algunos componentes. Además, el tiempo de residencia ha sido el parámetro más importante en el diseño de dicho sistema, ya que tenía que ser el mínimo posible para evitar algunos problemas de reacciones químicas y contaminación del gas en el sistema.

Finalmente, los regímenes transitorio y permanente (tiempo de residencia) para tomar buenas medidas fueron calculados para ambos analizadores, obteniendo 60 segundos de régimen permanente para el analizador GASMET y 40 segundos para el analizador ULTRAMAT. Además, un test de combustión fue realizado para comprobar que todo el sistema funcionaba correctamente, siendo los resultados más que satisfactorios.

Acknowledgements

This Master's Thesis was written in the Department of Mechanical Engineering at Aalto University during year 2016.

I want to thank my supervisor Mika Järvinen for the possibility to work with this team and for all the valuable help and advices. I am also grateful to my advisors Loay Saeed and Jonatan Skagersten who have helped me during all these months with their instructions and comments. Also thanks to everybody in the Department of Mechanical Engineering for creating a nice working atmosphere and for the nice company during coffee breaks.

Finally, special thanks to my friends, family and Ana Chari without whom this work would have not been possible.

Because I know grandfather that you are watching this and you would be proud...

Porque sé abuelo que lo estás viendo y estarías orgulloso...

Raúl García Hernández

Espoo, 04.10.2016

Preface

This Master's Thesis has been done during my Erasmus exchange student programme at Aalto University in the academic year 2015/2016. Mika Järvinen (Department of Mechanical Engineering) has been my supervisor at Aalto University, while María Teresa Montañés Sanjuan (Department of Chemical and Nuclear Engineering) has been my supervisor at Universitat Politècnica de València. With this Master's Thesis, I apply for the procurement of Master in Industrial Engineering at Universitat Politècnica de València.

CONTENTS

| | | |
|-------|---|----|
| 1 | Introduction..... | 1 |
| 1.1 | Objectives | 5 |
| 2 | Literature Review | 5 |
| 2.1 | Physicochemical Processes in Combustion and Gasification in Fluidized Beds..... | 5 |
| 2.2 | Operation Principles of Gas Analysers | 9 |
| 2.3 | Pre-Treatment of the Gas Samples | 13 |
| 2.4 | Residence Time in Gas Sampling System | 18 |
| 3 | Focus of this Master’s Thesis | 23 |
| 4 | Experimental Setup..... | 24 |
| 4.1 | Circulating Fluidized Bed Reactor (CFB). | 24 |
| 4.2 | Solid Recovered Fuel..... | 27 |
| 4.3 | Gas Analysers | 33 |
| 4.3.1 | Siemens ULTRAMAT 23 Gas Analyser | 33 |
| 4.3.2 | GASMET Gas Analyser | 34 |
| 5 | Multilevel Sampling System for Gas Analyser | 34 |
| 5.1 | Steel Pipes..... | 35 |
| 5.1.1 | Convection Inside of the Pipe..... | 37 |
| 5.1.2 | Conduction..... | 38 |
| 5.1.3 | Convection Outside of the Pipe | 38 |
| 5.1.4 | Radiation..... | 40 |
| 5.1.5 | Length of the Steel Pipe..... | 40 |
| 5.1.6 | Heat Transfer Experiments | 41 |
| 5.1.7 | Comparison of the Experimental Results and Model Results | 42 |
| 5.1.8 | Insulation of the Steel Pipe | 44 |
| 5.2 | Tar Trap | 46 |
| 5.3 | Solenoid and Pressure Valves..... | 48 |
| 6 | Test and Validation..... | 52 |
| 6.1 | Residence Time Test..... | 52 |
| 6.1.1 | Residence Time Test with CO | 56 |
| 6.2 | Valve Controlling Algorithm..... | 63 |
| 6.3 | Cycles of Measurements with the Sampling Gas System..... | 67 |
| 7 | Results and Discussions..... | 69 |

| | |
|---|----|
| 7.1 Combustion Test in the CFB | 69 |
| 7.1.1 Results for the Solenoid Valve Algorithm..... | 71 |
| 7.1.2 Comparison of the Results between ULTRAMAT and GASMET Gas Analysers . | 72 |
| 7.1.3 Comparison of the Results with Older Tests | 74 |
| 7.1.4 Results from the Tar Trap with Oil Scrubbers..... | 75 |
| 8 Conclusions and Future Research..... | 76 |
| 9.Appendix..... | 79 |
| 9.1 Model of the Heat Transfer for the Steel Pipes | 79 |
| Bibliography | 80 |

Nomenclature

Symbols

| | |
|---------------|--|
| $C(t)$ | Concentration of a trace respect to the time |
| $C_o(t)$ | Initial concentration |
| c_p | Specific heat capacity |
| D | Diameter of the pipe |
| ε | Emissivity of the material |
| $E(t)$ | Residence time distribution function |
| h_i | Convection coefficient inside of the pipe |
| h_o | Convention coefficient outside of the pipe |
| h_{rad} | Equivalent radiation coefficient |
| k | Thermal conductivity of the material |
| \dot{m} | Mass flow of gas |
| ΔN | Increase in the amount of injected trace |
| N_o | Initial amount of injected trace |
| Nu_D | Nusselt number |
| Pr | Prantdl number |
| Q | Heat released from the gas |
| q' | Heat released from the gas per meter of pipe |
| Re_D | Reynolds number |
| r_i | Internal radius of the pipe |
| r_o | External radius of the pipe |
| ε | Stefan-Boltzmann constant |

| | |
|------------|-----------------|
| T | Temperature |
| Δt | Step time |
| Y | Volumetric flow |

Operators

| | |
|----------------------|--------------------------------------|
| $\frac{d}{dt}$ | Derivate with respect to variable t |
| $\int_0^{\infty} dt$ | Integrate with respect to variable t |

Abbreviations

| | |
|-------|---|
| APC | Air pollution control |
| BFB | Bubbling fluidized bed |
| CFB | Circulating fluidized bed |
| ER | Equivalent ratio |
| FM | Flow meter |
| FT-IR | Fourier transform infrared spectrometer |
| HX | Heat exchange |
| IGCC | Integrated gasification combined cycle |
| IR | Infrared spectrometer |
| LCV | Lower calorific value |
| NCV | Net calorific value |
| PH | Preheater connected to the riser |
| PH2 | Sand-lock preheater |

| | |
|-----|--|
| PVC | Polyvinyl chloride |
| RH | Riser heating elements |
| SRF | Solid recovered fuel |
| VF | Ball valve controlling the fuel flow |
| VI | Valve controlling the inlet gas |
| VPS | Valve controlling the gas flow to the sand-lock and the aeration |

1 Introduction

Gasification is a relatively old technology, which was invented already at the end of the 18th Century and used mainly to produce town gas from coal during the 19th Century (Basu, 2006). Gasification refers to a group of different thermochemical processes that convert solid or liquid fuels into a synthesis gas (syngas). The used air in gasification is less than the theoretically needed stoichiometric air for complete combustion of the fuel.

This process occurs in reactors called gasifiers, where different fuels such as coal, biomass, and petroleum coke are converted into a combustible gas (syngas). It is a mixture of different gases, mainly CO and H₂ with other gases like CO₂, CH₄, H₂S, HCl, etc. The composition of the gas depends on the system and operational parameters (type of gasifier, temperature, raw material, pressure,...)(Williams, 2013).

There are different types of gasifiers categorize based on some characteristics of the reactors like gasification medium (air, oxygen or steam) or how the gas and fuel contact each other (Basu, 2006). If categorized by how the gas and fuel contact each other, there are 4 types of gasifier:

1. Entrained bed.
2. Fluidized bed (Bubbling or Circulating).
3. Spouted bed.
4. Fixed or moving bed (Basu, 2006).

Figure 1.1 shows examples of some these of gasifiers.

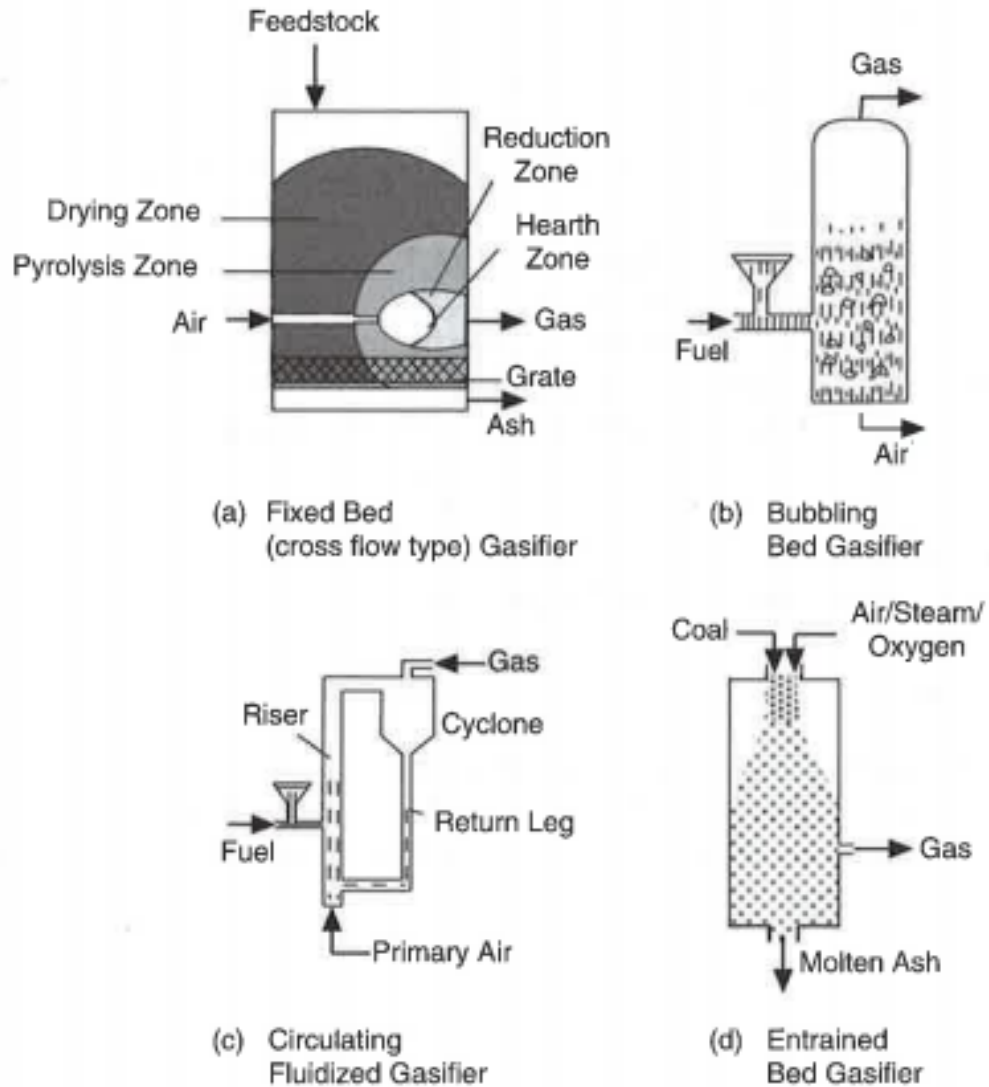


Figure 1.1 Different types of gasifier (Basu, 2006).

In a fluidized bed the fuel is mixed with the air in a hot bed of granular solids like sand; these reactors are used very frequently in gasification of biomass (Basu, 2006). Within this type of reactors, there are two different reactors that are fluidized bed gasifiers:

1. Bubbling fluidized bed gasifier (BFB).
2. Circulating fluidized bed gasifier (CFB).

The main difference between them is that the bubbling fluidized bed (BFB) cannot achieve a high solid circulation, while circulating fluidized bed (CFB) has an excellent heat and mass transfer and longer residence time (Basu, 2006).

The working principle of the circulating fluidized bed reactor (CFB) is that upward flow of air makes the solids suspended. Operating the CFB in the turbulent regime ensures high heat and mass transfer. This kind of reactors can be used in many applications like production of bio-gas, production of liquid transportation fuels (Siedlecki et al., 2011), treatment of waste and production of heat and electricity, etc. Figure 1.2 shows an example of a circulating fluidized bed reactor and Table 1.1 shows for-typical operational conditions of this type of reactors.

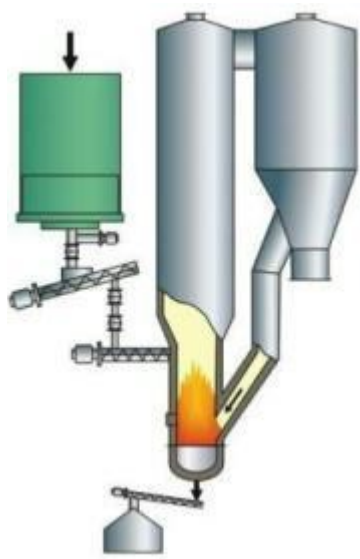


Figure 1.2 Circulating fluidized bed gasifier (ANDRITZ, 2016).

Table 1.1 Typical operational conditions for circulating fluidized bed gasifiers in commercial use (Grace, 2003).

| Parameters | Accepted Values |
|---|-----------------|
| Superficial gas velocity (m/s) | 2-12 |
| Net solids flux through the riser (kg/m ² s) | 10-1000 |
| Temperature (°C) | 20-950 |
| Pressure (kPa) | 100-2000 |
| Mean particle diameter (µm) | 50-500 |
| Overall riser height (m) | 15-40 |

Gasification offers some advantages over direct combustion. For example the gas flow in gasification is less than in the direct combustion of the fuel, since the amount of required oxygen in the gasification is less than the stoichiometric oxygen. Gasification thus needs smaller equipment, which results in lower capital costs (Basu, 2006).

Another advantage is that the end product gas from gasification has more applications than the direct combustion of the fuel. For example the syngas can be used to generate electricity or thermal energy in power plants, produce methanol, ammonia or other products in chemical or industrial processes.

In addition, because syngas can be produced from biomass, it means that a great amount of waste from cities, industries, forests, etc, can be treated. This could solve a big problem for emerging countries like China or India, so gasification is a good process to take advantage of such waste, in a better way for the environment instead of disposing the waste in landfills.

Syngas from gasification can be burnt directly in boilers in order to produce heat or it can also be cleaned in order to prevent corrosion and problems with tar. After the cleaning, it can be used in turbines or internal combustion engines to generate electricity and the gas could also be upgraded to e.g. liquid fuels through fuel synthesis (Williams, 2013), with the quality requirements shown in Table 1.2.

Table 1.2 Gas quality of raw producer gas from atmospheric, air blown biomass gasifier (Laurence and Ashenafi 2011).

| Component | Unit | Ic engine | Gas turbine | Methanol synthesis |
|-----------------------|--------------------|------------------|--------------------|---------------------------|
| Particles | mg/Nm ³ | <50 | <30 | <0,02 |
| Particle size | µm | <10 | <5 | |
| Tar | mg/Nm ³ | <100 | | <0,1 |
| Alkali | mg/Nm ³ | | 0,24 | |
| NH ₃ | mg/Nm ³ | | | <0,1 |
| H ₂ S& COS | mg/Nm ³ | | | <1 |
| Cl | mg/Nm ³ | | | <0,1 |
| CO ₂ | Vol. % | No limit | No limit | <12 |

Shown the importance of gasification and combustion nowadays, there are many studies and research on gasification and combustion in order to understand these processes better and to be able to improve this. Some studies like (Yang, 2008) tried to understand the different physiochemical processes in gasification and see what happens with the composition of the syngas if some parameters such as temperature, pressure, fuel, etc, are changed in the reactor. Others such as (Gómez-Barea and Leckner, 2010) studied different numerical models to estimate how the physiochemical processes change if the parameters of the reactor are modified, so the composition of the syngas will also change and with numerical models this composition can be estimated too.

On the other hand in comparison with the others, (Niu et al., 2008) developed a multilevel sampling system for gas analysers. With this system, instead of estimating with numerical models or studying the gas composition in only one place of the reactor, (Niu et al., 2008) could study the gas composition in different levels and understand better the physicochemical processes in each level of the reactor. In this study, the gas is treated and cleaned until it arrives to the gas analyser, because some substances like tar has to be removed and in this way avoid that the system will be damaged.

(Nakamura et al., 2016); (Phuphuakrat et al., 2011) and (García-Labiano et al., 2016) explained different methods to remove dangerous substances like tar from gas flow. (Phuphuakrat et al., 2011) studied the difference to use absorbents like diesel, biodiesel, vegetable oil and engine oil instead of water in scrubbers. The result was that vegetable oil is the best option for tar removal, and so (Nakamura et al., 2016) describes the use of oil scrubbers as they have a high tar removal efficiency. However, (García-Labiano et al., 2016) describes the use of filters instead of scrubbers to remove tar. Nevertheless, their efficiency is lower than the efficiency of scrubbers and they have some clogging problems as well.

A multilevel sampling system for gas analyser is developed in this thesis, which permits the gas composition from three different levels in the gasifier to be analysed with only one gas analyser. In this way, the different physicochemical reactions, which take place inside of the reactor, can be better understood. Besides, the treatment system of the gas is carefully designed in order to protect the system from unwanted substances like tar. Another of the objective of this work is to design the system so that the gas flow remains as short time as possible in the system, and avoid problems like contamination of the gas or even that the physicochemical reactions continue to occur in the treatment system.

1.1 Objectives

The main objective of this Master's Thesis is to develop a multilevel gas analysis system for a pilot scale circulating fluidized bed reactor. Only one gas analyser is used in the multilevel sampling system to analyse the gas composition, however measurement data is collected from 3 different vertical levels.

2 Literature Review

2.1 Physicochemical Processes in Combustion and Gasification in Fluidized Beds

When the gasification process of a fuel takes place, there are 4 different physicochemical processes, which take place in different levels of the reactor: drying, pyrolysis (devolatilization), combustion and reduction or gasification. These processes occur within different temperature ranges inside of the gasifier (Basu, 2006):

| | |
|------------------------------|---------------|
| Drying | (<150°C). |
| Pyrolysis (devolatilization) | (150-700°C). |
| Combustion | (700-1500°C). |
| Reduction or gasification | (800-1100°C). |

Drying, pyrolysis and reduction are endothermic processes, which absorb heat provided by combustion (exothermic process).

Knowing what happens in each level helps to understand the different gasification and combustion reactions (Basu, 2006), that take place in the reactor and the final gas composition, since it depends on which reactions are favoured in the gasification process:

Water-gas reaction.



Boudouard reaction.



Shift reaction.



Methanation.



Since the understanding of different processes in gasification and combustion is very important, several articles have been published about chemical reactions involved in gasification (Yang, 2008);(Gómez-Barea and Leckner, 2010); (Niu et al., 2008). According to (Yang, 2008), there are 3 different physicochemical processes or zones inside of the reactor:

Oxidation zone.

Reduction zone.

Destructive distillation or dry zone.

In the oxidation zone the oxygen reacts with the fuel (combustion) and produces a great amount of heat that is absorbed by the endothermic reactions in the other zones. When the oxygen is consumed, then the reduction reactions take place in the reactor and they produce mainly CO and H₂. Later the gas begins to flow into the destructive distillation or dry zone, where some cracking and dry processes occur.

In addition, (Yang, 2008) analysed the effect of different parameters such as temperature, pressure, type of coal, the length and cross section of the riser over each physicochemical process and the gas composition. For example, when the temperature in the reactor drops, the amount of CO decreases, while the amount of CH₄, H₂ and CO₂ increase. The effect of the temperature is shown in Figure 2.1.

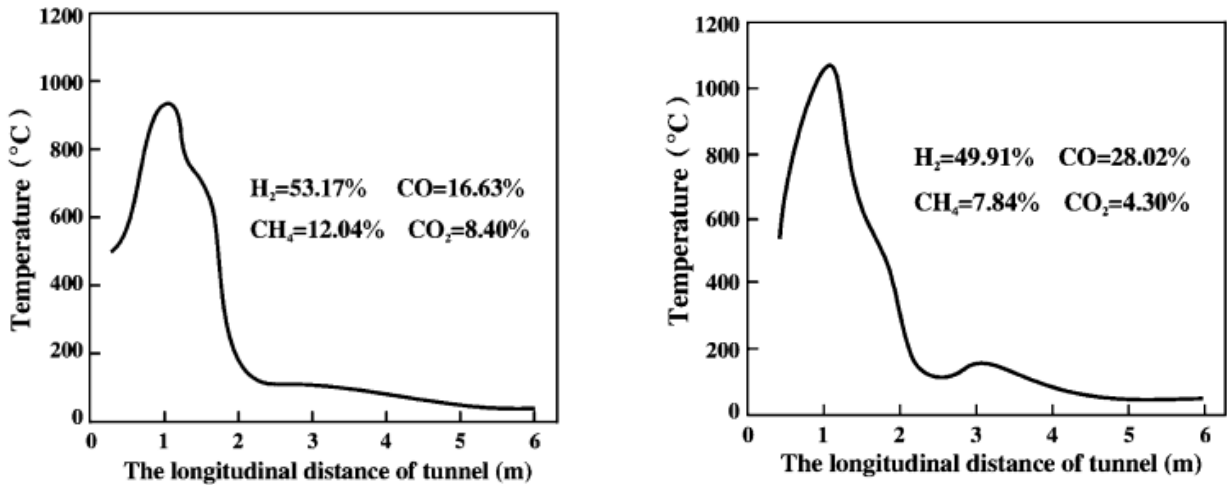


Figure 2.1 The temperatures in 3 and 10 min respectively after steam supply (Yang, 2008).

This happens because when the temperature drops gradually, the following reaction (reduction zone) becomes weaker:



However, other reactions that produce CH₄, H₂ and CO₂ are favoured.

Gómez-Barea and Leckner (2010) studied the physicochemical processes and the gas composition in biomass gasification. They simulated and did numerical modelling in order to predict the gas composition in different levels of a reactor. For this reason (Gómez-Barea and Leckner, 2010) developed a numerical model from conservation equations in order to predict what happen inside of the reactor. For fluidization modelling, they predicted the distribution of gas species in different levels of the reactor, their results are shown in Figure 2.2.

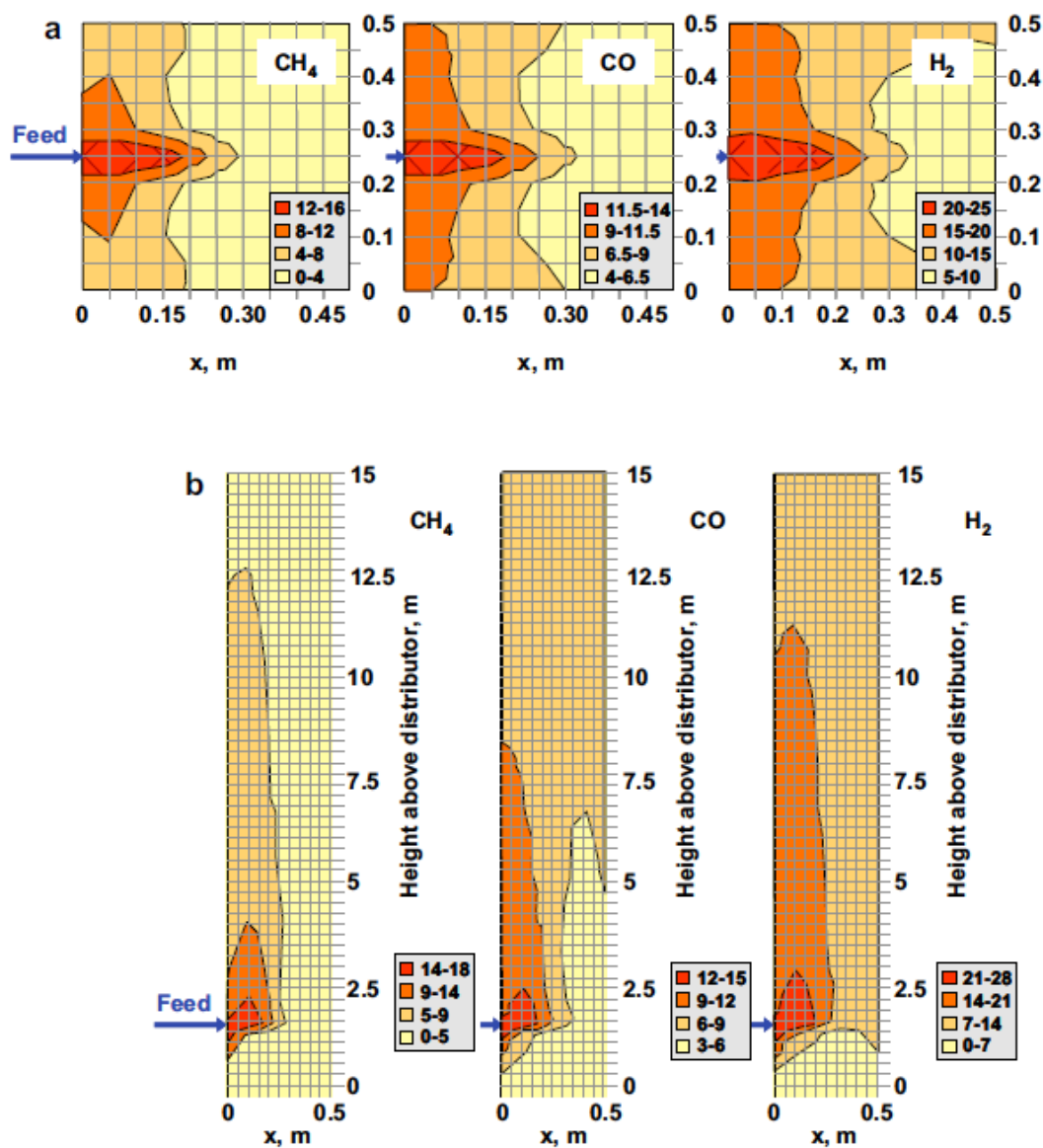


Figure 2.2 Distribution of the concentrations of CH_4 , CO and H_2 over the cross-section of a CFBG with 0.5 m square cross-section burning sewage sludge (Petersen and Werther 2005).

Figure 2.2 shows that the formation of CH₄, CO and H₂ are different in each level of the reactor. H₂ is formed almost in all levels of the reactor, while for example the CH₄ is almost completely produced at the bottom of the reactor. It occurs because the reactions and the favoured conditions for generating CH₄ are mainly located at bottom of the reactor.

However, although (Yang, 2008) and (Gómez-Barea and Leckner, 2010) tried to understand the different reactions in the reactor, none of these articles analysed the gas composition in different levels of the reactor. For example (Yang, 2008) analysed the gas down-streams of the cyclone and not in different levels of the reactor.

On the other hand, (Gómez-Barea and Leckner, 2010) developed and improved numerical models that predict the gas composition in the different physicochemical processes of the gasification, but their work did not study the gas composition in different levels of the reactor, it was only a prediction.

Because of the importance of the analysis of the gas composition in different levels of the reactor, in the next chapters, the different methods and types of gas analysers used to measure and analyse the gas composition in a reactor are explained. How to protect these systems from dangerous substances like tar and some important parameters like residence time, which have to be taken into consideration in gas analyser systems is also explained.

2.2 Operation Principles of Gas Analysers

Analysis of the gas composition of the flue gases in combustion or the final products of gasification has a high importance, since it can help to understand how the system is working and it can give us ideas how to improve the system or the process. There are different methods and equipment available on the market to analyse the gas composition. These equipment are called gas analysers and some of them and their working principles are going to be explained in this chapter.

There are two different methods to measure and analyse the gas composition in a reactor: continuously (on-line) or through discrete samples taken from the syngas flow. However in both methods, the gas should be cleaned from tar, particles and other substances using filters or scrubbers before it goes into a gas analyser (Reed and Das, 1988).

The on-line gas analyser systems are continuously measuring the gas composition that otherwise would not be possible with discrete samples, since the sample gas analyser system requires time to measure the gas composition (Reed and Das, 1988). On the other hand, the discrete samples measuring can be very useful, for example in the case that a company wants to analyse the sample in a laboratory with better conditions and equipment than in the reactor place.

Although, the type of gas analyser can be the same in both methods, the on-line and the discrete samples measuring, there are different types of gas analysers on the market such as infrared absorption (IR), electrochemical analysers, etc (Reed and Das, 1988).

One of the most common used gas analysers is the infrared absorption (IR) gas analyser. The working principle of this type of gas analyser is that when the infrared radiation pass although the sample gas, some of the radiation is absorbed by the gas molecules (GASMET, 1997a). This absorbed radiation can be seen as a decrease in the intensity of some wavelengths in the spectrum of the transmitted infrared radiation. If the infrared absorption spectrum is studied, it is possible to know which wavelengths have been absorbed and which gas has made this. As an example, Figure 2.3 shows the absorbance spectrum of CH_4 (GASMET, 1997a).

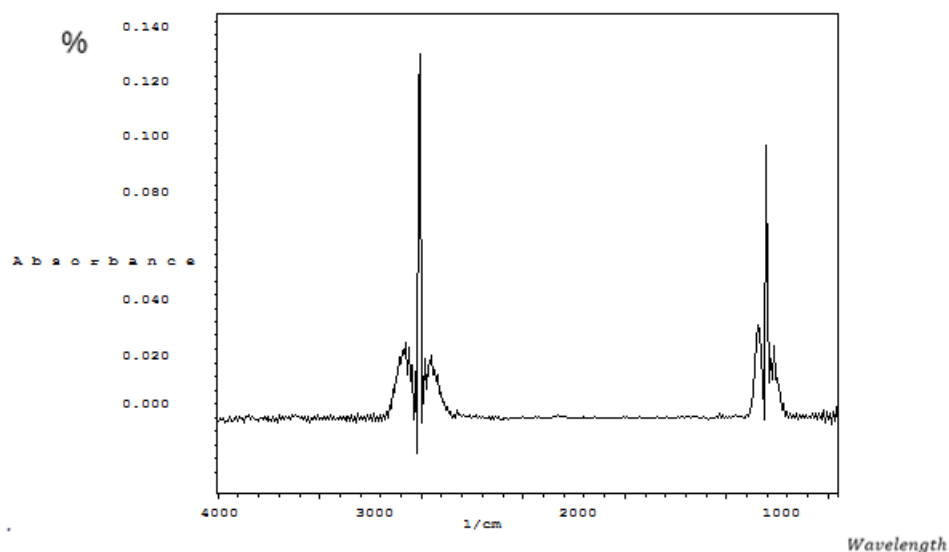


Figure 2.3 Absorbance spectrum of CH_4 (GASMET 1997).

One important operational parameter for gas analysers is the time-scales or sampling frequency. It is important because if the gas analyser analyses the gas compositions lower than the gas composition changes in reality, the obtained results will be inaccurate. This is due to the fact that the higher sample frequency is, more data is acquired and more accurate are the final results. Figure 2.4 shows the measured amount of CO in a gas with two different gas analyser (Siemens ULTRAMAT and Dx-4000 GASMET).

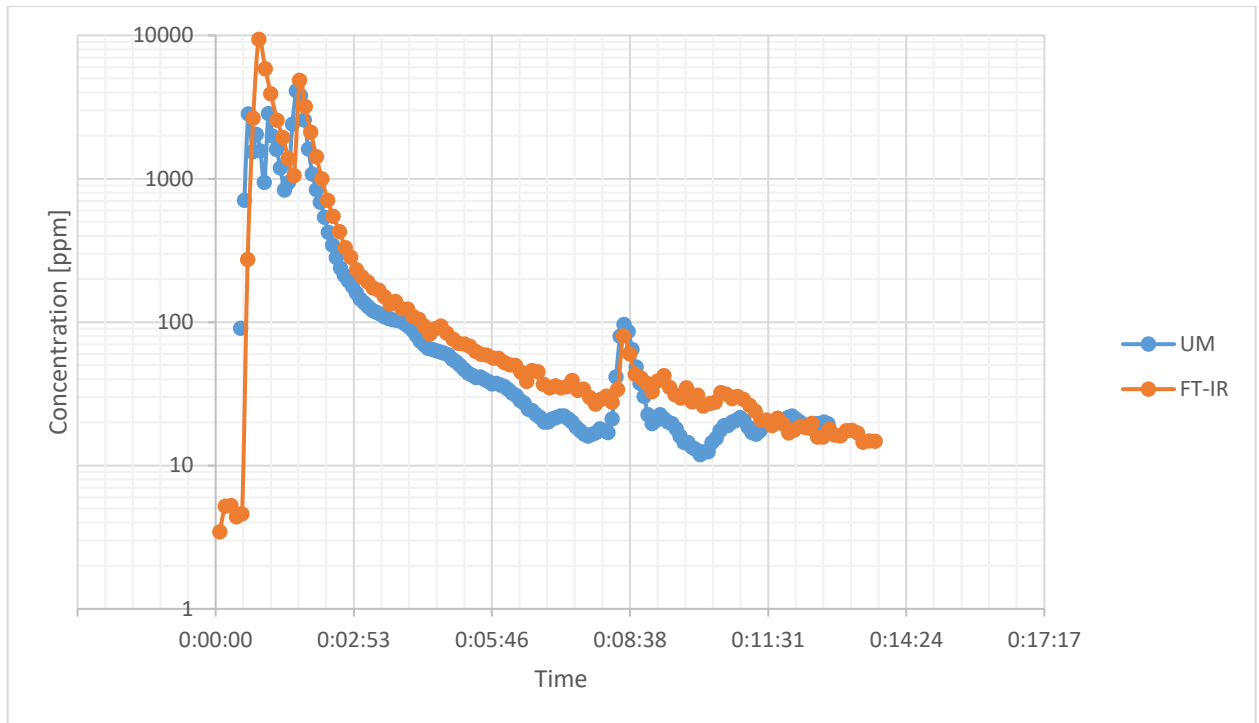


Figure 2.4 Amount of CO with two different gas analyser.

In Figure 2.4, it is possible to see that the results from both analysers, FT-IR and ULTRAMAR are very close. However, there are some differences due to the different sample frequency of each analyser. So when a gas analyser has to be chosen for a new project, the sample frequency is one of the most important properties to be taken into account.

Normally, the gas sampling point is located at the top of gasifier, since in this part of the reactor, the gas has been cleaned of particles. However, if other experiments have to be done for understanding what happens in different levels of the reactor, the gas sampling point has to be located in other places. (Niu et al., 2008) have developed some ideas, which permit to analyse the gas composition in different levels. The work obtained by (Niu et al., 2008) detailed local measurements of the gas composition in order to clarify the different reactions and mechanisms occurring in gasification or combustion. For this, the researchers developed a system that permit to take samples of the gas in different levels of the reactor. One example of such a system is shown in Figure 2.5.

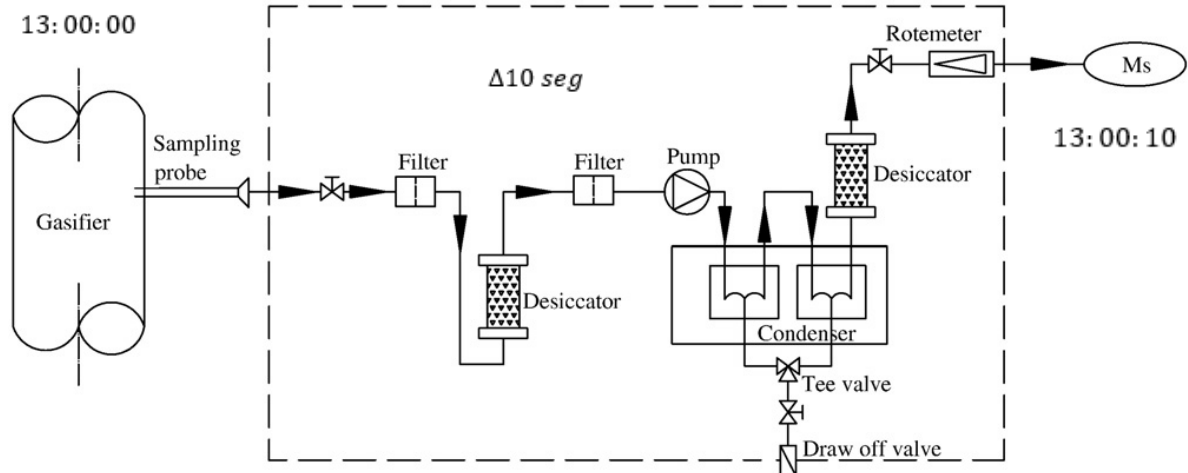


Figure 2.5 The gas pre-treatment system (Niu et al. 2008).

In this design, the samples of the gas are firstly cooled and cleaned with different filters, desiccators and a condenser to remove the particles, tar and water before the gas is analysed in mass spectrometry. This is an important step, since if these substances are not removed, the analyser could be damaged.

However, the previous work did not take into consideration the residence time of the gas in the cooling and cleaning system. It is a very important parameter because if the gas remains longer time, it could be contaminated with metals or other substances in the analyser system, as well the physicochemical reaction could further react through the sampling system. So the longer the gas remains in the pre-treatment, less reliable results of the gas composition will be obtained.

Another important thing to know is that the delay (residence time) between when the gas is taken from the reactor and when the gas is analysed in the gas analyser is not taken into account in (Niu et al., 2008). It could pose a big problem, since it is impossible to know when the analysed gas was inside of the reactor and how much time the gas was in the gas analyser system. An example is shown in Figure 2.5, in which the gas was inside of the reactor at 13:00:00, and the residence time (delay) of the gas in the sampling system was 10 seconds.

For this reason, if the residence time or delay that the gas is in the gas sampling system is known, it is possible to know when each taken measurement of the gas composition was inside of the gasifier. So if the residence time is very short, it means that likely the measurements are closer to the real situation inside of the reactor than if the gas remains for too long time in the gas sampling system (long residence time).

Because of the importance of the residence time and the protection of the system, how to protect the gas analyser system from unwanted substances like tar and the importance to know the residence time in the gas analyser system will be explained in the next chapters.

2.3 Pre-Treatment of the Gas Samples

Whether the gas is sampled continuously or discretely, the gas analysers have to be always protected from substances such as tar, particles and liquid water that are produced in gasification.

Tar is a substance produced in gasification or pyrolysis that consists of several hundreds of hydrocarbons and aromatic compounds. The most important ones are shown in Table 2.1. Apart from other problems, one of the main problems related to when the tar dew point is reached, tar condensates resulting in clogging of fuel lines, filters, engines and gas analysers. The amount of tar produced in gasification processes depends on the conditions inside of the reactor, the fuel and the type of gasifier. In an updraft gasifier 10–15 g/Nm³ of tar is normally formed (Nakamura et al., 2016) and in the case of the gasification plant in Lahti 7-12 g/Nm³ is formed (Kurkela et al., 2003). Table 2.1 shows one classification of tar composition.

Table 2.1 Classification of tar based on molecular weight (Wolfesberger et al., 2009).

| Tar class | Class name | Property | Representative compounds |
|-----------|---|--|---|
| 1 | GC-Undetectable | Very heavy tars, cannot be detected by GC | - |
| 2 | Heterocyclic aromatics | Tars containing hetero atoms, highly water soluble compounds | Pyridine; phenol; cresols; quinolone; isoquinoline; dibenzophenol |
| 3 | Light aromatic (one ring) | Usually light hydrocarbons with single ring; do not pose a problem regarding condensability and solubility | Toluene; ethylbenzene; xylenes; styrene |
| 4 | Light PAH compounds (two to three rings) | Two and three rings compounds; condense at low temperature even at very low concentration | Idene; naphthalene; methylnaphthalene; biphenyl; acenaphalene; fluorine; phenanthrene; anthracene |
| 5 | Heavy PAH compounds (four to seven rings) | Larger than three rings; these components condense at high-temperature at low concentration | Fluoranthene; pyrene; chrysene; perylene; coronene |

There are many available technologies to remove tar, which can be divided into primary and secondary methods.

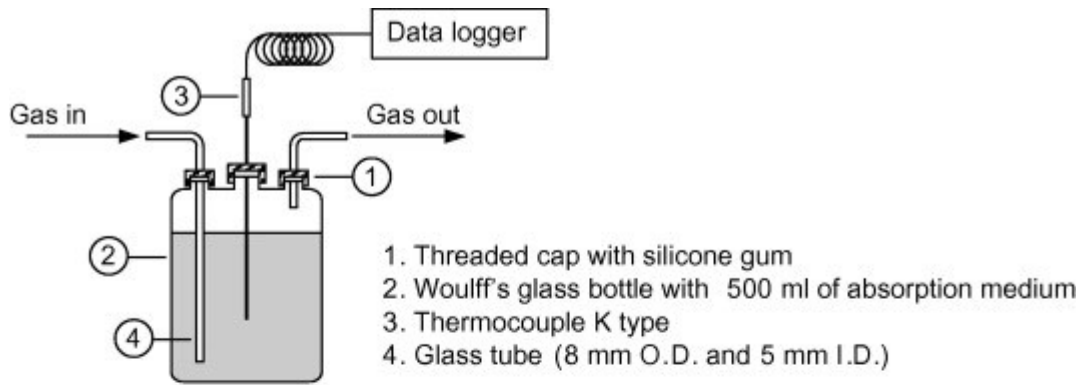
Primary methods are: thermal cracking, catalytic cracking and plasma gasification (Nakamura et al., 2016). Some of these methods, which use catalysts like Ni, remove tar with a high efficiency, over 98-99%. However, these primary methods have some disadvantages such as higher initial and running costs because of high temperature, short life of the catalysts and difficult construction of adapted reactors (Nakamura et al., 2016).

Secondary methods use scrubbers, filters and centrifuges. Such equipment are easier to commercialize because of their low initial and operational costs (Nakamura et al., 2016). In the case of scrubbers, there is a problem if water is used, since tar is soluble in water requiring expensive water treatment units (Nakamura et al., 2016). For this reason the use of scrubbers with oil is one alternative to water, since oil is non-polar, unlike tar, thus tar is not soluble in oil (Nakamura et al., 2016).

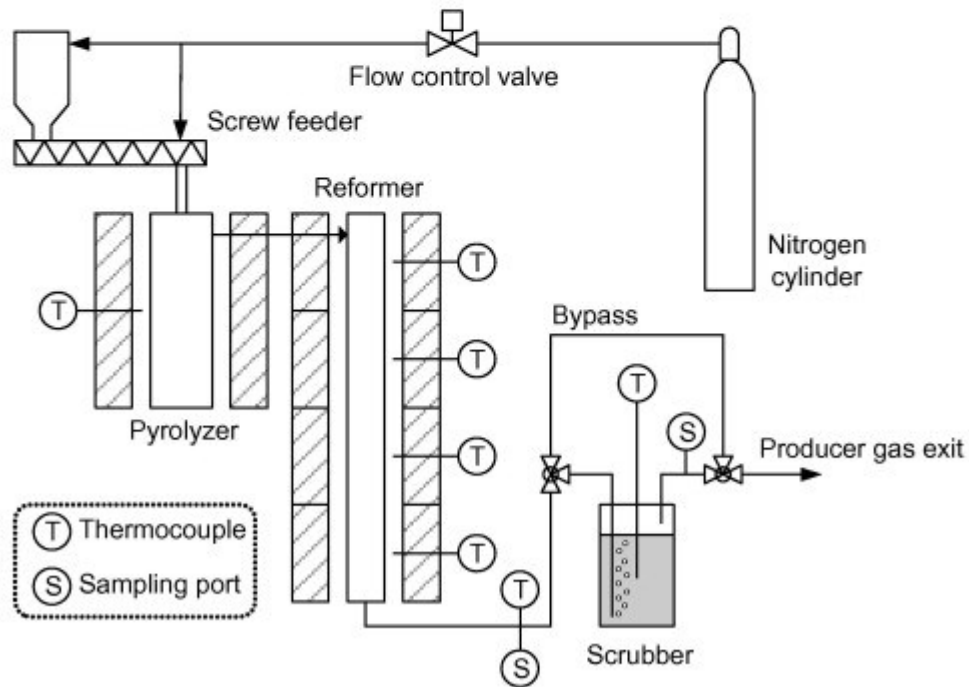
Besides (Phuphuakrat et al., 2011) studied the efficiency of removing tar with different substances, and the results were from highest to lowest efficiency in tar removal:

Diesel fuel → vegetable oil → biodiesel fuel → engine oil → water.

Figure 2.6 shows the scrubber used in (Phuphuakrat et al., 2011) and its connection to the tar removal system.



a



b

Figure 2.6 (a) Detail of the scrubber used for tar absorption study and (b) schematic diagram of the experimental setup (Phuphuakrat et al., 2011).

However, in this study an increase in gravimetric tar was observed for diesel fuel and biodiesel fuel absorbents because they evaporate easily. Therefore vegetable oil is the best option in scrubbers to remove tar in gasification systems (Phuphuakrat et al., 2011). Table 2.2 shows the tar removal efficiency with different absorbents, while Figure 2.7 shows the gravimetric tar of these absorbents used for the tar removal.

Table 2.2 Absorption efficiencies of tar components by different absorbents (%) (Phuphuakrat et al., 2011).

| | Water | Diesel fuel | Biodiesel fuel | Vegetable oil | Engine oil |
|---|-------|-------------|----------------|---------------|------------|
| Benzene (C ₆ H ₆) | 24,1 | 77,0 | 86,1 | 77,6 | 61,7 |
| Toluene (C ₇ H ₈) | 22,5 | 63,2 | 94,7 | 91,1 | 82,3 |
| Xylene (C ₈ H ₁₀) | 22,1 | 730,1* | 97,8 | 96,4 | 90,7 |
| Styrene (C ₈ H ₈) | 23,5 | 57,7 | 98,1 | 97,1 | 91,1 |
| Phenol (C ₆ H ₆ O) | 92,8 | 111,1* | 99,9 | 99,7 | 97,7 |
| Indene (C ₉ H ₈) | 28,2 | 97,9 | 97,2 | 97,6 | 88,7 |
| Naphthalene (C ₁₀ H ₈) | 38,9 | 97,4 | 90,3 | 93,5 | 76,2 |

* Higher than 100% because of the evaporation of the absorbent.

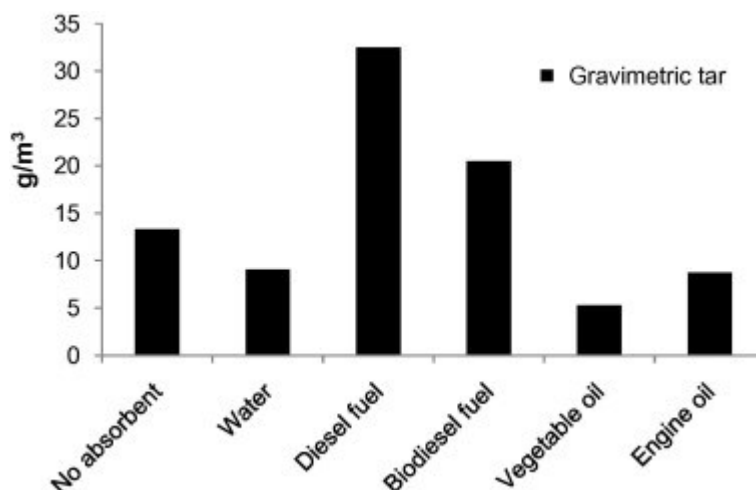


Figure 2.7 Concentration of gravimetric tar in the tar trap using different absorbents (Phuphuakrat et al., 2011).

Apart from scrubbers, there are other components that are used to protect gas analysers, engines, or any equipment installed down-stream of the reactor. For example filters are also used for tar and particulate matter removal. There are many different types of filters like catalytic filters, granular bed filters, ceramic filters, etc.

Filters can be used directly in the air pollution control (APC) system to remove most of the unwanted substances, but they can also be used after scrubbers in order to remove the substances that the scrubbers could not remove. In this way, any down-stream equipment of the reactor are protected from tar, particles, etc. Figure 2.8 shows a catalytic filter used in (García-Labiano et al., 2016), while Figure 2.9 shows a dual layer granular bed filter used in (Hu et al., 2016).

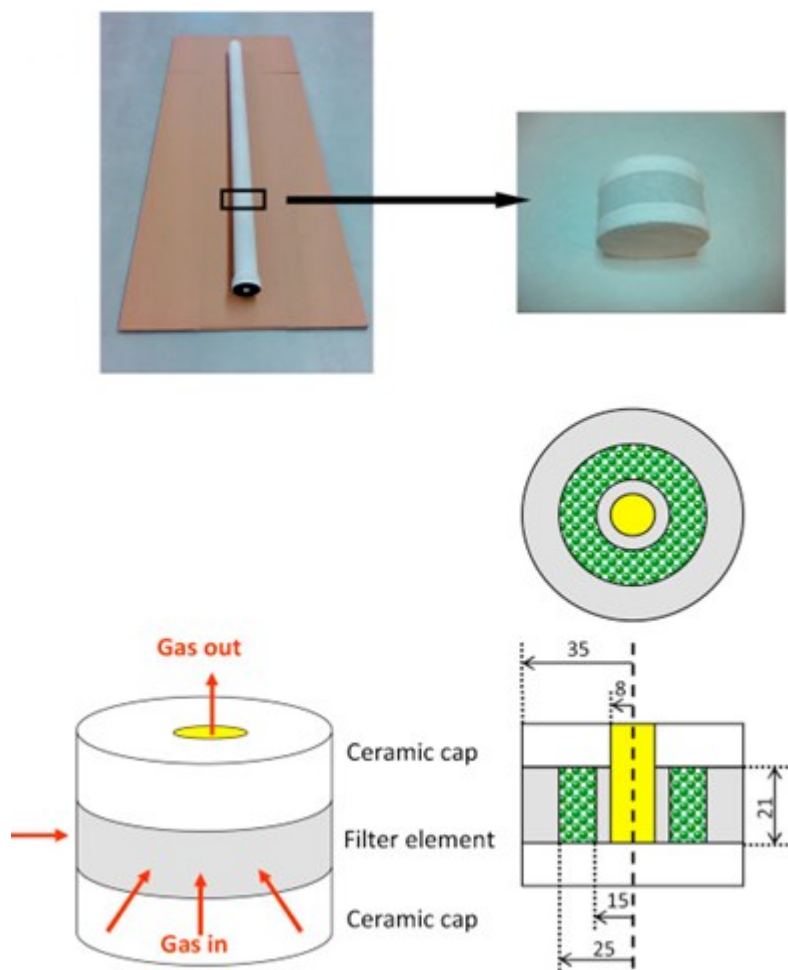


Figure 2.8 Catalytic filter (García-Labiano et al., 2016).

Removing tar using ceramic filters can be problematic, since sometimes these filters can get blocked or clogged and as result, the whole process should be stopped in order to clean or change the filters (Bridgwater, 2013). Filters depend on operational conditions, type of reactors and fuel used. For example in Lahti, the use of wood instead of SRF reduces the production of tar, avoiding the clogging problem of the ceramic filters (Uuskallio, 2014).

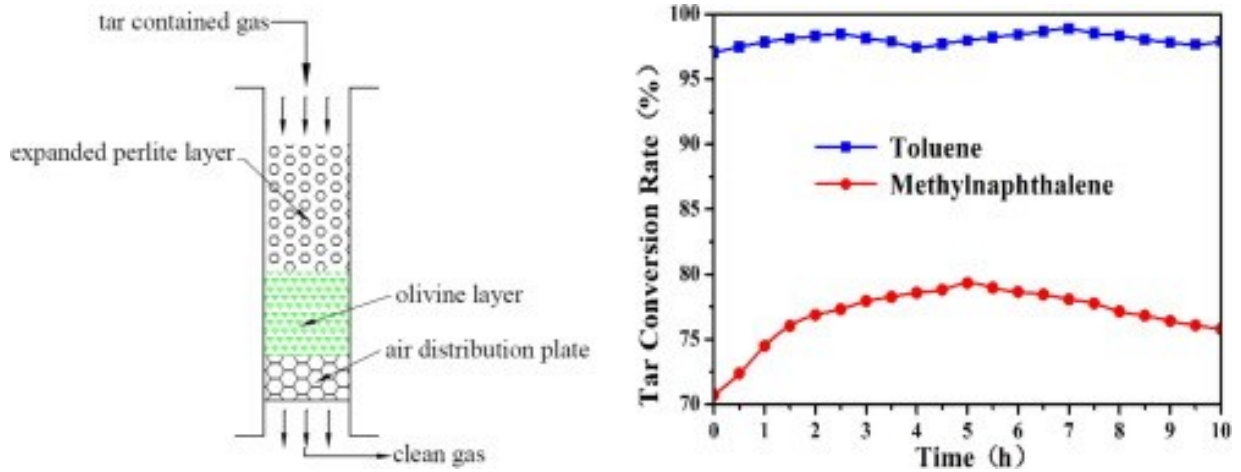


Figure 2.9 Dual layer granular bed filter (Hu et al., 2016).

After the gas flow has been cleaned from unwanted substances, the next step is to assure that the gas flow will remain in the sampling system as short time as possible, the residence time of the gas in the whole system is going to be explained in the next chapter.

2.4 Residence Time in Gas Sampling System

The residence time is defined as the time that the gas spends in the gas sampling system, which includes the equipment and piping between the reactor and the gas analyser. If this time is very long the measurements can be inaccurate. It is because some reactions continue in the gas analyser system and valuable data can be lost. Besides that, during the time that the gas spends inside of the gas analyser system, there is more probability that the gas is contaminated by any substance. So the knowledge of the residence time has a big importance in the multilevel sampling gas system.

There are two different methods to measure the residence time and the residence time distribution function in deposits, reactors or pipes of gases or liquids: pulse input and step input (Fogler, 2006). In the pulse input method, a trace of coloured, radioactive or inert (CO_2 , N_2 , etc) elements are injected in the reactor or pipe and later the time that the trace remains in the system can be measure checking when the concentration of this trace in the system starts to appear in the pulse response and until when there is not any trace in the system (Fogler, 2006). The pulse injection and the pulse response of the trace are shown in Figure 2.10.

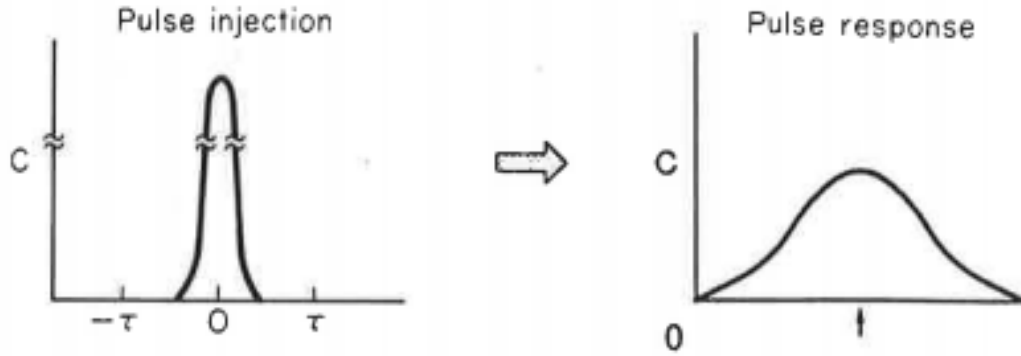


Figure 2.10 Pulse input for residence time measurement (Fogler 2006).

In this method, an amount of tracer N_0 is injected in one shot for as short time as possible. Later the amount of this tracer is calculated with the concentration of this tracer in the flow with Equation 2.1 (Fogler, 2006):

$$\Delta N = C(t)v\Delta t \quad (2.1)$$

Where ΔN is the increase of the amount of trace with time, v is the volumetric flow, $C(t)$ is the concentration of the trace in the flow and Δt is the time from the injection of the trace to the concentration is measured (Fogler, 2006). If Equation (2.1) is divided by the amount of tracer injected N_0 , it is possible to obtain the residence-time distribution function:

$$E(t) = \frac{v C(t)}{N_0} \quad (2.2)$$

Finally if Equation (2.1) is derivated and then integrated, combining Equation (2.2), Equation (2.3) is obtained.

$$E(t) = \frac{C(t)}{\int_0^{\infty} C(t) dt} \quad (2.3)$$

Where $C(t)$ is the concentration of tracer at time and the integral is the area under the C curve, as shown in Figure 2.11.

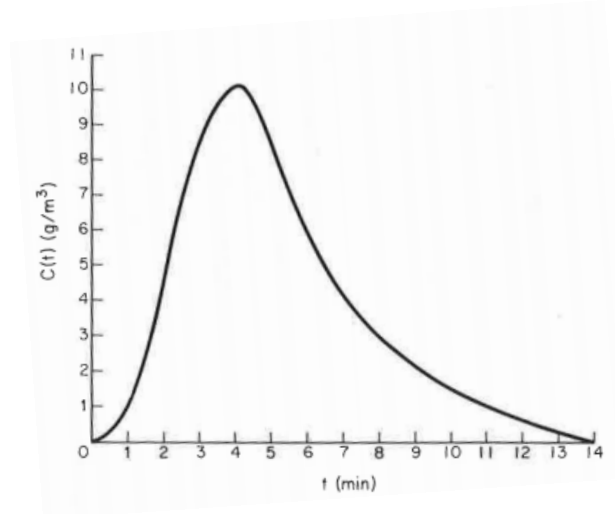


Figure 2.11 Concentration of the trace in the flow over time (Fogler, 2006).

The difference between the step input and the previous method is that the injection of the trace remains constant until there is a trace of inert element in the step response. So the residence time of the trace can be calculated only with watching the time between when the injection of the trace is produced and when the trace appears in the step response (Fogler, 2006). Figure 2.12 shows an example of this method.

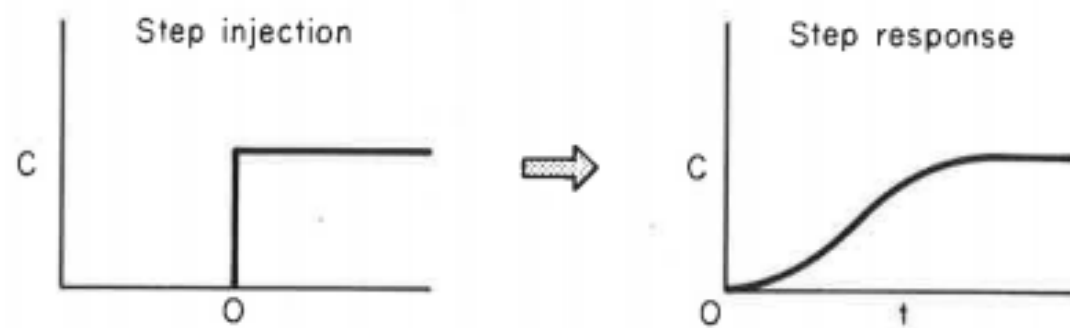


Figure 2.12 Step input for residence time measurement (Fogler 2006).

In the step injection method the concentration of the trace in the flow is constant after the injection (Fogler, 2006):

$$C_o(t) = 0 \quad t < 0$$

$$C_o(t) = \text{constant} \quad t \geq 0$$

In this method the residence-time distribution function can be calculated with Equation (2.4) (Fogler, 2006).

$$E(t) = \frac{d}{dt} \left[\frac{C(t)}{C_o} \right]_{step} \quad (2.4)$$

Finally, independently of the method used, the residence time can be calculated from the residence-time distribution function in Equation (2.5) (Fogler, 2006):

$$t_m = \frac{\int_0^{\infty} tE(t)dt}{\int_0^{\infty} E(t)dt} = \frac{\int_0^{\infty} tE(t)dt}{1} = \int_0^{\infty} tE(t)dt \quad (2.5)$$

Overall, the step input method is more accurate than the pulse input (Fogler, 2006) and therefore the step input method will be used in this work.

On the other hand, if only the residence time is known, it is not enough, since the residence time measured is composed by two different parts: transitional time and steady time. The transitional time is the time within the amount of trace in the response is increasing until this achieves the same concentration. However the steady time is the time when the concentration of trace in the response is all the time the same, i.e. without any change.

If this is applied to the step input method, the injection of trace is almost instant, which can be seen in Figure 2.12. However in the response it is very clear that at the beginning there is a time when the amount of trace is increasing until it is stabilized. This is the transitional time, while after the trace is stabilized the steady time follows. Figure 2.13 shows the transitional and steady times in the step response.

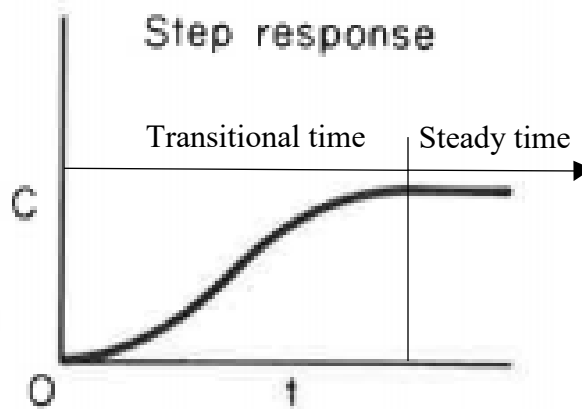


Figure 2.13 Transitional and steady time in step response.

This can be applied to sampling lines, since if a valve is installed before the gas analyser and it is opened and closed, there is a transitional time and a steady time in the gas flow. Gas analysers work during this time, but only data from the steady state is reliable. For this reason it is necessary to know how long the steady time takes, because this is the time within the data acquired from the gas analyser will be reliable. Figure 2.14 shows the transitional times and the steady times when a valve is opened and closed before a gas analyser.

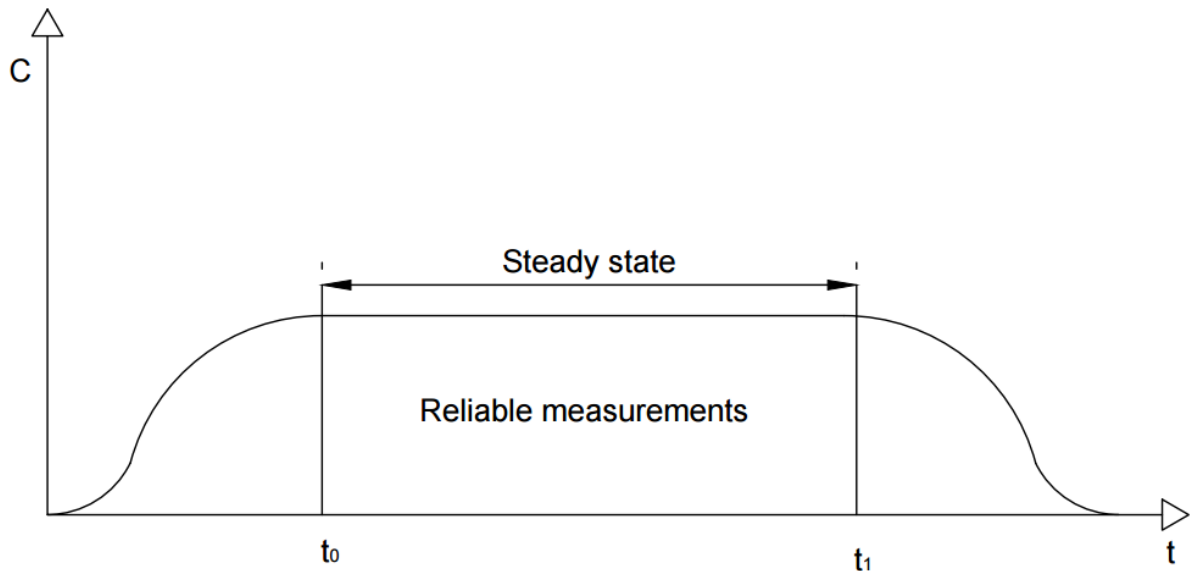


Figure 2.14 Transitional and steady states for one measurement with gas analyser.

As the measurements are only reliable during the steady state, the reliable data of gas composition should be taken from t_0 to t_1 . Therefore, knowing this steady state and the two transitional times after t_1 and before t_0 , it is possible to know how long one cycle of measurement takes with the gas analyser.

On the other hand, if instead of measuring only one level in a gasifier, three levels are measured with the same gas analyser, it is very important to know how long each level takes. It is so because two levels cannot be measured at the same time, i.e. when one has been measured, it is possible to start to measure the next one. For this reason, if the time of one cycle of measurement in one level is known, it is possible to calculate when the next level can be measured. Figure 2.15 shows an example of measurements in three different levels with one gas analyser.

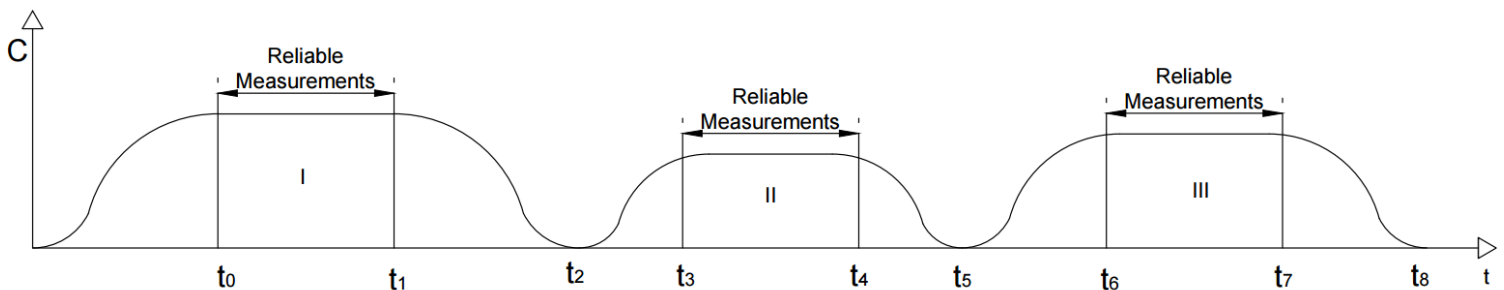


Figure 2.15 Measurements of three levels with one gas analyser.

The working principle of the system shown in Figure 2.15 is that at the beginning the valve of the first level is opened and when the transitional time in this level ends at t_0 , the data acquired by the gas analyser from this level is reliable until t_1 . After t_1 the valve at the first level is closed and at t_2 the valve at the second level is opened. On t_3 the steady state of the second level starts, so the acquired data from the second level is reliable until t_4 and in t_5 the valve on the third level is opened. The process is repeated with the third level, and at t_8 if the experiment has not finished, this cycle can be done again.

This process can in principle be done with any number of levels. t_8 is in this case the time of the cycle necessary to measure all the levels. Knowing the total time that an experiment in the gasifier takes, it is possible to calculate how many measurements can be taken in all levels in one experiment. Equation 2.6 shows how to calculate this.

$$\text{number of measurements} = \frac{t_{\text{experiment}}}{t_{8 \text{ cycle of measurements}}} \quad (2.6)$$

3 Focus of this Master's Thesis

The main objective of this Master's Thesis is the development of a multilevel gas sampling system for gas analyser in circulating fluidized bed reactor, i.e, the sampling of the gas flow can be taken in three different vertical levels and analysed with only one gas analyser.

This permit for future works to study the different physiochemical reactions that are taking place in gasification and the concentration of the gasification products in each level. Besides, some parameters of the gasification like temperature, particle size distribution, fuel, etc can be varied and so it permits to study how change the products or the physiochemical reactions in the different levels of the reactor.

Other of the important objectives of this work is to develop a good treatment system for the gas flow. It means that some equipment like oil scrubbers, filters, etc, have to be used in order to remove all the unwanted substance from the gas flow like tar, particles, etc. In addition, it permits to study the composition of these substances and acquire reliable data for other studies or researches.

On the other hand, this sampling system has to be designed so that the gas remains as less time as possible inside of it. This is because some reaction can also be produced in this treatment system, so some valuable data could be lost, as well as if the gas remains too long in the system, there are more opportunities that it might be contaminated. Besides, knowing residence time, it is possible to calculate when the acquired data from the gas analyser is reliable and decide a sampling frequency in order to get as maximum as possible samples of the three levels in one experiment.

4 Experimental Setup

The main objective of this work is to develop a multilevel sampling system for a gas analyser in a circulating fluidized bed reactor. Before this Master's Thesis the gas was only analysed down-stream from the cyclone of the reactor only in one level. However, after this work and with the newly built multilevel sampling system the gas could be analysed in three different levels of the reactor. It is done in order to understand in a better way how the gas composition changes along the riser, and to be able to compare with the gas composition obtained down-stream from the cyclone.

In this chapter all the equipment and material (reactor, gas analysers, fuel, etc.) used for the experiments and the development of this Master's Thesis are going to be explained.

4.1 Circulating Fluidized Bed Reactor (CFB).

The reactor used in this Master's Thesis is a circulating fluidized bed reactor (CFB). It is located in the Department of Mechanical Engineering at Aalto University. The reactor is a pilot scale CFB, in which the test conditions are more similar to the conditions found in commercial reactors than in lab scale CFBs. Figures 4.1 and 4.2 show the reactor used in this work.

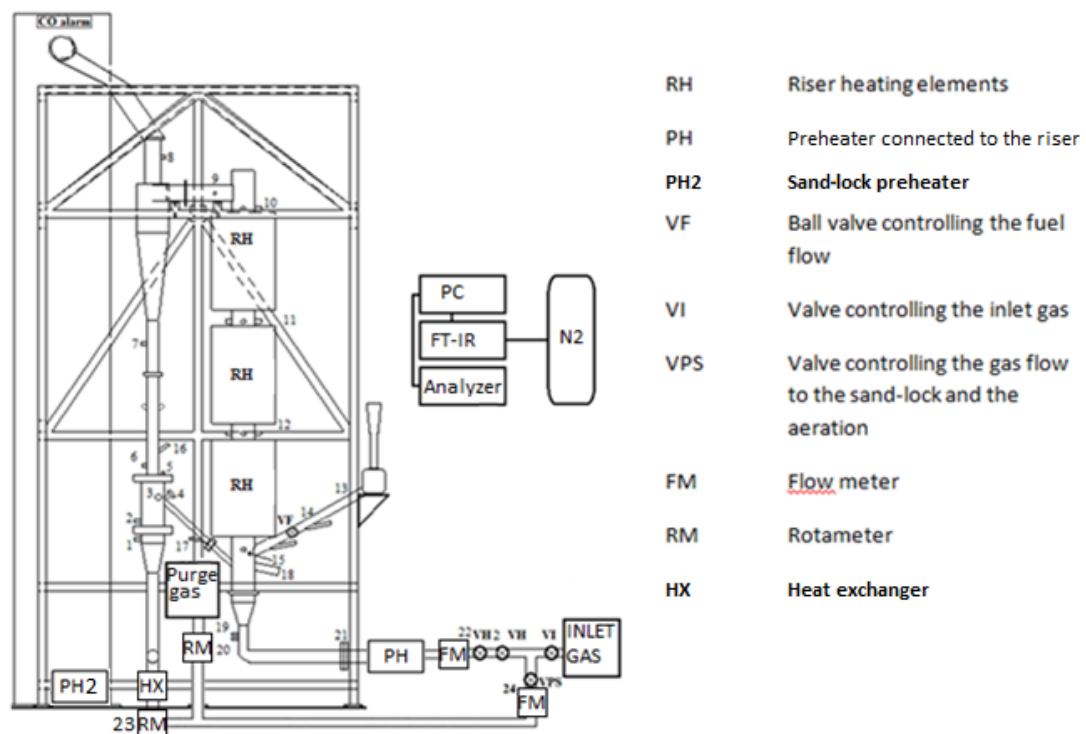


Figure 4.1 Schematic view of the CFB reactor.



Figure 4.2 CFB reactor.

The reactor is an atmospheric reactor, which is made of acid resistant steel (316L) in order to resist corrosion. The distribution plates are perforated plates in both the riser and the sand lock. The riser is covered by 3 heating element sections of 4,6 kW and its internal diameter is 128 mm. Besides, there are windows on the three sampling levels for monitoring what is happening inside of the riser and other windows in the downcomer and the sand lock.

Apart from the reactor, there are other needed equipment for the correct work of the reactor. There are two pre-heaters, the first one heats the air injected into the riser (LHS 61L PREMIUM, LEISTER), whose power is 11 kW. The other pre-heater indirectly heats the air injected into the sandlock through a heat exchanger. The pre-heater (CH-6056, LEISTER) has a maximum power of 10 kW. Figure 4.3 shows the air pre-heater (LHS 61L PREMIUM, LEISTER).

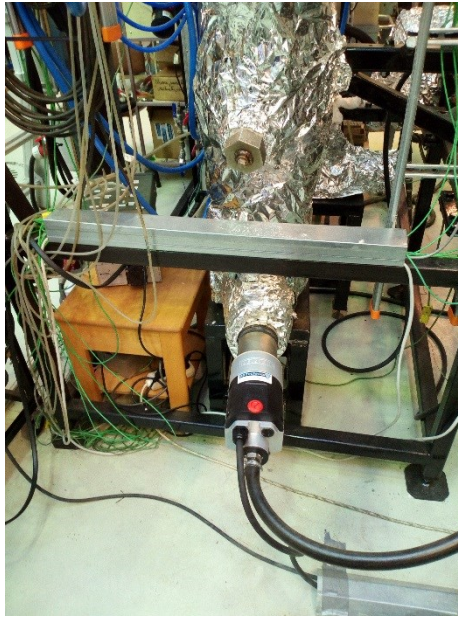


Figure 4.3 Air pre-heater (11 kW).

At the top of the reactor there is a cyclone that separates the solids, before these are recirculated to the sand lock and later to the riser. Figure 4.4 shows the heater for the sand lock.

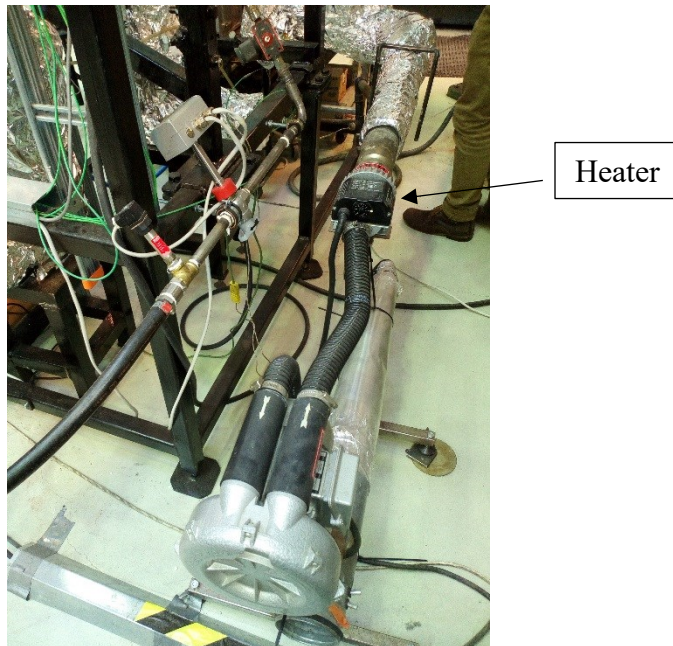


Figure 4.4 Blower and heater for the sand lock.

Finally, there is other equipment, for controlling and measuring the air and gas flows like valves, rotameters, etc. Table 4.1 shows the normal operating parameters of the system.

Table 1 Normal running parameters of the system.

| Design parameters | CFB |
|--|----------------|
| Temperature, °C | < 900 |
| Circular diameter, m | 0.128 |
| Height, m | 2.3 |
| Bed material (sand) mean diameter, mm | 0.2 |
| Residence time of fuel, s | 1-2 |
| Fluidising gas | Air |
| Distributor plate type | perforated |
| Numbers of orifices; diameter , mm | 141 ; 3 |
| Reactor construction material | ASTM 316 steel |
| Superficial gas velocity, m/s | ~2 (@ 800°C) |
| Heating power, riser | 3x4,6 kW |
| Air preheater, riser | 11 kW |
| Air preheater, sand lock | 10 kW |

4.2 Solid Recovered Fuel

The synthesis gas (syngas) can be produced from many different feedstocks such as coal, biomass, solid recovered fuel (SRF), etc. The gasification of coal has been used mostly through the history, but other feedstocks like biomass have also been used frequently in the past, moreover in the production of tar (Basu 2006). In addition, in emerging countries, where the total population is higher than in the industrialized countries, are producing great amounts of waste. Therefore, solutions for the treatment of these waste have to be found in countries like China, India or Brazil.

Gasification of SRF is one of the best ways to control the increase of produced waste in these countries, since the waste can be used to produce energy and it is always better than waste disposal in landfills. Besides, gasification has a higher efficiency than the direct combustion of the waste, as the syngas can be used in combined cycles. It also has some advantages regarding emissions, since the amount of gas is smaller than in combustion so that smaller equipment can be used for cleaning the gas which in turn leads to less investment costs

SRF comprises a lot of different waste fractions, however from analysis it is possible to know the moisture content, amount of volatile matter and content of fixed carbon and ash (Saeed, 2015). There are different analysis like ultimate fuel analysis, dry and ash free analysis, dry analysis and received analysis. Figure 4.5 shows what is possible to know with each analysis of the solid recovered fuel (Saeed, 2015).

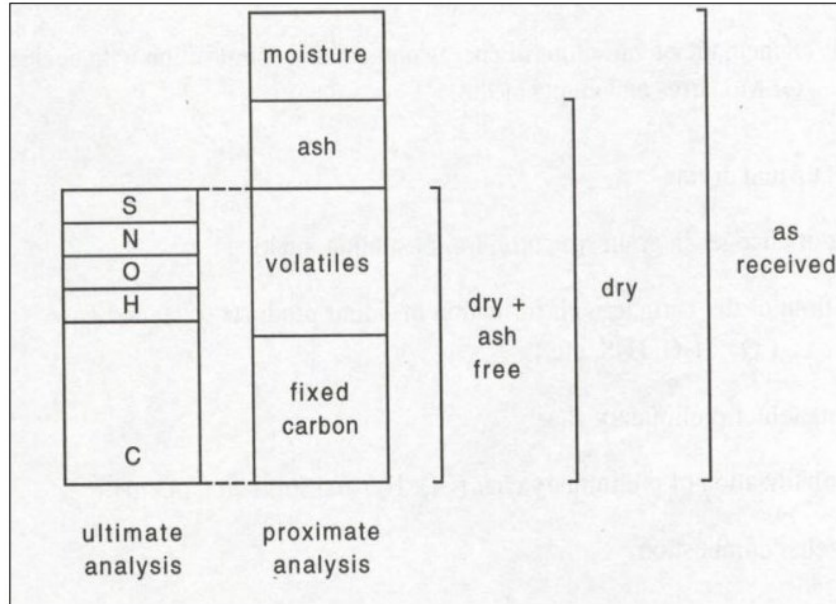


Figure 4.5 Different analysis of solid waste (Saeed, 2015).

Knowing the fuel composition is very important because it influences the thermal treatment of the fuel, as an example the influence of the moisture content in the lower calorific value (Görner, 2008). Figure 4.6 shows one example of this effect.

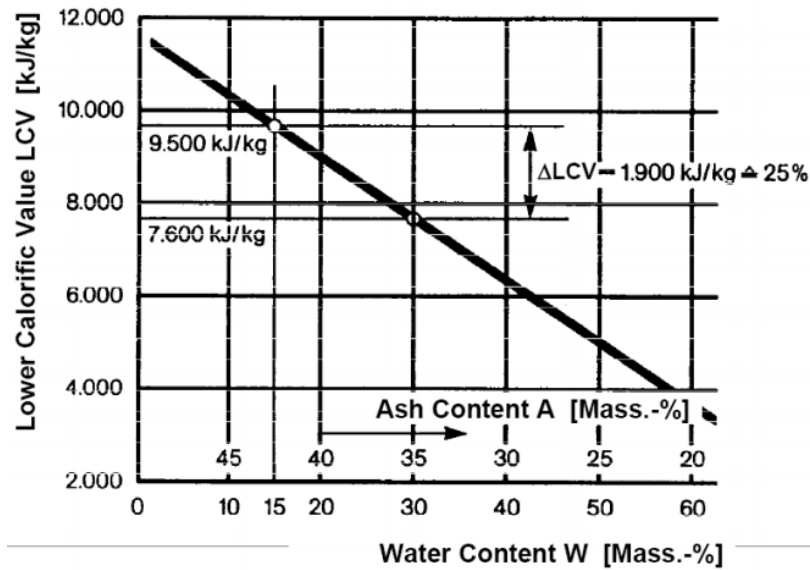


Figure 4.6 Influence of the water in the lower calorific value of solid waste (Görner, 2008).

In addition, the composition of solid waste is not at the same in all countries, since the waste depend on the culture and lifestyle of each country (Görner, 2008). For example Figure 4.7 shows the difference of combustibles, ash and water content of waste in Europe and Japan.

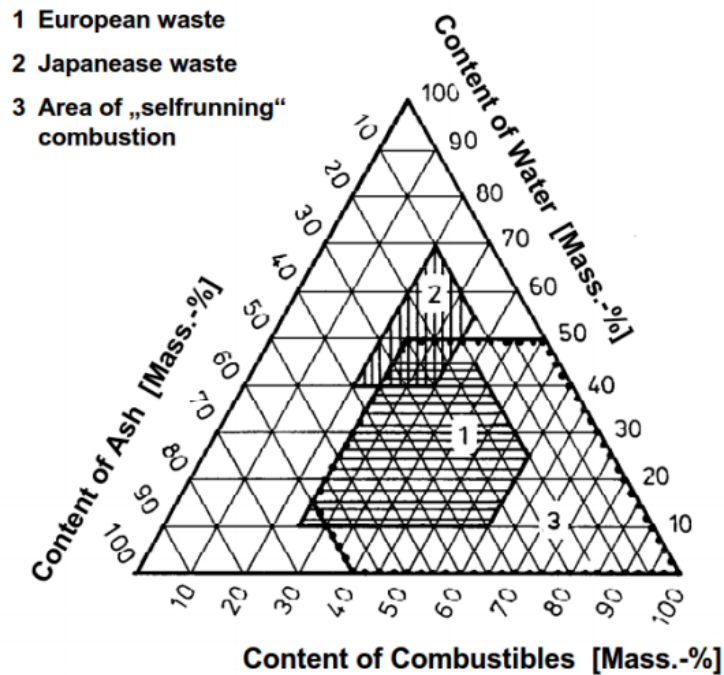


Figure 4.7 Influence of water in lower calorific value of waste (Görner, 2008).

Although the main objective is the same in all the countries, the use of SRF in gasification or combustion to obtain energy, the composition of the waste is not the same and neither are the treatment methods. So different regions have different standards regulating the quality and the use of SRF.

SRF have to comply with the specification established by the European Standard CEN/TC 343. This standard defines the solid recovered fuels as “prepared fuel from non-hazardous waste to be utilized for energy recovery in waste incineration or co-incineration plants, excluding fuels that are included in the scope of CEN/TC 335 (solid biofuels)” (Olabarria Uzquiano, 2013).

This standard sets the following specifications of solid recovered fuels (Olabarria Uzquiano, 2013):

1. Terminology.
2. Fuel specifications and classes.
3. Quality management system.
4. Sampling.
5. Sample reduction.
6. Physical and mechanical tests.
7. Chemical tests.
8. Supplementary tests.

According to the standard CEN/TS 15359, the SRFs are grouping into classes based on three important parameters:

1. Net calorific value.
2. Chlorine content.
3. Mercury content.

Each parameter is divided into 5 classes as Table 4.2 shows.

Table 4.2 Solid recovered fuel classification (CEN/TS 15359).

| Classification property | Statistical measure | Unit | Classes | | | | |
|---------------------------|---------------------|------------|-----------|-----------|-----------|-----------|----------|
| | | | 1 | 2 | 3 | 4 | 5 |
| Net calorific value (NCV) | Mean | MJ/kg (ar) | ≥ 25 | ≥ 20 | ≥ 15 | ≥ 10 | ≥ 3 |

| Classification property | Statistical measure | Unit | Classes | | | | |
|-------------------------|---------------------|-------|------------|------------|----------|------------|----------|
| | | | 1 | 2 | 3 | 4 | 5 |
| Chlorine (Cl) | Mean | % (d) | $\leq 0,2$ | $\leq 0,6$ | ≤ 1 | $\leq 1,5$ | ≤ 3 |

| Classification property | Statistical measure | Unit | Classes | | | | |
|-------------------------|-----------------------------|------------|-------------|-------------|-------------|-------------|-------------|
| | | | 1 | 2 | 3 | 4 | 5 |
| Mercury (Hg) | Median | Mg/MJ (ar) | $\leq 0,02$ | $\leq 0,03$ | $\leq 0,08$ | $\leq 0,15$ | $\leq 0,50$ |
| | 80 th percentile | Mg/MJ (ar) | $\leq 0,04$ | $\leq 0,06$ | $\leq 0,16$ | $\leq 0,30$ | ≤ 1 |

Gasification of SRF is challenging, since they sometimes have some problems. There are high concentrations of Cl or S which can produce contaminants like HCl, H₂S, tar, etc. One of the most problematic elements in SRF is Cl, which can come from organic waste, like chlorinated polymers (PVC) and inorganic waste like salt in food (NaCl). The organic and inorganic Cl produces HCl during thermal processes, which is very harmful and corrosive for the environment and the gasification system respectively (Berrueco et al., 2015).

(Berrueco et al., 2015) tried to study how to reduce the amount of minor contaminants produced in the gasification of SRF like HCl, H₂S, etc, without changing other gasification performance parameters apart from the temperature or the equivalence ratio (ER). The gas composition and the amount of contaminants are analysed for different temperatures and equivalence ratios in order to find optimal ranges, for operational parameters, regarding efficiency and emissions. For example Figure 4.8 shows how the temperature influences the amount of contaminants.

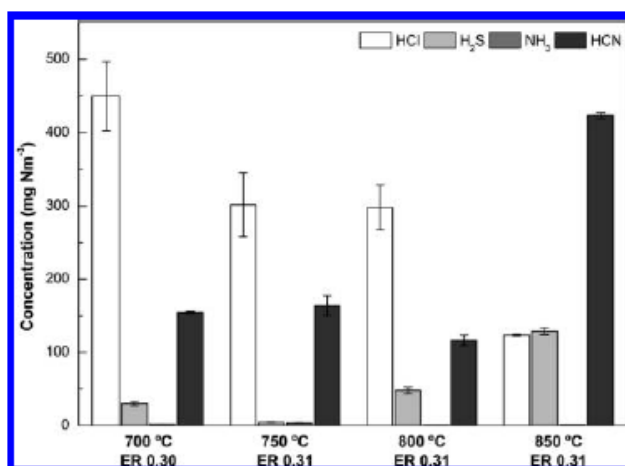


Figure 4.8 Effect of the gasification temperature on producer gas composition with ER=0,31 (Berrueco et al. 2015).

Therefore, studies like this are very important for understanding how to remove or avoid these pollutants in gasification of SRF. Besides, it helps to solve the problems with the SRF treatment, since it is a cheap fuel that reduces the use of fossil fuels and avoids landfilling (Frankenhaeuser et al., 2008).

For this reason the fuel used in this Master’s Thesis is a SRF of class 3 compound of wood, paper and cardboard, plastics and textiles. In addition, it is the same fuel that is used in Lahti Energia in gasification process in Kymijärvi II power plant. The fuel composition and properties are shown in Table 4.3.

Table 4.3 Solid recovered fuel composition (Skagersten et al., 2015).

| | |
|---------------------------------|-------|
| Moisture, wt% (ar) | 16,5 |
| Ash, wt% (dry) | 9,6 |
| Lower heating value, MJ/kg (ar) | 17,3 |
| C, wt% (dry) | 51,6 |
| H, wt% (dry) | 6,87 |
| O, wt% (dry) | 37,8* |
| N, wt% (dry) | 0,48 |
| S, wt% (dry) | 0,21 |
| Cl, wt% (dry) | 0,33 |
| Ca, wt% (dry) | 1,99 |

*Calculated by difference taking also some species into account which are not listed in the table.

Before feeding the fuel to the reactor, it has to be crushed in order to ensure homogeneity. The mill used for this process was Wiley mill type. After that, the fuel is pelletized with a size less than 6 mm for avoiding rat holes and plugging in the feeding system. Figure 4.9 shows some examples of fuel before and after it is crushed and pelletized.



a) Solid recovered fuel (SRF) as received.

b) Solid recovered fuel (SRF) after being crushed



b) Solid recovered fuel pelletized

Figure 4.9 Solid recovered before and after it is crushed and pelletized.

Finally, the fuel is fed to the reactor by a screw conveyor, whose flow can be adjusted with a frequency converter. The feeding hopper is made of transparent acryl in order to be able to monitor the fuel flow with a video camera and estimate the volume flow of the fuel by analyzing the video. Figure 4.10 shows the fuel feeding system in the reactor.

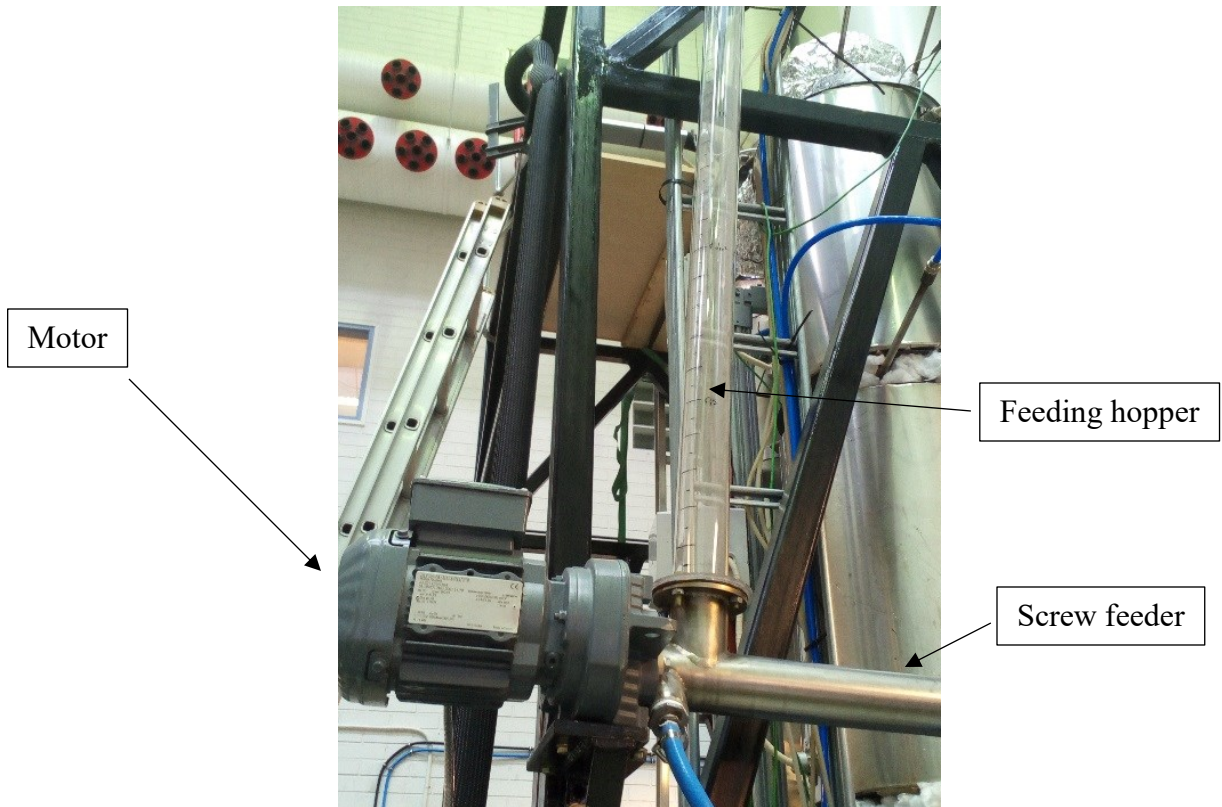


Figure 4.10 Fuel feeding system.

4.3 Gas Analysers

There are two gas analysers connected to the reactor: Siemens ULTRAMAT 23 and GASMET FT-IR. Both, ULTRAMAT and GASMET take the gas sample down-stream of the cyclone of the reactor. After this work, they will be able to be connected to the multilevel sampling system. These gas analysers are explained in the chapters 4.3.1 and 4.3.2.

4.3.1 Siemens ULTRAMAT 23 Gas Analyser

Siemens ULTRAMAT 23 gas analyser is an infrared absorption gas analyser, which contains three infrared (IR) active constituents. Besides, it also contains an electrochemical cell for measuring the O_2 . Therefore, this gas analyser can measure gases produced in gasification or combustion like CO, CO_2 , as well as O_2 , which is a very useful feature (SIEMENS, 2015).

4.3.2 GASMET Gas Analyser

The other gas analyser connected to the reactor is the Dx-4000 GASMET gas analyser. This analyser is a Fourier transform infrared spectrometer (FT-IR), but in contrast to the gas analyser explained in chapter 4.3.1, this analyser cannot analyse O_2 . This is due to the fact that this analyser is an infrared spectrometer but it does not contain any electromechanical cell to measure the O_2 (GASMET, 1997b). However, the gas analyser was mainly calibrated for analysing: H_2O , CO_2 , CO , HCl , CH_4 , SO_2 , NO , NO_2 , N_2O and other hydrocarbons like benzene C_6H_6 , ethane C_2H_4 , styrene C_8H_8 , ethane C_2H_6 , toluene C_7H_8 , butadiene C_4H_6 , propene C_3H_6 , methanol CH_4O , formaldehyde CH_2O , acetaldehyde C_2H_4O , α -pinene $C_{10}H_{16}$, propane C_3H_8 , propanol C_3H_8O and acetone C_3H_6O . (Saeed, 2004).

5 Multilevel Sampling System for Gas Analyser

In this chapter all parts of the multilevel sampling system for gas analyser in the reactor are explained. The main objective of this work is to build a multilevel sampling system for a gas analyser in a circulating fluidized bed reactor (CFB). Figure 5.1 shows a Schematic view of the system.

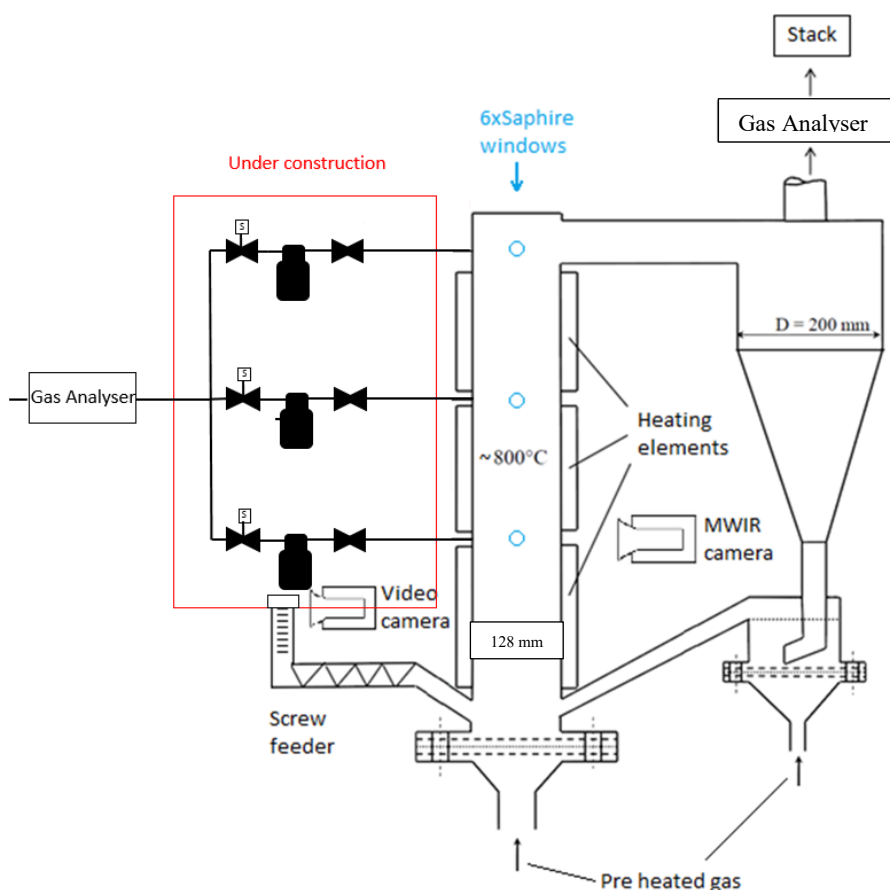


Figure 5.1 Diagram of the system.

The multilevel sampling system comprises following components:

- a) Three steel pipes, which are connected to three different levels of the riser.
- b) Ball valves, which open and close the sampling system to the reactor for protection or maintenance.
- c) Tar trap, which remove the tar, condensing it in a glass bottle.
- d) Three solenoid valves, which control from what level of the riser the gas is analysed by the analyser.
- e) Vitryl pipes, which connect the solenoid valves to the gas analyser.
- f) Support structure, mechanically supporting the sampling system.

In this chapter, the implementation of different processes and the construction of all parts of multilevel sampling system are explained in detail.

5.1 Steel Pipes

In this system, there are three steel pipes that are connected to three different levels of the CFB riser and to the solenoid valves that control the gas flow into the gas analyser. The heat transfer in these pipes is very important, since the temperature of the gas inside of the reactor is about 800-850°C and the pressure operated valves can only resist 250°C. Besides, condensation is unwanted, so the temperature has to be within a safe range. Therefore, heat transfer is the main design criteria for deciding the size and length of these steel pipes.

Since the heat transfer is the main method to dimension the size and the length of the steel pipes of the multilevel sampling system, a model of heat transfer in excel (example in appendix 9.1) was made in order to calculate the dimensions of these pipes.

The first step in this model is to calculate how much heat (Q) has to be released in order to cool the gas flow from an initial temperature (T_1) to a final temperature (T_2). The amount of heat can be calculated from Equation 4.1 as follow.

$$Q = \dot{m} * c_p * (T_1 - T_2) \quad (5.1)$$

Where:

Q is the amount of released heat from the gas in the pipe [W]

\dot{m} is the mass flow of gas [kg/s],

c_p is the heat capacity of the gas [KJ/KgK],

T_1 is the temperature of the gas at the beginning of the pipe [K],

T_2 is the temperature of the gas at the end of the pipe [K].

To calculate this heat flow, c_p has to be calculated first, since it depends on the composition of the gas which in the case of gasification is mainly CO, CO₂, H₂, CH₄, etc. The c_p of each substance can be calculated using Equation (5.2) and the needed coefficients a,b,c and d found in (Thermodynamic Department Univeritat Politècnica de València, 2005).

$$c_p = a + bT + cT^2 + dT^3 \quad (5.2)$$

Based on the volume and mass fraction of the composition of the syngas, the heat capacity (c_p) of this gas can be calculated.

There are three different forms of heat transfer: conduction, convection and radiation. In case of a pipe, the heat transfer is divided into:

- Inside convection, between the gas flow and the inside surface of the pipe.
- Conduction, through the thickness of the pipe.
- Outside convection, between the outside surface of the pipe and the ambient air.
- Radiation, between the outside surface of the pipe and the ambient.

Figure 5.2 shows a scheme of the equivalent electrical model of the heat transfer.

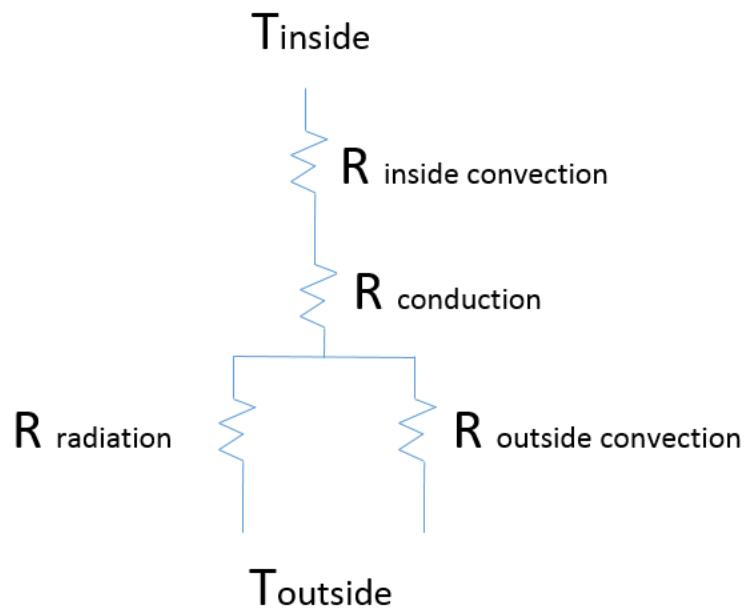


Figure 5.2 Equivalent electrical model of the heat transfer.

According to that model, the amount of heat per unit of length (q') that is released due to the difference of temperature can be calculated with the Equation (5.3):

$$q' = \frac{(T_{ins} - T_{out})}{R_{iconv} + R_{cond} + R_{oconv+rad}} \quad (5.3)$$

Where:

q' is the heat transfer of the gas to the ambient per unit of length [W/m],

T_{ins} is the temperature of the gas inside of the pipe [K],

T_{out} is the temperature outside of the pipe [K],

R_{iconv} is the resistance to the heat transfer of the convection inside of the pipe [$K/mK/W$],

R_{cond} is the resistance to the heat transfer of the conduction in the material of the pipe [$K/mK/W$],

$R_{oconv+rad}$ is the resistance to the heat transfer of the convection and radiation outside of the pipe [$K/mK/W$].

Selecting a diameter of a pipe in order to calculate the different resistances of heat transfer, it is possible to calculate the amount of heat per unit of length. With the results of Equations (5.1) and (5.3) the needed length of the steel pipe is calculated with equation (5.4).

$$Length\ of\ the\ pipe = \frac{Q}{q'} \quad (5.4)$$

Where:

Q is the heat transfer of the gas to the ambient [W],

q' is the heat transfer of the gas to the ambient per unit of length [W/m].

5.1.1 Convection Inside of the Pipe

The heat transfer between the gas flow and the inside surface of the pipe is convection. The resistance to heat transfer can be calculated with equation (5.5) for convection in pipe flow. (Heat Transmission Course Universitat Politècnica de València, 2011a).

$$R_{iconv} = \frac{1}{2\pi r_i h_i} \quad (5.5)$$

Where:

r_i is the internal radius of the pipe [m],

h_i is the heat transfer coefficient [W/m^2K].

The heat transfer coefficient can be calculated with correlation based Equations (5.6) or (5.7) depending on whether the gas flow regime is laminar or turbulent (Reynolds number) (Heat Transmission Course Universitat Politècnica de València, 2011b).

$$\text{laminar} \rightarrow Nu_D = \frac{h_i D}{k} = 4,36 \quad (5.6)$$

$$\text{turbulent} \rightarrow Nu_D = 0,023 Re_D^{0,8} Pr^n \rightarrow h_i = \frac{Nu_D k}{D} \quad (5.7)$$

Where:

Nu_D is the Nusselt number,

Re_D is the Reynolds number,

Pr is the Prandlt number,

h_i is the heat transfer coefficient $[W/m^2K]$,

D the diameter of the pipe $[m]$,

k the thermal conductivity of the material of the pipe $[W/mK]$.

5.1.2 Conduction

After the convection inside of the pipe the heat is transferred through the material of the pipe by conduction. The resistance of the conduction is (Heat Transmission Course Universitat Politècnica de València, 2011b):

$$R_{cond} = \frac{\ln\left(\frac{r_o}{r_i}\right)}{2\pi k} \quad (5.8)$$

Where:

r_o is the external radius of the pipe $[m]$,

r_i is the internal radius of the pipe $[m]$,

k is the thermal conductivity of the material of the pipe $[W/mK]$.

5.1.3 Convection Outside of the Pipe

The resistance to the heat transfer outside of the pipe (convection) is shown in Equation (5.9) (Heat Transmission Course Universitat Politècnica de València, 2011b).

$$R_{outconv} = \frac{1}{2\pi r_o h_o} \quad (5.9)$$

Where:

r_o is the external radius of the pipe [m],

h_o is the heat transfer coefficient [W/m^2K].

The ambient air is moving at low speed (laminar flow) due to the temperature gradient between the steel pipe and the ambient air. Equation (5.10) is used to calculate the heat transfer coefficient of convection outside of the pipe (Heat Transmission Course Universitat Politècnica de València, 2011a).

$$N_{uD} = C Re_D^m Pr^{\frac{1}{3}} \rightarrow h_o = \frac{N_{uD} k}{D} \quad (5.10)$$

Where:

N_{uD} is the Nusselt number,

Re_D is the Reynolds number,

Pr is the Prandlt number,

h_o is the heat transfer coefficient [W/m^2K],

D the diameter of the pipe [m],

k the thermal conductivity of the material of the pipe [W/mK].

C and m are constants that depend on the Reynolds number (Heat Transmission Course Universitat Politècnica de València, 2011a).

Table 5.1 Coefficients for equation (5.10)

| Re_D | C | m |
|-----------------|-------|-------|
| 0,4 to 4 | 0,989 | 0,33 |
| 4 to 40 | 0,911 | 0,385 |
| 40 to 4000 | 0,683 | 0,466 |
| 4000 to 40000 | 0,193 | 0,618 |
| 40000 to 400000 | 0,027 | 0,805 |

5.1.4 Radiation

The last mechanism for heat transfer is radiation between the external surface of the pipe and the ambient. The resistance to heat transfer due to radiation can be calculated with Eq. (5.11) (Heat Transmission Course Universitat Politècnica de València, 2011b).

$$R_{rad} = \frac{1}{2\pi r_o h_{rad}} \quad (5.11)$$

Where:

r_o is the external radius of the pipe [m],

h_{rad} is the heat transfer coefficient of radiation [W/m^2K].

h_{rad} has been calculated with Equation (5.12) (Heat Transmission Course Universitat Politècnica de València, 2011b).

$$h_{rad} = \sigma \varepsilon \frac{(T_{su}^4 - T_{sky}^4)}{(T_{su} - T_{sky})} \quad (5.12)$$

Where:

T_{su} is the average temperature of the outside surface of the pipe [K],

T_{sky} is the temperature of the outside ambient, which in this model is equal to the room temperature [K],

ε is the emissivity of the material of the pipe,

σ is the Stefan-Boltzmann constant [W/m^2K^4].

5.1.5 Length of the Steel Pipe

Once all the heat transfer mechanism have been calculated, the amount of heat per unit of length exchanged between the gas inside of the pipe and the ambient can be obtained combining Eq. (5.5) and (5.8) with (5.9) and (5.11) (Heat Transmission Course Universitat Politècnica de València, 2011b).

$$q' = \frac{(T_{ins} - T_{out})}{\frac{1}{2\pi r_i h_i} + \frac{\ln(\frac{r_o}{r_i})}{2\pi k} + \frac{1}{2\pi r_o (h_{rad} + h_o)}} \quad (5.13)$$

Finally the length of the steel pipe can be calculated with Equation (5.4).

5.1.6 Heat Transfer Experiments

After creating the model, two experiments have been done in the laboratory without gasification, just with fluidization with air. In these experiments the reactor was heated up to a normal working temperature of 800-850 °C and a steel pipe was installed in the top of the riser. After the air was pumped from the riser into the pipe (4 L/min) equipped with thermocouples the temperature of the gas inside of the pipe was measured. The first experiment was made with a steel pipe (pipe 1) like in Figure 5.3.

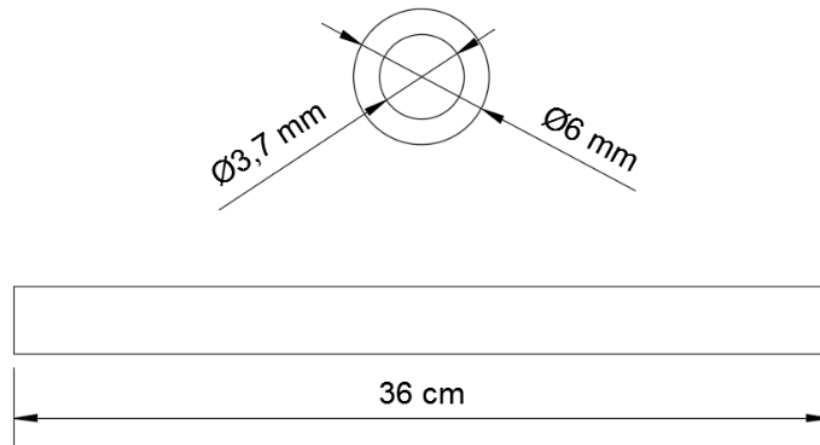


Figure 5.3 Properties of the steel pipe in experiment 1.

And the second experiment with a pipe (pipe 2) like in Figure 5.4.

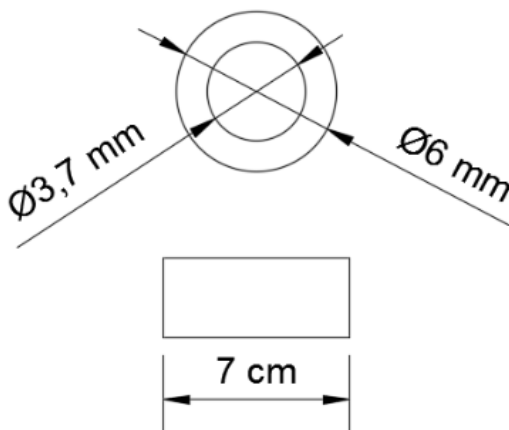


Figure 5.4 Properties of the steel pipe in experiment 2.

The results of temperature in the pipes were:

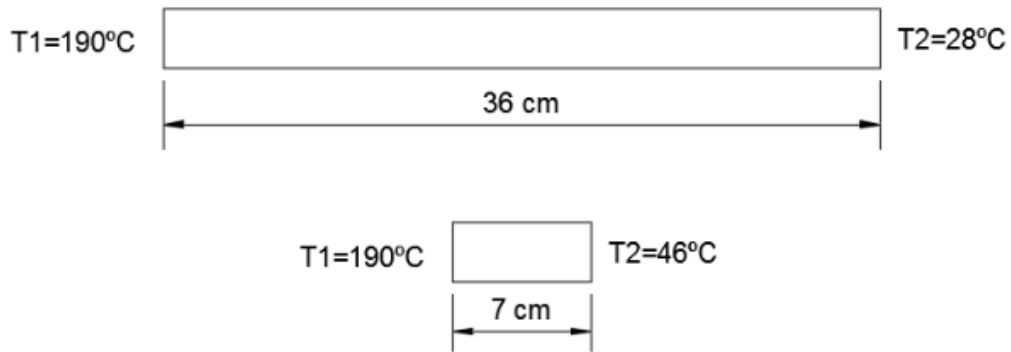


Figure 5.5 Results from experiments in the laboratory.

The difference between the temperature of the gas inside of the riser and at the beginning of the pipe is due to the fin effect, since the connection between the riser and the steel pipe has the shape shown in Figure 5.6. The temperature of the gas at the beginning of the pipe is between 180-190°C, not 850 °C like inside of the riser.

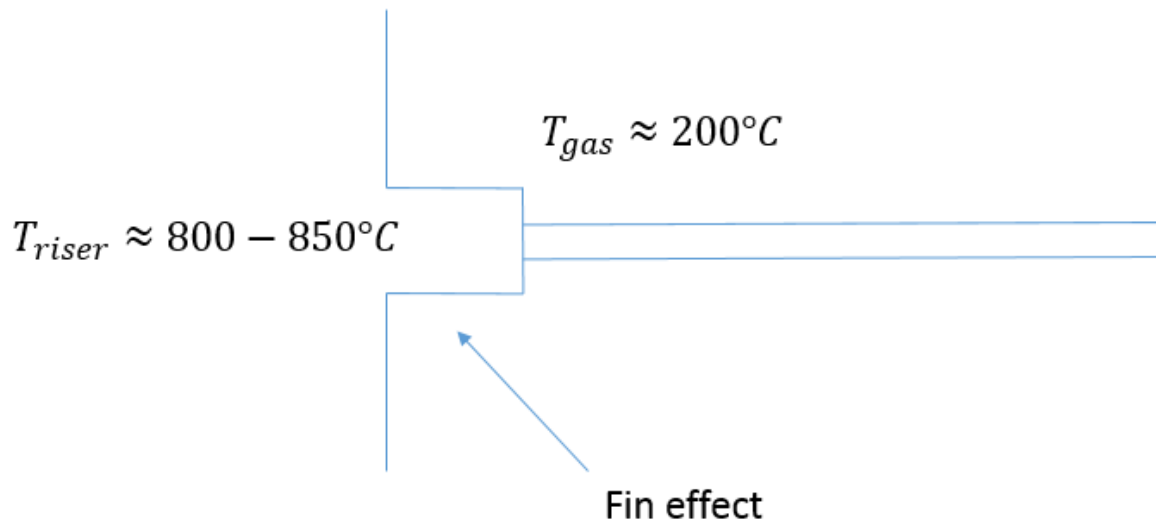


Figure 5.6 Connection between steel pipe and the riser.

5.1.7 Comparison of the Experimental Results and Model Results

The next step is to check that the heat transfer model works. For that the properties of the pipes 1 and 2 are introduced in the model. In order to represent real operational conditions, the gas composition in the model is air, i.e. in volumetric fraction 21% of O₂ and 79% of N₂. In addition, all the temperatures of the gas at the beginning and end of the pipe and also the outside conditions are introduced.

The results from the model and the results from the experiments are shown in Table 5.2.

Table 5.2 Comparison between experimental and model results.

| | Experiment (Pipe 1) | Model Results | Experiment (Pipe 2) | Model Results |
|----------------------------|------------------------|------------------|------------------------|------------------|
| T1 (°C) | 190 | 190 | 190 | 190 |
| T2 (°C) | 28 | 28 | 46 | 46 |
| gas flow (L/min) | 4 | 4 | 4 | 4 |
| length of the pipe (cm) | 36 | 36,64 | 7 | 32,6 |

It is possible to see in Table 5.2, that the model works for pipes that are long enough, since for very short pipes, the gas flow is undeveloped flow and the equations used in the heat transfer model only work for developed flow. Figure 5.7 shows the effect of undeveloped flow on the temperature of the gas in short pipes (data taken from experiments).

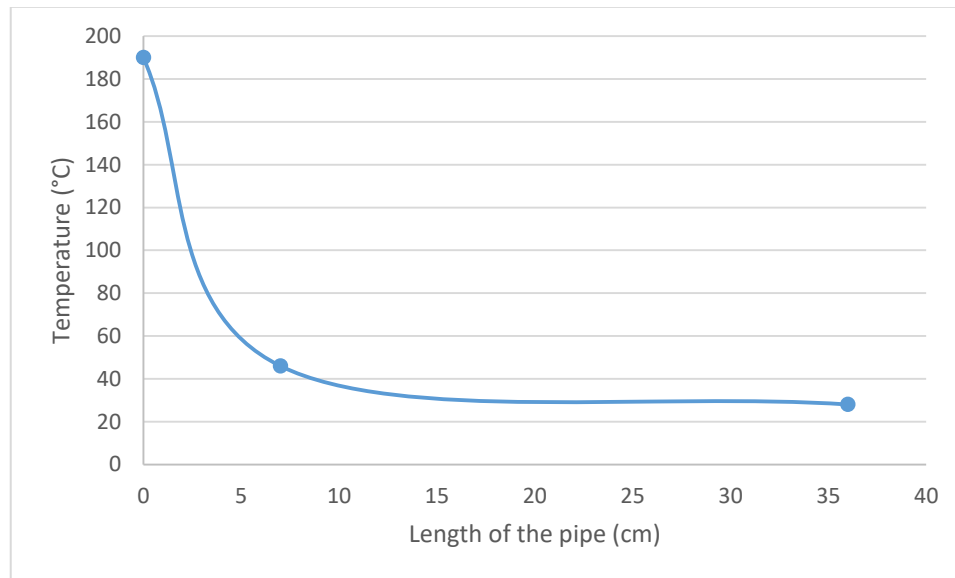


Figure 5.7 Effect of the undeveloped flow in the gas temperature.

From Figure 5.8 it is possible to see that the model works for pipe 1, while for pipe 2, which is the shortest pipe, the model does not work (undeveloped flow).

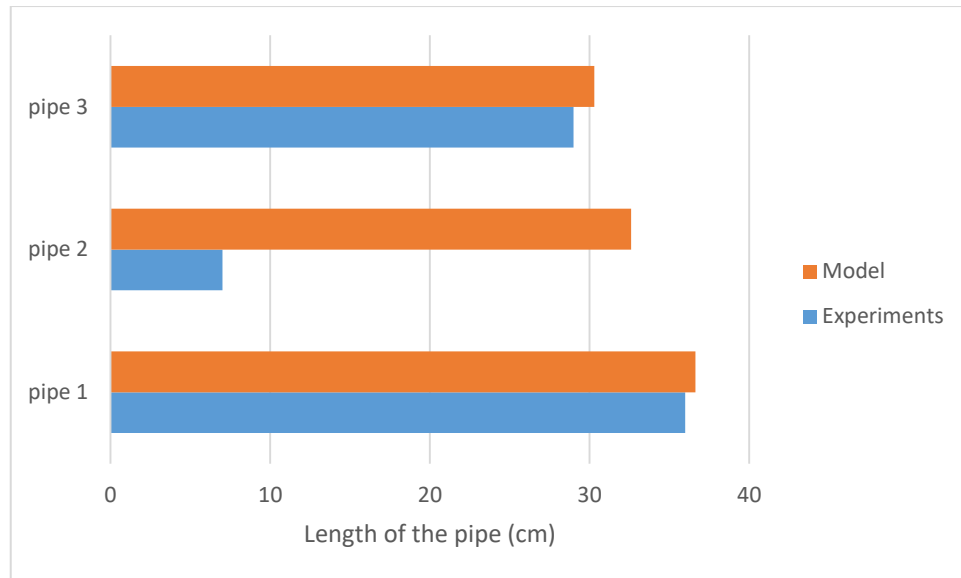


Figure 5.8 Comparison between models and experiments results.

5.1.8 Insulation of the Steel Pipe

After studying the heat transfer, pipes with a length of 19 cm and an inner diameter of 4 mm are installed in the three different levels of the riser. In order to increase the temperature at the end of the pipe, the resistance of conduction in the heat transfer of Equation (5.13) has to be increased, therefore the pipes were insulated with a 2,5 cm thick of insulator Insulfrax blanket S 128/2,5. Figure 5.9 shows the main properties of this insulator.

| Insulfrax S Blanket | | | | |
|--|-------------|-----------|------------|------------|
| Typical Chemical Analysis (wt.%) | | | | |
| SiO ₂ | 61.0 - 67.0 | | | |
| CaO | 27.0 - 33.0 | | | |
| MgO | 2.5 - 6.5 | | | |
| Al ₂ O ₃ | <1.0 | | | |
| Fe ₂ O ₃ | <0.6 | | | |
| Physical Properties | | | | |
| Colour | White | | | |
| Classification Temperature (°C) * | 1200 | | | |
| Melting Point (°C) | >1330 | | | |
| Mean Fibre Diameter (microns) | 4.0 | | | |
| Permanent Linear Shrinkage (%) 24 hour soak | | | | |
| 1200 °C | 1.0 | | | |
| Density (kg/m³) | 64 | 96 | 128 | 160 |
| Thermal Conductivity (W/mK) | | | | |
| Mean Temp. | | | | |
| 400 °C | 0.12 | 0.11 | 0.10 | 0.09 |
| 600 °C | 0.18 | 0.17 | 0.16 | 0.15 |
| 800 °C | 0.27 | 0.26 | 0.23 | 0.21 |
| 1000 °C | 0.43 | 0.36 | 0.31 | 0.29 |
| Tensile Strength (kPa) | | | | |
| | 30 | 50 | 70 | 90 |

Figure 5.9 Insulfrax S blanket properties (Unifrax, 2009).

The temperature of the pipe should not exceed 200°C to ensure the mechanical integrity of materials like vitryl and because some substances, which have to be removed like tar, condensates at temperatures below of 200°C.

An experiment was done to find out if the temperature of the gas inside the insulated pipes would be higher than 200°C. In this experiment, the reactor was heated up and the temperature of the pipe was stable over 100°C. Later, the gas flow of the reactor started to flow inside of the pipe during 1 hour until the temperature of the pipe was over 220°C. Finally, the gas flow in the pipe was stopped and the temperature of the pipe started to decrease again until the stable temperature. Figure 5.10 shows the results of this experiment.

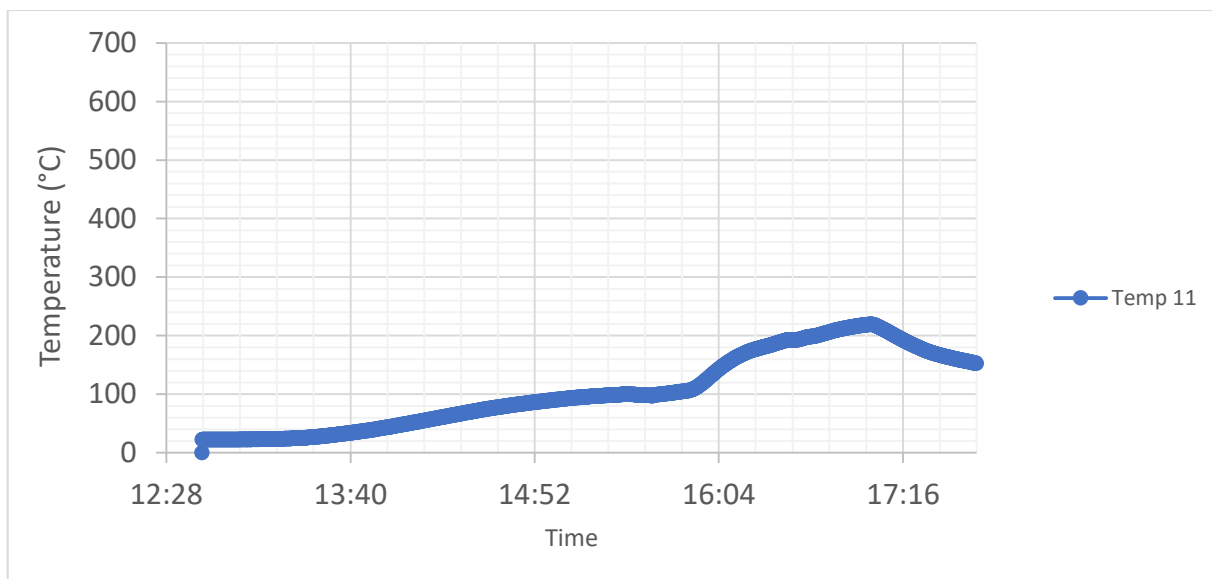


Figure 5.10 Experimental results of temperature of the insulated pipe when there is gas flow and not.

According to the results of this experiment, it is possible to say that the steel pipes installed with this layer of insulator are good, because it is necessary 1 hour of gas flow inside of the pipe to achieve 220°C, while the normal duration of the experiments with fuel in this reactor is 15-30 min. Therefore, it is never achieved a temperature higher than the safe temperature of 200°C and the unwanted substances like tar can condensate in the oil of the scrubbers, as well that the vitryl pipes cannot be destroyed for high temperatures.

Finally, the decision was to install steel pipes with a length of 19 cm in the three different levels of the riser. Besides, all of them were covered with 2,5 cm thick insulation, so that the temperatures at the end of the pipes and before the tar traps were over 100°C.

5.2 Tar Trap

After the length of the steel pipe has been chosen and the insulator too, the next equipment in the multilevel sampling system is the tar trap. The tar trap is the equipment that removes tar from the gas flow in order to avoid clogging. In addition, when the experiment has finished the tar can be taken from the trap for analysis of its composition.

There are different options for tar removal like scrubbers, ceramic filters, catalytic filters, etc. However the chosen solution for the tar removal is a scrubber. The tar trap consists of a bottle (500 ml) with a liquid absorbent inside, where the gas flow enters into the bottle and flows through the absorbent. The gas flow then continues going up to where it is sucked by the gas analyser pump through a pipe. The tar is detained in the liquid and after an experiment, the absorbent with the tar can be removed from the bottle and analysed. Figure 5.11 shows the bottle used as a scrubber in this work.



Figure 5.11 Bottle used in this work like scrubber.

There are many different substances that can be used as absorbents in scrubbers. For example (Good et al., 2005) collected tar by condensation and absorption in isopropanol, which was found to be the most suitable solvent. In (Good et al., 2005) tar collection is done in 6 impinger bottles with isopropanol, in which water and tar are stripped from the process gas by absorption in isopropanol. The heat released is removed in an external water bath. Figure 5.12 shows the method used in their experiments.

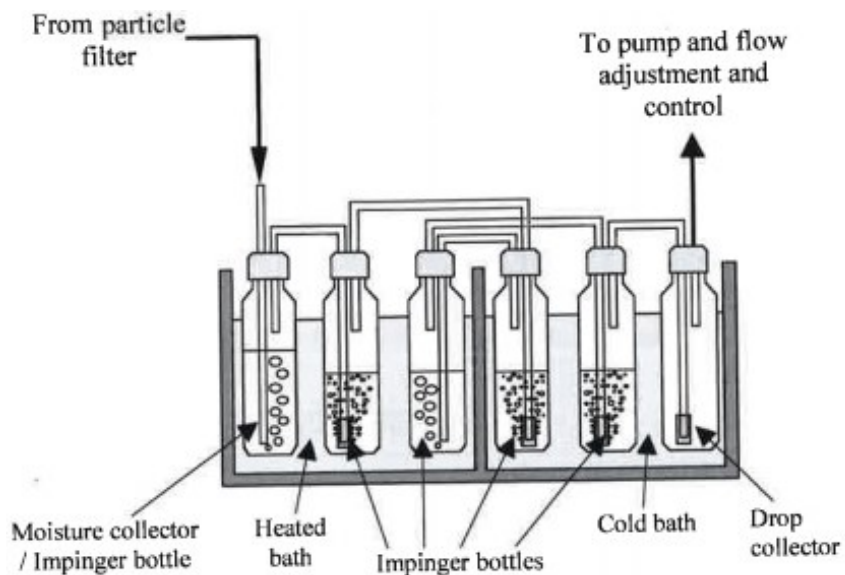


Figure 5.12 Tar collection using isopropanol (Good et al., 2005).

According to (Nakamura et al., 2016) and (Phuphuakrat et al., 2011), oil is a good absorbent because it is a non-polar substance, so tar is not soluble in oil and it can be separated easily from the oil. In water, the results are the opposite because the tar is soluble in water and if it is necessary to separate both of them in order to analyse tar, which is very difficult.

One problem that the oil can cause in the system is that the pressure losses become too high and an additional pump has to be installed. However, a test was conducted in order to predict the pressure losses in the scrubber. For that the bottle was connected to the gas analyser and its pumping unit and filled with different amount of oil. The results from the test are shown in Table 5.3.

Table 5.3 Pressure losses experiment with oil scrubber.

| Gas Flow Q (l/min) | Oil Volume (ml) |
|--------------------|-----------------|
| 1,55 | Without bottle |
| 1,5 | 0 |
| 1,5 | 100 |
| 1,5 | 200 |
| 1,5 | 300 |
| 1,5-1,45 | 400 |

Table 5.3 shows that the changes of the gas flow in the bottle caused by the use of oil scrubbers are negligible. Therefore, an additional pump is not needed and the oil scrubbers are going to be used for the tar removal in this Master's Thesis.

The next equipment installed in the multilevel sampling system are the pressure and solenoid valves that control from which level the gas analyser measures the gas composition. These valves are explained in the next chapter.

5.3 Solenoid and Pressure Valves

After the tar trap there are three pressures valves, which control from what part of the reactor the gas is taken for analysis. The valves used in this Master's Thesis are pressure operated valves with a stainless steel body and threaded PN40 ports from the company ASCO (model E298). Besides each pressure valve has one solenoid valve also from the company ASCO (model E314) that controls when the pressure valve has to open and close. The main properties of these pressure valves are shown in Figure 5.13 and a scheme of the valves is shown in Figure 5.14.

GENERAL

| | |
|-----------------------------------|---|
| Differential pressure | 0 to 40 bar [1 bar =100 kPa] |
| Maximum allowable pressure | 40 bar (within the specified limits, see diagram 1) |
| Ambient temperature range | -25°C to +180°C |
| Maximum viscosity | 5000 cSt (mm ² /s) |
| Pilot fluid | Air |
| Max. pilot pressure | 10 bar |
| Min. pilot pressure | See below |

| fluids (*) | temperature range | disc seal (*) |
|---|-------------------|---------------|
| DN 15-20-25: air and gas groups 1 & 2 DN 32-40-50: air and gas group 2 all DN: water, oil, liquids groups 1 & 2 and steam | - 10°C to + 250°C | bronze PTFE |

Figure 5.13 Properties of the solenoid valves.

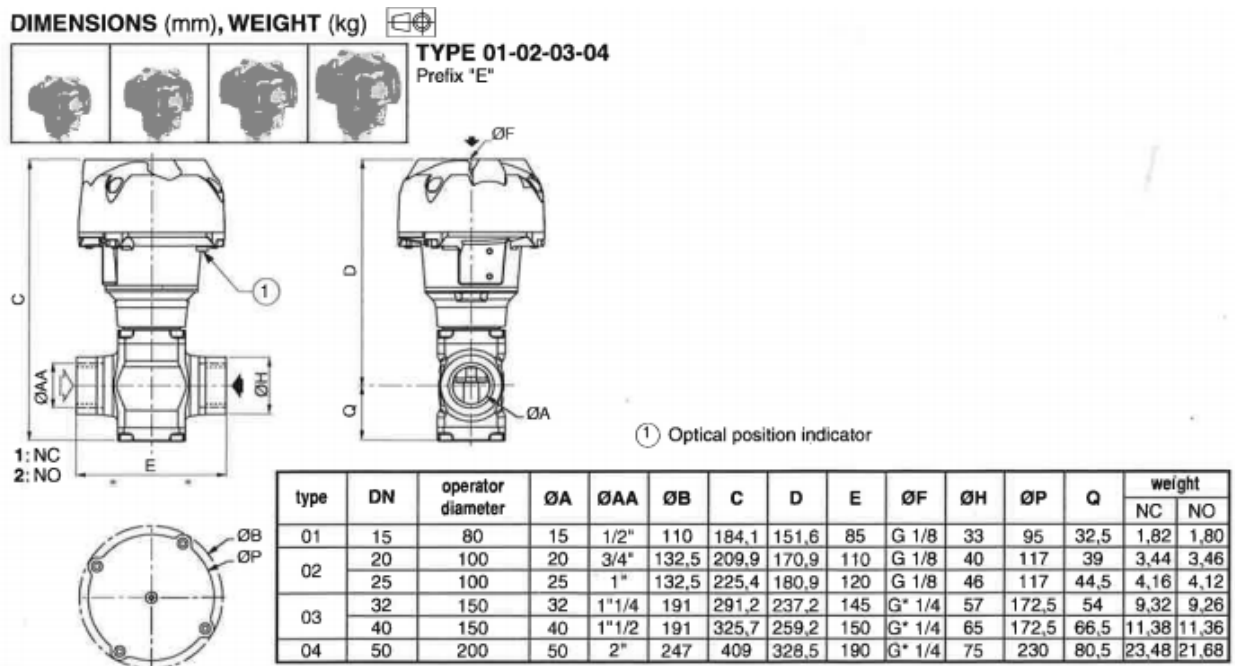


Figure 5.14 Diagram of the solenoid valves.

The size of the chosen solenoid valves is a nominal diameter (DN) of 15 mm or ½ inches. The maximum temperature that the solenoid valves can resist is 250°C, this was taken into account in the heat transfer calculations explained in chapter 4.1, and for this reason these pressure valves have been chosen. These valves were suitable as they can withstand flows with humidity.

The solenoid valves, which control the pressure valves, are shown along with some of their properties in Figure 5.15 and Figure 5.16.



Figure 5.15 Solenoid valves.

CONSTRUCTION

| MATERIALS IN CONTACT WITH FLUID | | |
|---|----------------------------|---------------------------|
| (*) Ensure that the compatibility of the fluids in contact with the materials is verified | | |
| Body | Brass | Stainless steel, AISI 304 |
| Shading coil | Copper | Silver |
| Core tube | Stainless steel, AISI 305 | |
| Core and pluggnut | Stainless steel, AISI 430F | |
| Springs | Stainless steel, AISI 302 | |
| Seals | NBR | |
| Disc | NBR | |
| Upper disc | FPM | |
| Core guide | POM | |

ELECTRICAL CHARACTERISTICS

| | |
|---------------------------------------|--|
| Coil insulation class | F |
| Connector | Spade plug (cable Ø 6-10 mm) |
| Connector specification | ISO 4400 / EN 175301-803, form A |
| Electrical safety | IEC 335 |
| Electrical enclosure protection | Moulded IP65 (EN 60529) |
| Standard voltages | DC (=) : 24V - 48V |
| (Other voltages and 60 Hz on request) | AC (~) : 24V - 48V - 115V - 230V/50 Hz |

| operator ambient temperature range (TS) (°C) | power ratings | | | | replacement coil | |
|--|---------------------|--------------------------|------|----------------------|------------------|--------------|
| | inrush ~ (VA) | holding ~ (VA) (W) | | hot/cold = (W) | ~ 230 V/50 Hz | = 24 V DC |
| | | 25 | 10,1 | | | |
| -25 to +55 | 50 | 25 | 10,1 | 8,5/11,6 | 238613-059 | 238713-006 |

Ergonomics reserves v2.0

Figure 5.16 Properties of the solenoid valves

Figure 5.17 shows the connection between the solenoid and pressure valves. The solenoid valves are connected by electrical cables to an optocoupler.

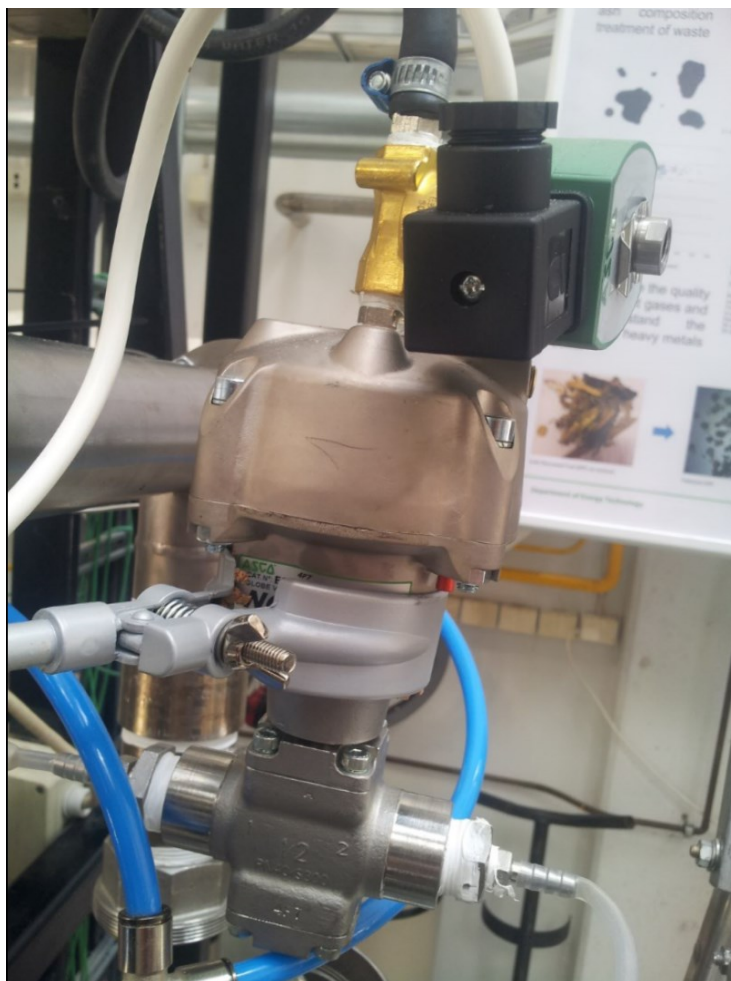


Figure 5.17 Solenoid and pressure valves assembled.

The optocoupler, which was made in house, is connected to a LabVIEW card, and this card is connected to a computer. The optocoupler has 3 LEDs that shows which valve is opened and another LED that shows when all the valves are closed. It is possible to control the time that each valve is opened or closed with the computer and the electronic control system (optocoupler and LabVIEW card). Figure 5.18 shows the optocoupler and its power supply.

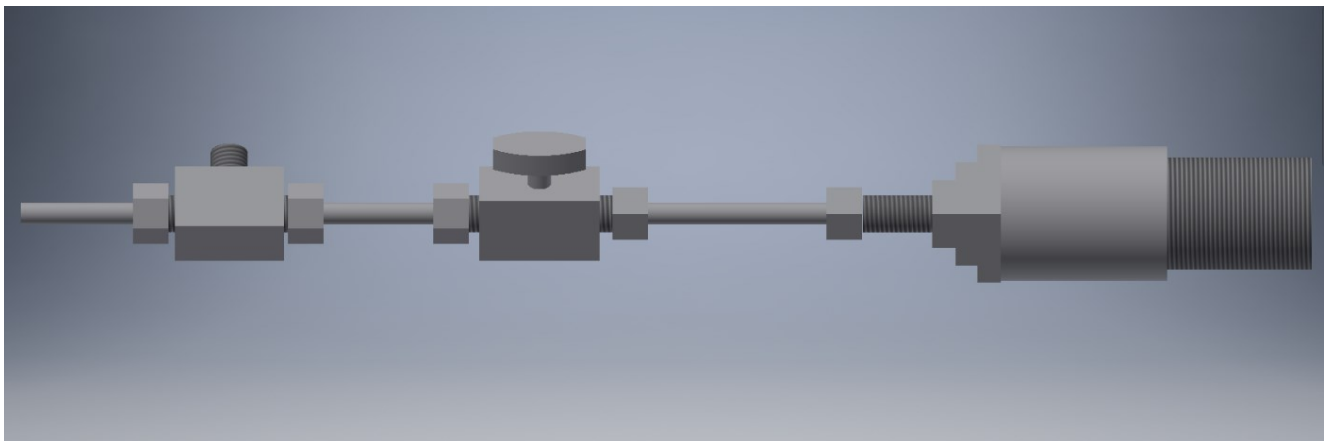


Figure 5.18 Optocoupler and power supply of the electronic control system for solenoid valves.

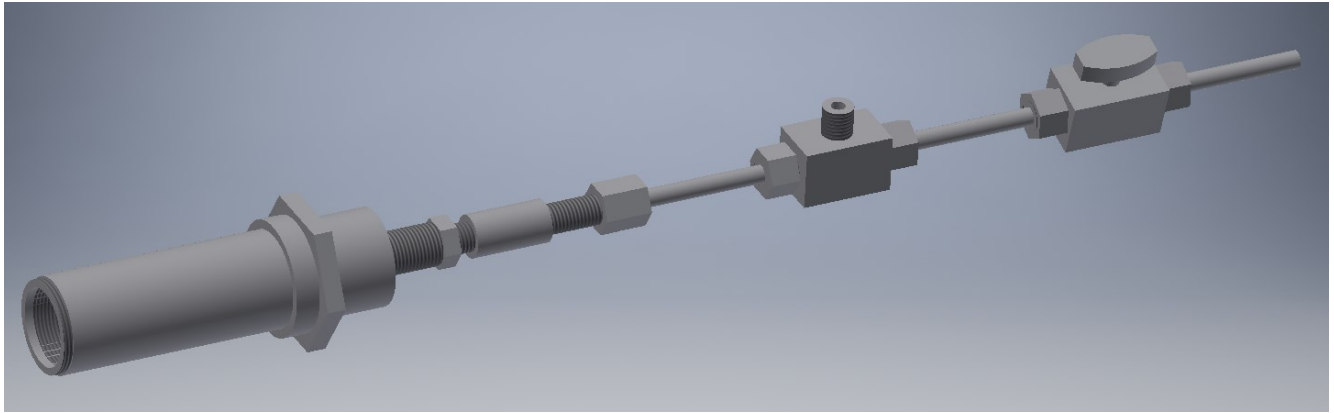
6 Test and Validation

6.1 Residence Time Test

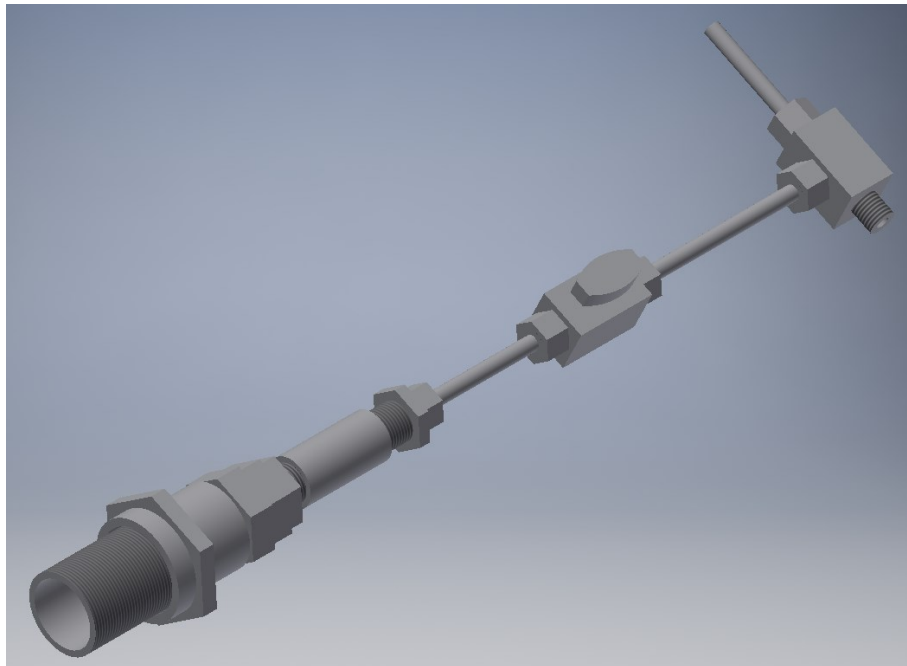
After steel pipes, solenoid valves and oil scrubbers have been connected to the reactor, the next step is to calculate the residence time of the gas going from the reactor to the gas analyser in each level of the multilevel gas sampling system. The residence time should preferably be the same in all levels of the sampling system. Therefore, the volume of the three levels should also be the same in all the levels. For this reason the length and diameter of each component of the three levels are measured and the total volume of each level is calculated. Figure 6.1 shows the three different levels of the sampling system.



a) Level 1 of the multilevel sampling gas system.



b) Level 2 of the multilevel gas sampling system.



c) Level 3 of the multilevel gas sampling system.

Figure 6.1 Levels of the multilevel gas sampling system.

The measurements of the length, diameter and the calculated volume using Equation (6.1) in each component are shown in Table 6.1. The total volume of each level of the sampling system is also shown in Table 6.1.

$$V = \frac{D^2 * \pi}{4} * L \quad (6.1)$$

Where:

V is the volume of the component of the pipe in cm^3 ,

D is the diameter of the component of the pipe in cm,

L is the length of the component of the pipe in cm.

Table 6.1 Volume of each component in the three levels and the total volume of the each level in the multilevel gas sampling system.

| Level 1 | | | |
|------------------|--------------------|----------------------|--|
| Component | Length (cm) | Diameter (cm) | Volume (cm^3) |
| 1 | 3,86 | 2,03 | 12,49 |
| 2 | 2,14 | 2,25 | 8,51 |
| 3 | 0,53 | 1,48 | 0,91 |
| 4 | 3,87 | 0,78 | 1,85 |
| 5 | 2,53 | 0,47 | 0,44 |
| 6 | 4,07 | 0,38 | 0,46 |
| 7 | 2,35 | 0,38 | 0,27 |
| 8 | 4,1 | 0,38 | 0,46 |
| 9 | 2,59 | 0,38 | 0,29 |
| 10 | 3,95 | 0,38 | 0,45 |
| 11 | 2,44 | 0,4 | 0,31 |
| 12 | 1,93 | 0,4 | 0,24 |
| | 34,36 | | 26,69 |

| Level 2 | | | |
|------------------|--------------------|----------------------|--|
| Component | Length (cm) | Diameter (cm) | Volume (cm^3) |
| 1 | 3,86 | 2,03 | 12,49 |
| 2 | 0,13 | 2,42 | 0,60 |
| 3 | 1,27 | 1,79 | 3,20 |
| 4 | 1,15 | 1,15 | 1,19 |
| 5 | 2,26 | 0,5 | 0,44 |
| 6 | 6,16 | 0,38 | 0,70 |
| 7 | 2,59 | 0,38 | 0,29 |
| 8 | 4,66 | 0,38 | 0,53 |
| 9 | 2,35 | 0,38 | 0,27 |
| 10 | 3,96 | 0,38 | 0,45 |
| 11 | 1,68 | 0,4 | 0,21 |
| 12 | 5,12 | 0,4 | 0,64 |
| | 35,19 | | 21,02 |

| Level 3 | | | |
|-----------|--------------|---------------|---------------------------|
| Component | Length (cm) | Diameter (cm) | Volume (cm ³) |
| 1 | 3,86 | 2,03 | 12,49 |
| 2 | 0,49 | 2,42 | 2,25 |
| 3 | 0,57 | 1,83 | 1,50 |
| 4 | 0,76 | 1,51 | 1,36 |
| 5 | 3,88 | 0,89 | 2,41 |
| 6 | 0,14 | 1,15 | 0,15 |
| 7 | 2,28 | 0,47 | 0,40 |
| 8 | 4,57 | 0,38 | 0,52 |
| 9 | 2,59 | 0,38 | 0,29 |
| 10 | 6,1 | 0,38 | 0,69 |
| 11 | 2,34 | 0,38 | 0,27 |
| 12 | 3,8 | 0,38 | 0,43 |
| 13 | 0,53 | 0,4 | 0,07 |
| 14 | 0,51 | 0,4 | 0,06 |
| | 32,42 | | 22,89 |

According to Table 6.1, the volume in the three levels is not the same. Therefore plastic pipes made of vitryl were installed after the solenoid valves to have the same volume in the three levels. Since the level 1 shown in Table 6.1 has the biggest volume, the extra length of plastic pipe needed for levels 2 and 3 can be calculated with Equation (6.2).

$$L = \frac{\Delta V * 4}{\pi * D^2} \quad (6.2)$$

Where:

L is the extra length of the plastic pipe in cm,

ΔV is the difference of volume between 2 levels of the sampling system in cm³,

D is the diameter of the plastic pipe in cm, in this case is 4 mm.

The results of the length of the plastic pipes needed in levels 2 and 3 are shown in Table 6.2.

Table 6.2 Length needed of plastic pipe in each level in order to ensure the same volume in the three levels of the multilevel gas sampling system.

| | Level 1 | Level 2 | Level 3 |
|--|---------|---------|---------|
| Volume (cm ³) | 26,69 | 21,02 | 22,89 |
| Difference to level 1 (cm ³) | - | 5,67 | 3,79 |
| Extra length needed of plastic pipe (cm) | - | 45,1 | 30,2 |

According to Table 6.2, level 2 needs a plastic pipe of 45 cm and level 3 of 30 cm longer than the pipe on level 1 to ensure equal volume for all levels.

6.1.1 Residence Time Test with CO

Once that the same volume has been ensured in the three levels of the sampling system, the next step is to test that the residence time really is the same in the three levels (step input method, chapter 2.4). For that experiments were done with CO. In these experiments the three levels of the sampling system were connected to a pressurized CO bottle (225ppm) and to the gas analysers. By checking the time that the CO flow takes to arrive to the gas analysers, it is possible to estimate the residence time in each level of the sampling system. Figure 6.2 shows how the levels were connected in the test to the pressurized CO bottle and the gas analysers.



Figure 6.2 CO Concentration test.

In the first experiment the three levels were connected to a Siemens ULTRAMAT 23 gas analyser. The CO flow was controlled and measured all the time in the experiment with a rotameter. The flow was 1,5 l/min but with an air rotameter, so first it needs to be converted into CO flow with Equation (6.3).

$$Q_{co} = \frac{\rho_{air} * Q_{air}}{\rho_{co}} = \frac{1,2 * 1,5}{1,17} = 1,53 \text{ l/min} \quad (6.3)$$

Where:

Q_{co} CO flow in l/min,

ρ_{co} CO density in kg/m³ at (20°C and 1 atm),

Q_{air} air flow in l/min,

ρ_{air} air density in kg/m³ at (20°C and 1 atm).

The flow was air with 225 ppm of CO in it, so the minimal difference in density and therefore in gas flow could be neglected.

In this way CO the flow is very similar to the gas flow in a real test in the reactor. After controlling the gas flow, the concentration of CO was measured in the three levels and the measured residence time in level 1, 2 and 3 are shown Figure 6.3.

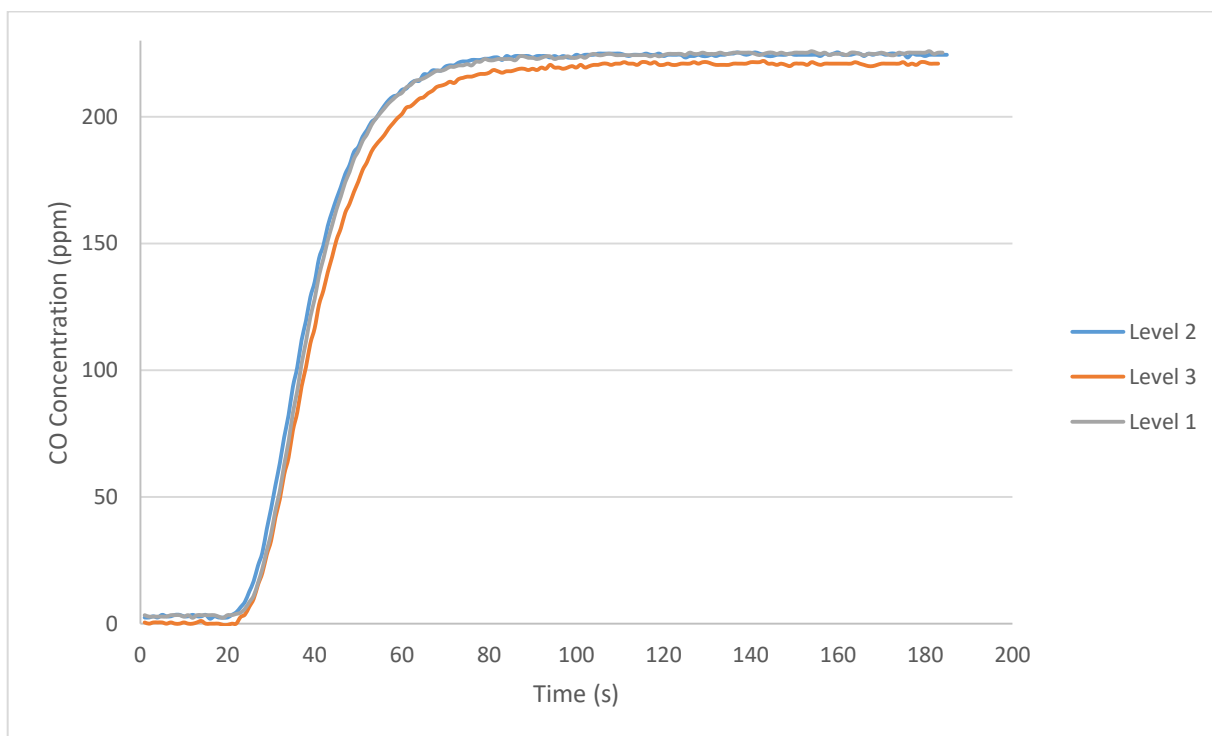


Figure 6.3 Results of the residence time test in ULTRAMAT gas analyser with CO concentration in the three levels of the sampling system.

In Figure 6.3, it is possible to see that the residence time is almost the same in the three levels of the sampling system. There is a small difference in the level 3 but it can be solved because 40 cm extra of plastic pipe was connected in each level in order to adjust the residence time.

In addition to finding out that the residence time is the same in the three levels of the sampling system, it is also possible to deduce the transitional and the delay time in each level. For example in Figure 6.4 it is possible to see that with a CO flow of 1,53 l/min, the gas analyser starts to detect non zero CO concentration after 21 seconds. Besides, it is possible to see that the transitional time is over 75 seconds, i.e, the gas takes 75 seconds to arrive to steady time.

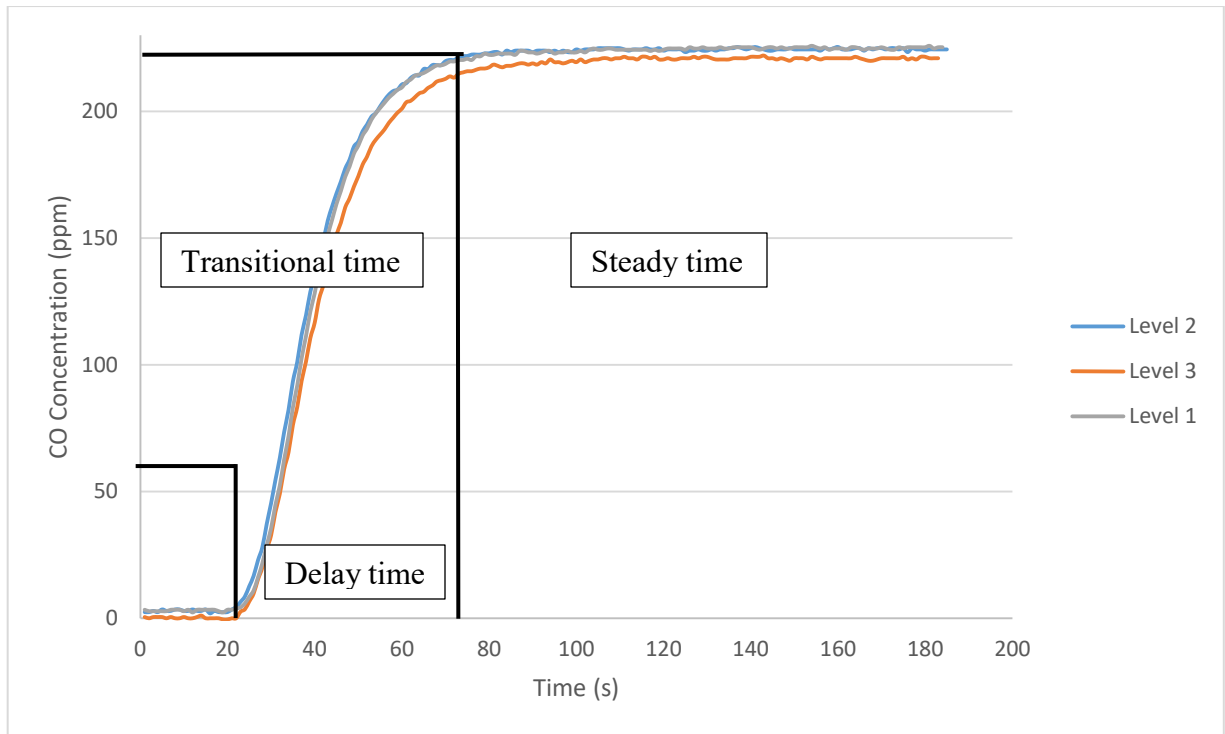


Figure 6.4 Transitional, steady and delay time in the three levels of the multilevel gas sampling system.

The next experiment was to repeat the same test but using the Dx-4000 GASMET gas analyser instead of the Siemens ULTRAMAT 23 gas analyser. The CO flow was 1,53 l/min again, and the results from this experiment are shown in Figure 6.5.

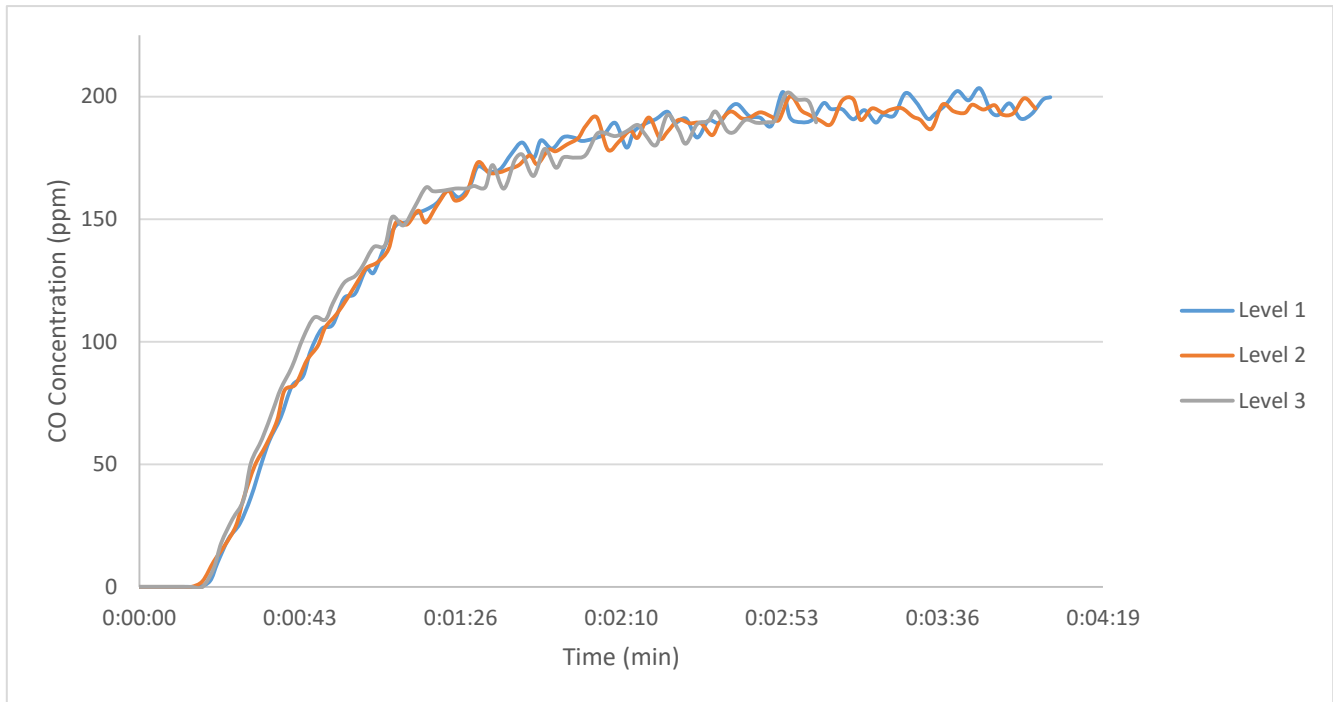


Figure 6.5 Results of the residence time in GASMET gas analyser with CO concentration in each level of the multilevel gas sampling system.

In Figure 6.5 it is possible to see that the maximum concentration of CO is barely over 200 ppm instead of 225 ppm (pressurized CO bottle). This is because of the analyser needs to be recalibrated, as well the pump of the gas analyser needs to be repaired because the pumping problems causes fluctuations in the measurements (Figure 6.5). Nevertheless it does not influence the test and results.

In Figure 6.5, it is possible to see that the residence time was also the same in the three levels of the sampling gas system. In this case the delay time was 18 seconds, which is shorter than in the case of the other analyser (different internal structure of the gas analyser), where the delay time was 20 seconds (Figure 6.4).

On the other hand, the transitional time is over 140 seconds, while in the other analyser it is only 80 seconds (Figure 6.4). The transitional, delay and steady time of the gas in this experiment with Dx-4000 GASMET gas analyser are shown in Figure 6.6.

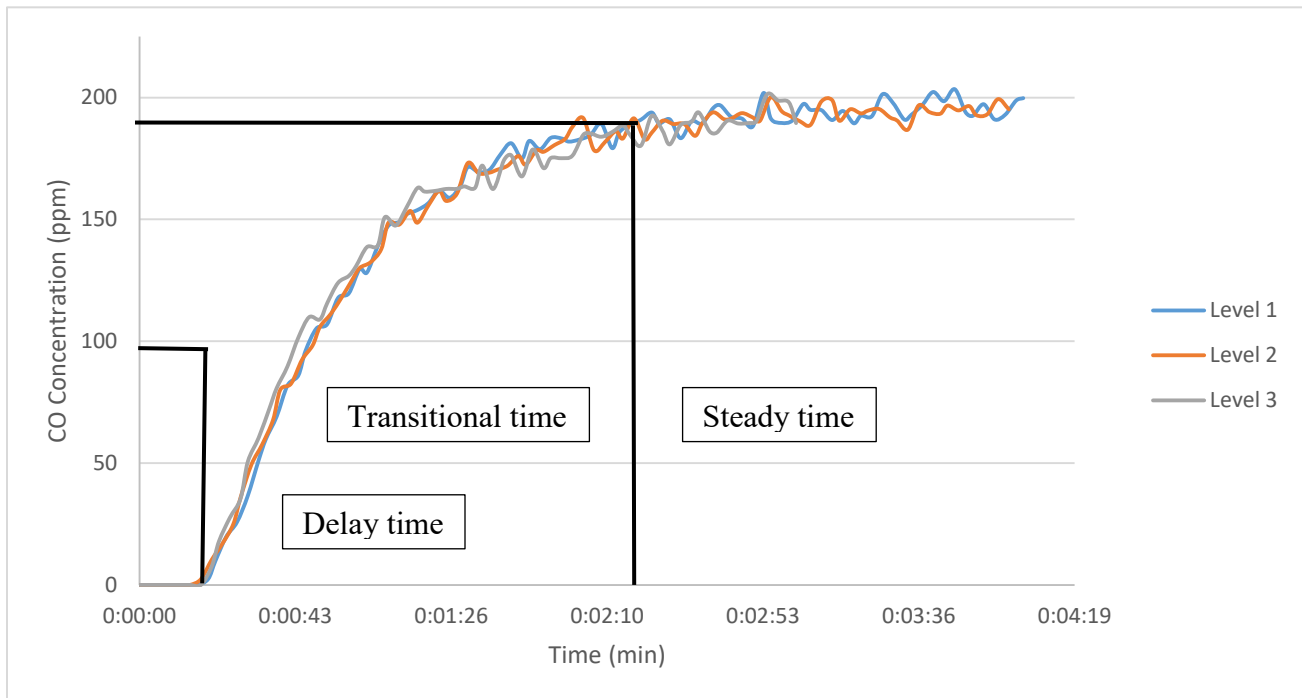


Figure 6.6 Transitional, steady and delay time in GASMET analyser in the CO concentration test.

The delay time with a CO flow of 1,53 l/min was 18 seconds, and the transitional time 140 seconds. The delay time is very similar in both analysers, Siemens ULTRAMAT 23 and Dx-4000 GASMET. However the transitional time, and so the time that it takes to reach a steady state after the solenoid valve is opened, is longer for the GASMET analyser than the ULTRAMAT analyser. Figure 6.7 shows the results of the two experiments together.

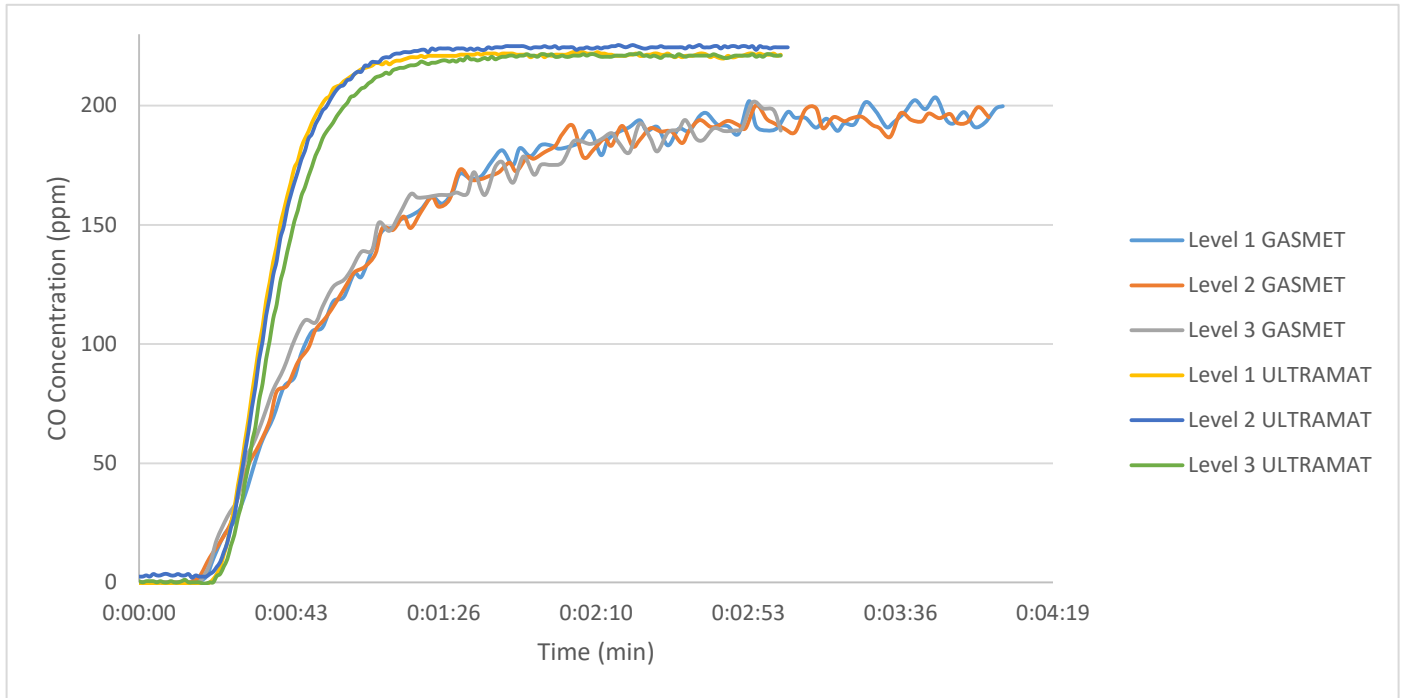


Figure 6.7 Comparison of both gas analysers in the CO concentration test.

Finally, it is possible to see that the delay time is almost the same in both analysers, in the case of ULTRAMAT analyser is 20 seconds and in GASMET analyser the delay time is 18 seconds. However the transitional time is different in each analyser, since in ULTRAMAT analyser the transitional time is 80 seconds and in GASMET analyser is over 140 seconds because of the internal structure and the working of the analysers are different.

The next step is to estimate the delay time theoretically in order to check if the volumes calculated in chapter 6.1 of each level and the experiments with CO are coherent. The volume of the different parts of one level of the sampling gas system is shown in Table 6.3.

| | Steel pipe | Oil scrubber | Solenoid valve | Plastic pipe | Analyser heating pipe | Total | Oil | Total gas volume |
|--------------------------------|------------|--------------|----------------|--------------|-----------------------|--------|-----|------------------|
| Volume (cm³) | 26,69 | 700 | 12,24 | 19,17 | 62,83 | 820,93 | 300 | 520,93 |

The total volume that the gas can fill is 520 cm³. With Equation (6.4), it is possible to calculate the delay time that the gas takes to arrive from the reactor to the gas analyser.

$$t = \frac{V}{Q} \quad (6.4)$$

Where:

t is the delay time,

V is the volume of the level,

Q is the volumetric gas flow.

Finally, with a volumetric gas flow of 1,5 l/min, as in the step input tests, the delay time is:

$$t = \frac{0,52093}{1,5} * 60 = \mathbf{20,8\ s}$$

The estimated value of the delay time is almost the same than the value obtained from the experiments with both gas analysers, Siemens ULTRAMAT 23 and Dx-4000 GASMET (Figure 6.3 and Figure 6.5). Therefore it is possible to say that the results of the measured volume of the levels and the obtained results from the experiments with CO flow are correct.

6.2 Valve Controlling Algorithm

Based on the results from the experiments the delay time has been estimated, the next step is to find out the transitional time that in one level the solenoid valve has to wait to and the analyser can start to measure the gas composition reliably from the next level.

Figure 6.4 and Figure 6.6 show that, the transitional time is over 80 seconds in Siemens ULTRAMAT 23 analyser and 140 s in Dx-4000 GASMET. Therefore the transitional time has to be over 80, i.e, the solenoid valve can open after 80 s if the ULTRAMAT analyser is connected to the multilevel sampling gas system, or 140 s if GASMET analyser is connected. Another important point is that after the solenoid valve of one level closes the gas analyser continues measuring for 140 s the gas composition of that level in the case of ULTRAMAT analyser, as it is shown in Figure 6.8.

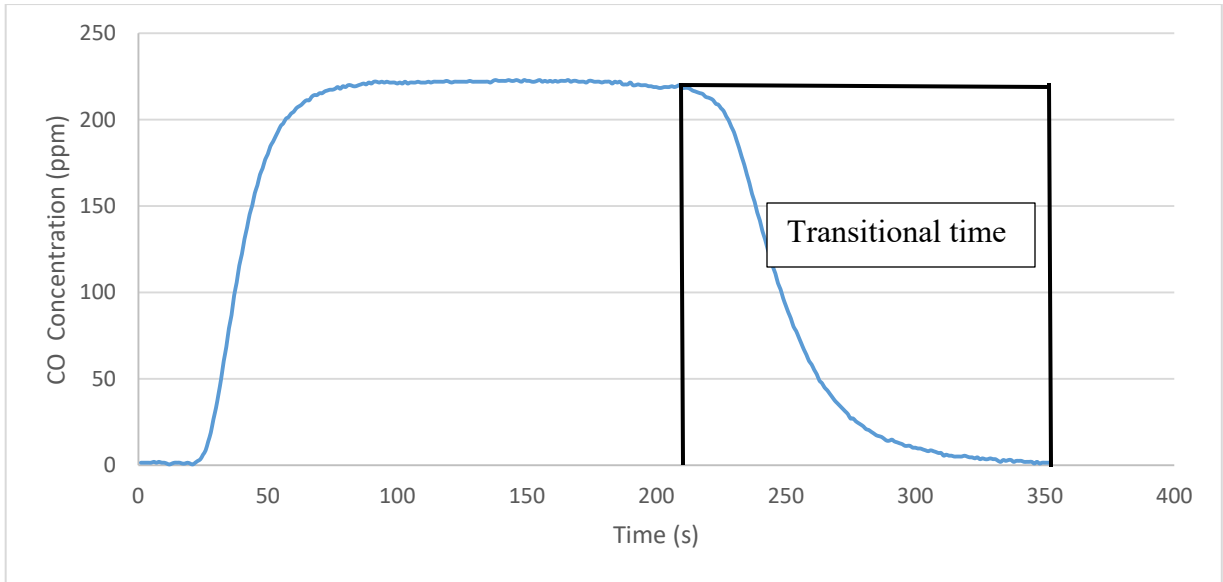


Figure 6.8 Transitional time in ULTRAMAT gas analyser after close the solenoid valve.

After these 140 seconds the gas analyser has been cleaned from all the substances from that level and it is ready to measure another level. Therefore, the most important is to know if with 80 seconds of transitional time, the gas analyser is ready to measure one level after it has measured another level before. Figure 6.9 shows that a delay time of 80 seconds is enough.

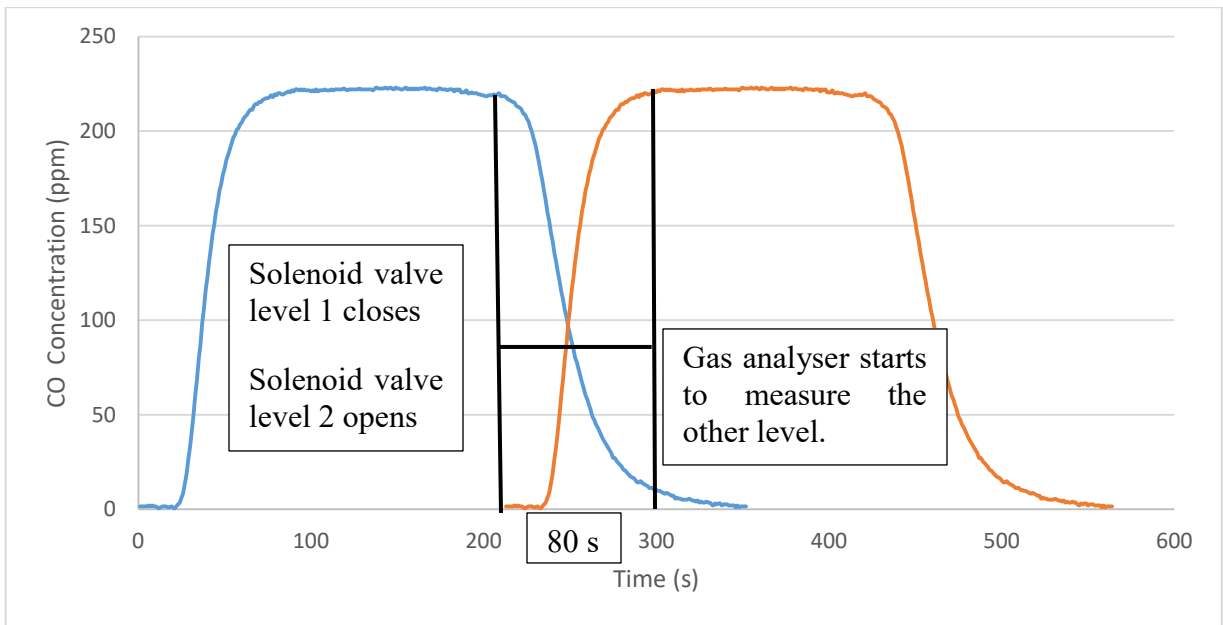


Figure 6.9 Transitional time between 2 levels with ULTRAMAT gas analyser.

According to Figure 6.9, 80 seconds as transitional time is enough because the amount of substance remaining in the system that the gas analyser measures when it is measuring a new level is neglectable.

In the GASMET analyser case, the gas analyser continues measuring the gas composition from the previous level during 114 seconds, as shown in Figure 6.10.

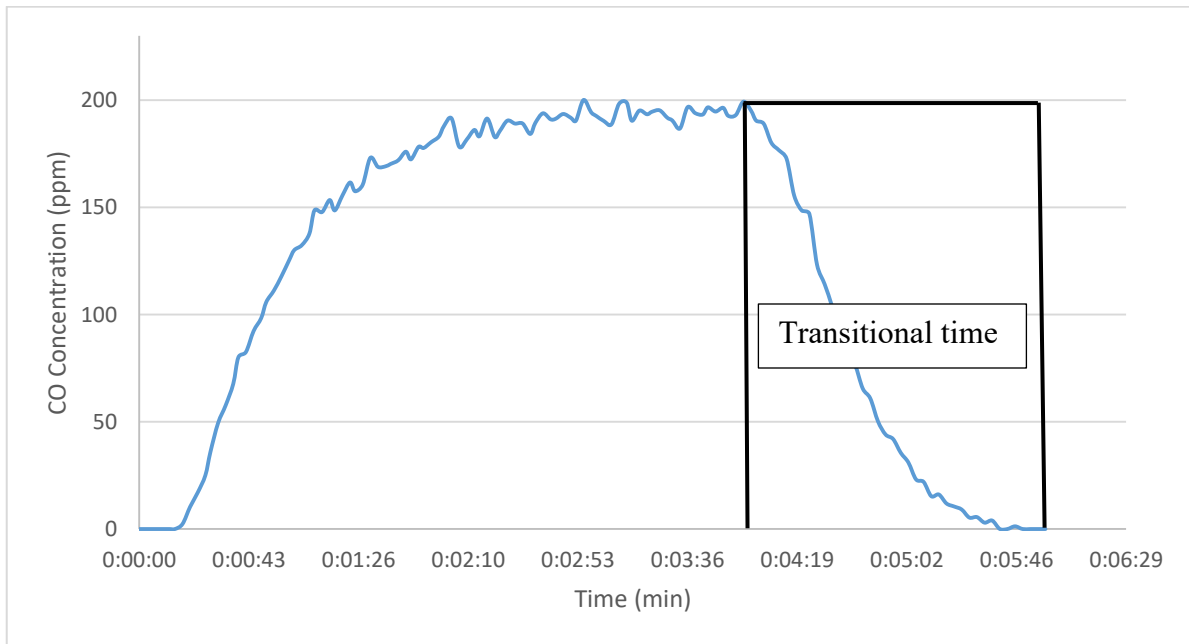


Figure 6.10 Transitional time after close solenoid valve GASMET gas analyser.

In this case, the transitional time to clean the gas analyser is 114 seconds. Therefore it is not necessary to check if the analyser will be ready to start to measure another level, because the transitional time to clean the analyser is 114 seconds, while the transitional time to start to measure the gas composition is 140 seconds. Figure 6.11 illustrates an example of this.

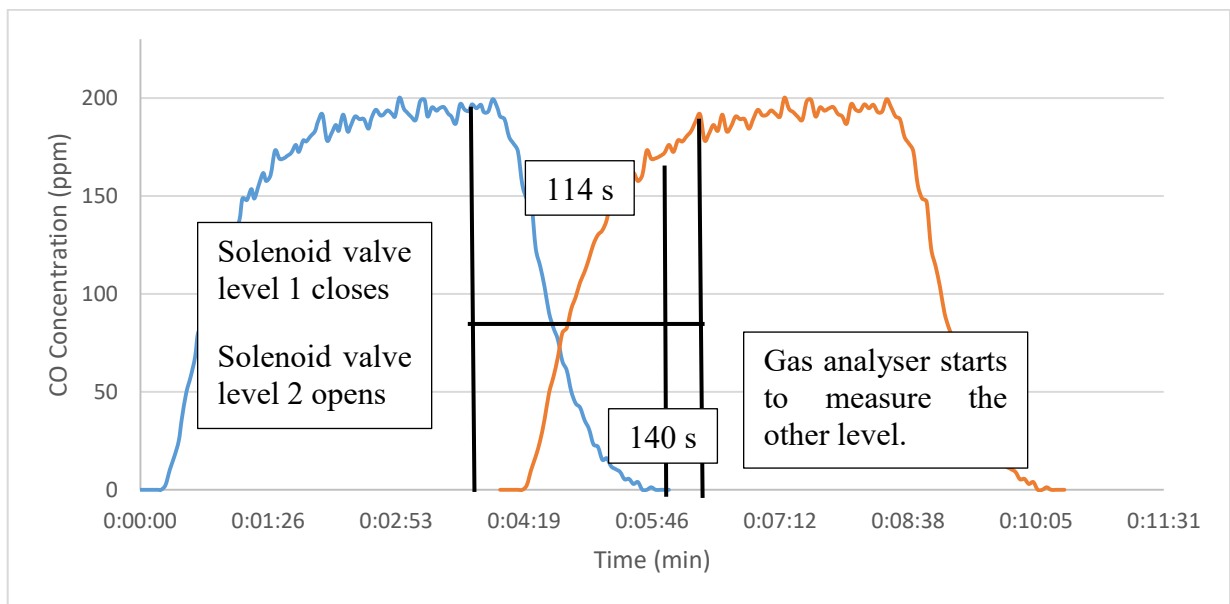


Figure 6.11 Transitional time between two levels with GASMET gas analyser.

Figure 6.11 shows that the time the analyser needs to be cleaned from the previous level is less than the transitional time to start measuring the next level. Therefore, 140 seconds of transitional time is the minimum time a valve should be opened.

In conclusion, the transitional time that the ULTRAMAT analyser has to wait to start to measure is 80 seconds, so when a solenoid valve is opened, the gas analyser has to wait 80 seconds to start to measure, and when that solenoid valve is closed and another valve from another level is opened, the gas analyser needs to wait again other 80 seconds to measure the new level. Figure 6.12 shows an example of the time needed for the gas analyser takes to start measuring the next level reliably.

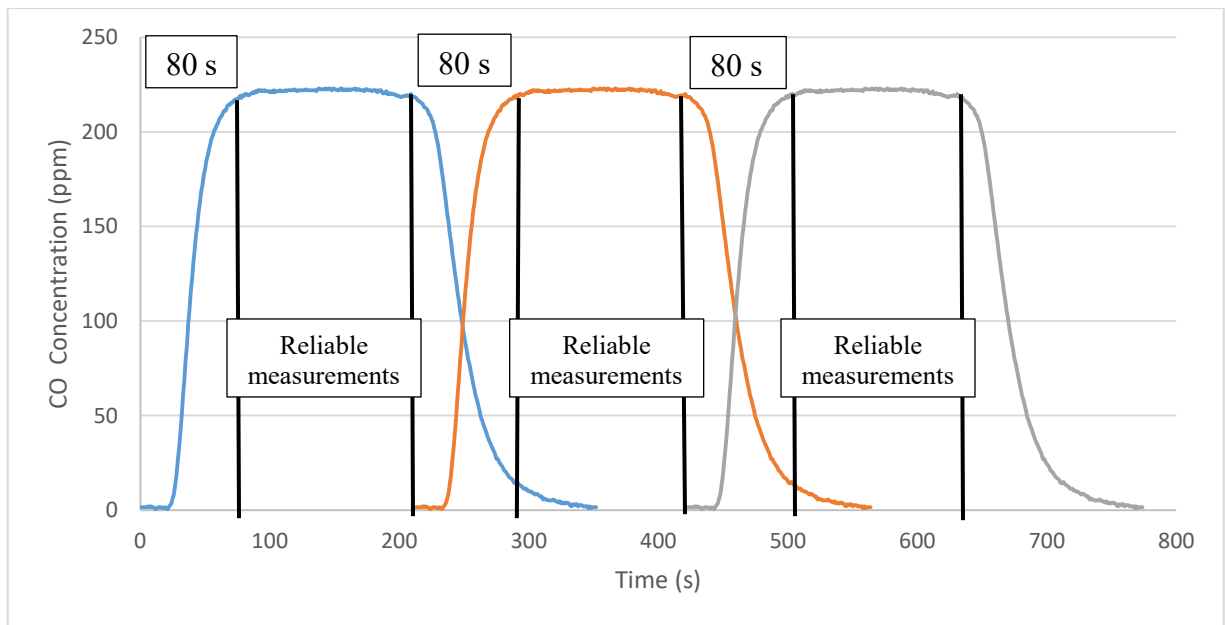


Figure 6.12 Reliable measurements and transitional times of the three levels with ULTRAMAT gas analyser.

Similarly for the GASMET gas analyser the transitional and delay time that the analyser has to wait for analysing the gas composition of another level of the multilevel sampling gas system is 140 seconds. Figure 6.13 shows an example.

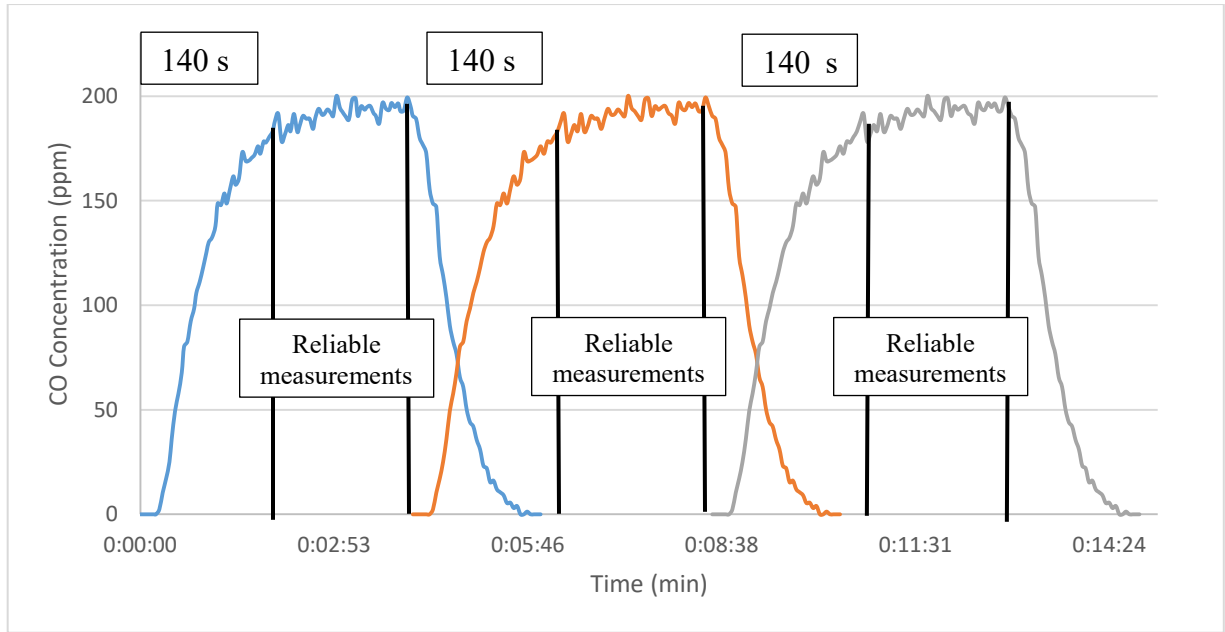


Figure 6.13 Reliable measurements and transitional times of the three levels with GASMET gas analyser.

In Figure 6.13 and Figure 6.12, the value of the reliable measurements have been taken when the CO concentration reached 95% of the steady state value.

Overall, the transitional time for Siemens ULTRAMAT 23 gas analyser is 80 seconds at the beginning of a real test in the reactor and among different levels of the multilevel sampling gas system, while the transitional time for Dx-4000 GASMET gas analyser is 140 seconds.

6.3 Cycles of Measurements with the Sampling Gas System

Once that the transitional time has been estimated, the next step is to decide how many cycles of measurements can be taken with the sampling gas system in one real test in the CFB.

In chapter 6.2 it was concluded that 80 seconds is the minimum transitional and delay time of waiting when changing levels, with the Siemens ULTRAMAT gas analyser and 140 seconds with the Dx-4000 GASMET gas analyser. Apart from transitional time, it is also necessary additional time for reliable measurements in each level (steady time).

The duration of one test in the CFB is 30 min, in the case of ULTRAMAT gas analyser one feasible algorithm for the numbers of cycles in each level to control the valves might be as it is shown in Figure 6.14.

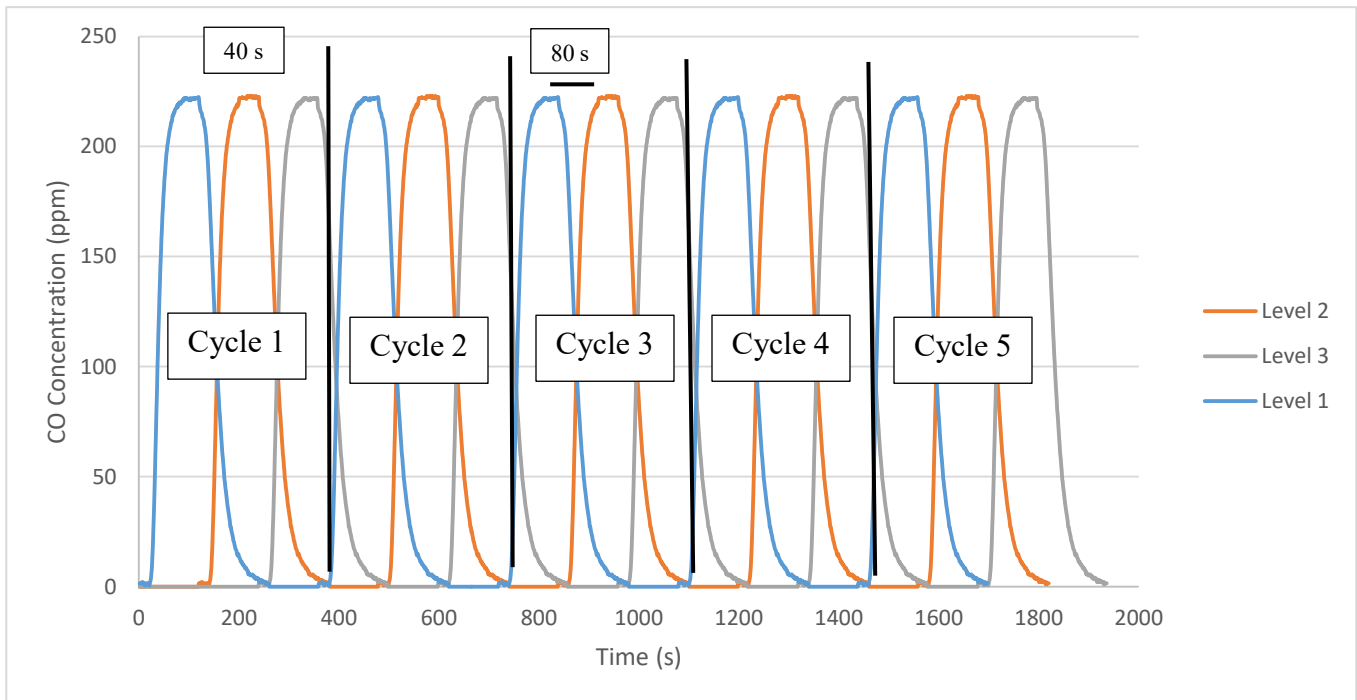


Figure 6.14 Five different cycles of measurements with ULTRAMAT gas analyser in the three levels.

In this case, it is possible to do 5 cycles, waiting 80 seconds for transition between levels followed by 40 seconds of reliable measurements. Therefore it is necessary to use 120 seconds per level, i.e, 360 seconds per cycle.

For the GASMET gas analyser, a feasible algorithm for controlling the valves is shown in Figure 6.15.

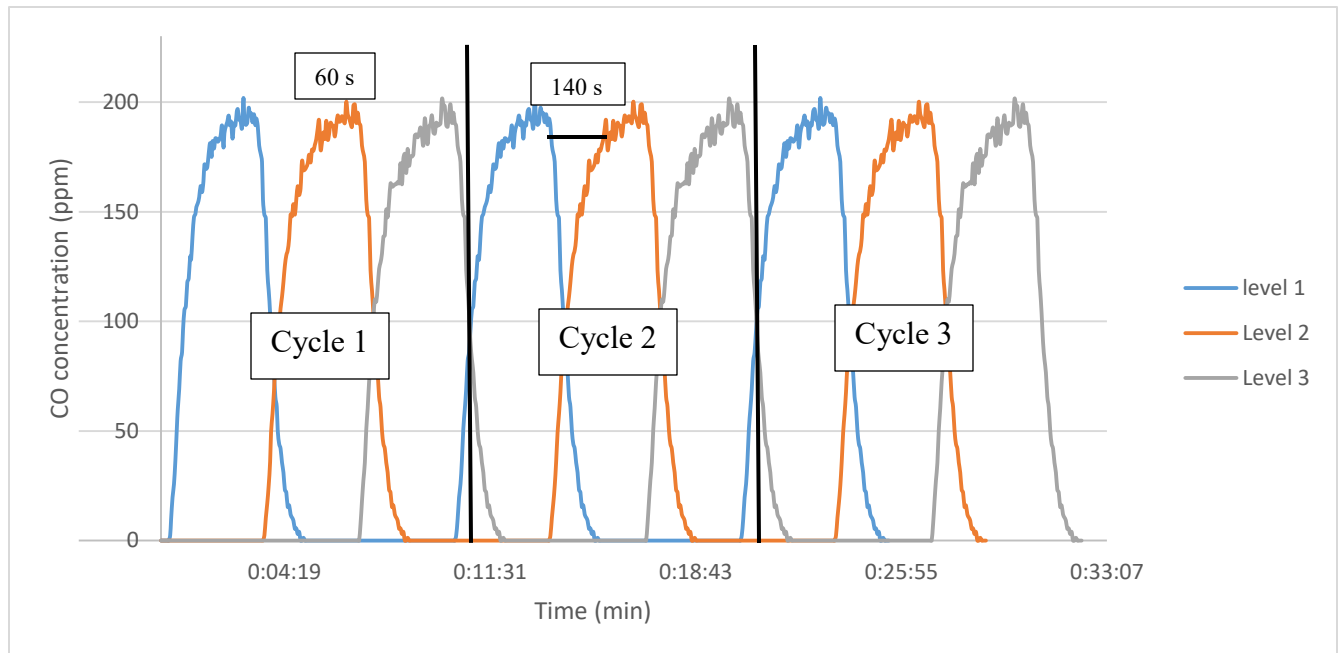


Figure 6.15 Three different cycles of measurements with GASMET gas analyser of the three levels.

In this case, it is possible to do only 3 cycles in each level of the sampling gas system. In each level, there are 140 seconds of transitional time, and 60 seconds of steady time when reliable measurements are taken with the gas analyser.

In conclusion, with ULTRAMAT gas analyser it is possible to do 5 cycles of measurements per level and with GASMET gas analyser, it is only possible to do 3 cycles because the transitional time is longer. The next step is to test the multilevel gas sampling system in a real tests with the CFB in order to know if the proposed design in this Master's Thesis, works correctly.

7 Results and Discussions

7.1 Combustion Test in the CFB

Once that all the components of the multilevel sampling gas systems were installed, a real test in the CFB was done. This test was conducted to check that the multilevel gas sampling system, designed in this thesis, works correctly.

The test conducted was a combustion test of 30 min, that was carried out in the CFB on 20/06/2016, in which the fuel feeding took over 17 min. The selection of a combustion test instead of a gasification test was because of safety measures, since the multilevel sampling system was used for the first time and the gases produced in combustion are less dangerous than in gasification.

14 kg of sand was used such as bed material. It had a Gaussian particle size distribution with a mean Sauter mean diameter of 200 μm . The composition of the sand is shown in Table 7.1.

Table 7.1 Sand composition (XRF-analysis/ ICP-OES in Oulu).

| Na ₂ O (%) | MgO (%) | Al ₂ O ₃ (%) | SiO ₂ (%) | P ₂ O ₅ (%) | S (%) | Cl (PPM) | K ₂ O (%) | CaO (%) |
|-----------------------|---------|------------------------------------|----------------------|-----------------------------------|-------|----------|----------------------|---------|
| 0,00 | 0,00 | 0,14 | 2,84 | 0,00 | 0,00 | 498 | 0,06 | 0,34 |

Besides, other parameters for the real test were:

- Fuel feeding: 2,3 kg/h
- Superficial gas velocity: 2 m/s
- Gas flow approx.: 390 l/min
- Air ratio: 2
- Riser temperature: 800°C

The procedure for the test is to first heat up the reactor until 700°C and then feed 1,2 kg of SRF (6%-w H₂O) into it. During fuel feeding, the screw feeder has to be regulated to keep the air ratio as stable as possible. As well, the temperature has to be controlled by adjusting the heating power of the riser and the air pre heater. The temperature of the reactor during the test is shown in Figure 7.1.

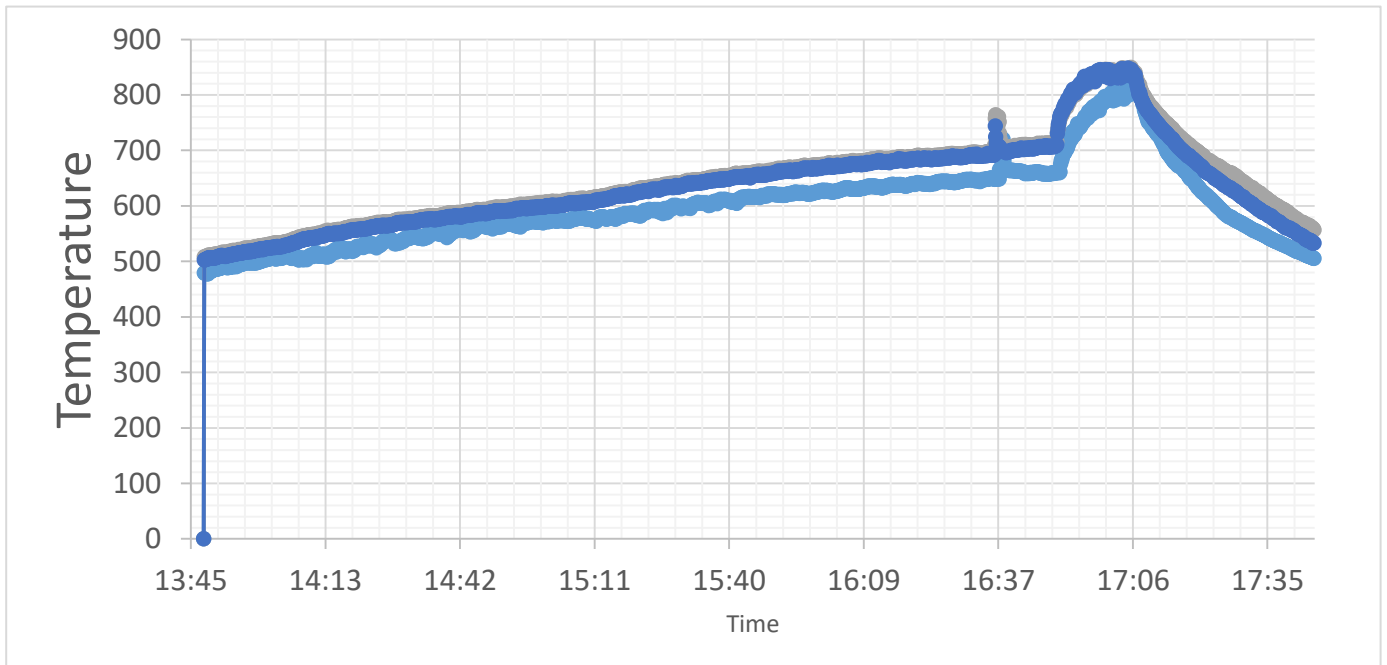


Figure 7.1 Temperatures of the three levels of the riser during the combustion test.

In Figure 7.1, the variation of temperatures of the three levels of the riser are shown. At 16:50 the fuel was fed, so the temperature increases from 700°C to 800°C. The fuel feeding was stopped at 17:07. According to Figure 7.1 the temperature was more or less stable over 800°C during the fuel feeding.

7.1.1 Results for the Solenoid Valve Algorithm.

The solenoid valve algorithm chosen to control the valves was the algorithm explained in chapters 6.2 and 6.3. The Dx-4000 GASMET gas analyser was connected to the multilevel sampling gas system for the combustion test, the delay and transitional time chosen were 140 seconds and the steady time (reliable measurements) was 60 seconds per level. Therefore the time per level was 200 seconds, and the number of cycles was 3 times per level (30 min) as shown in Figure 6.15.

Figure 7.2 shows the results for the CO₂ concentration measured in all levels in the combustion test.

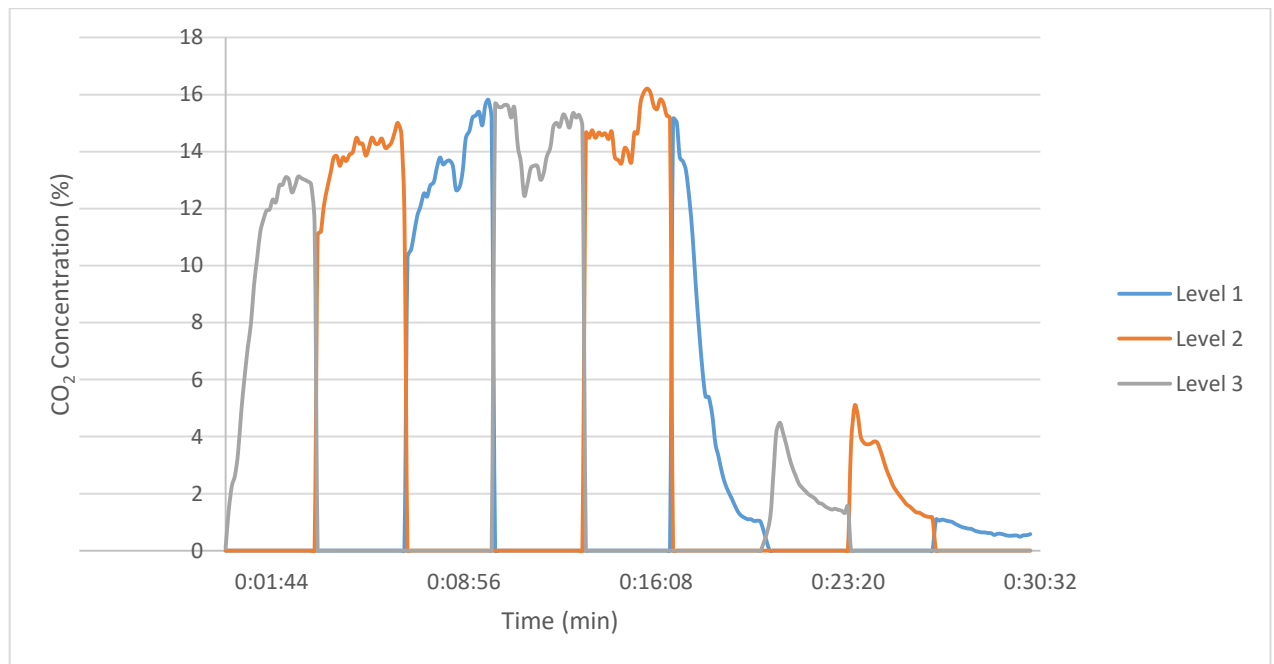


Figure 7.2 Working of the multilevel gas sampling system for CO₂ from combustion test.

Figure 7.2 shows that each level is measured during 200 seconds, although not all the data is reliable, which depends on the solenoid valve algorithm chosen. Figure 7.3 shows the reliable measurements (steady time) of CO₂ during the combustion test in each level.

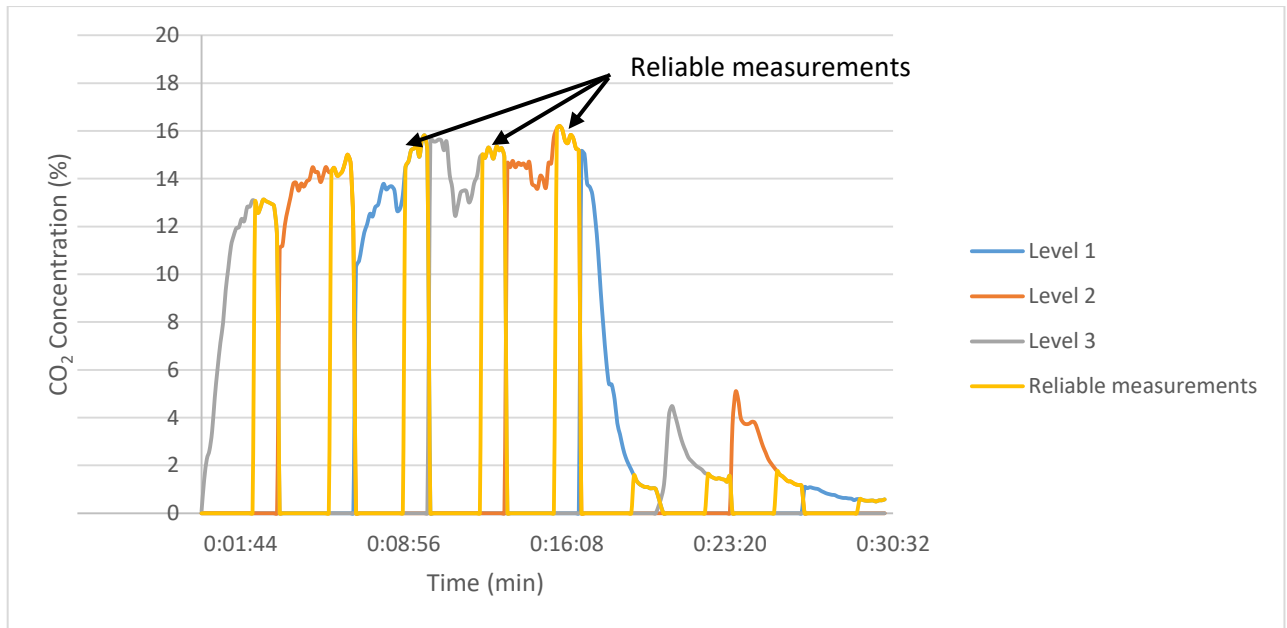


Figure 7.3 Reliable measurements of CO₂ in each level in a combustion test in CFB.

According to Figure 7.3, it is possible to see that the algorithm used to open and close the solenoid valve is coherent, since when the GASMET gas analyser is measuring one level, the gas composition is from this level and there is not any contamination from other levels. In addition, in Figure 7.3 it is possible to see that in reliable data of each level the gas composition is more or less stable during the measurement. This is a first indication that the multilevel gas sampling system designed in this Master's Thesis works.

7.1.2 Comparison of the Results between ULTRAMAT and GASMET Gas Analysers

The other gas analyser, Siemens ULTRAMAT gas analyser, was connected to the top of the CFB in order to compare its measurements with the ones obtained with the GASMET gas analyser. Figure 7.4 shows the results of CO₂ concentration from both analysers. In the GASMET gas analyser case, the results from the three levels are shown together in order to be able to compare them with the results obtained with the ULTRAMAT.

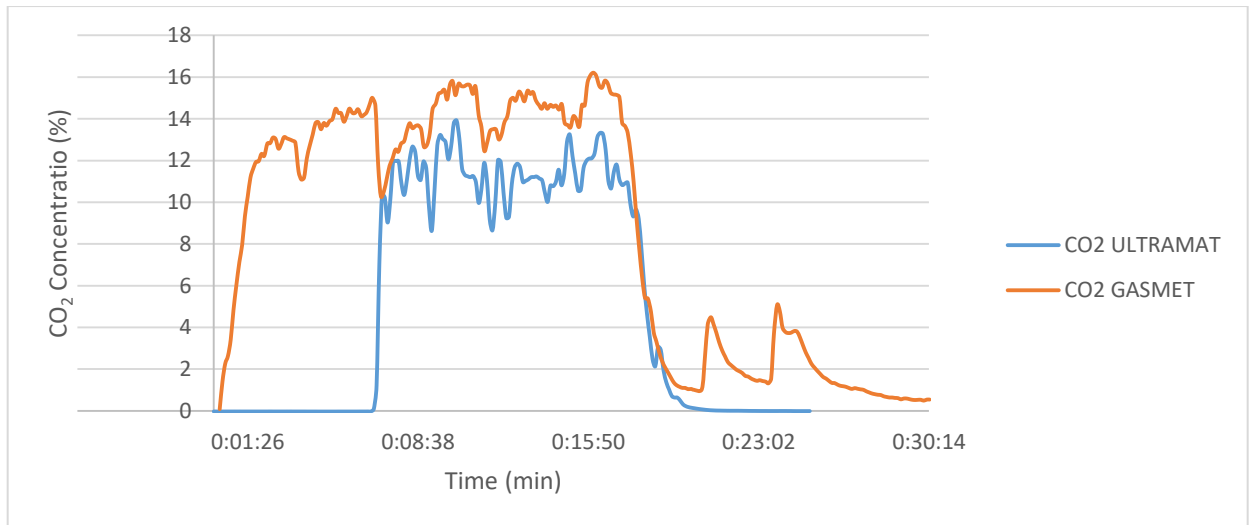


Figure 7.4 CO₂ Concentration from both gas analysers in the combustion test.

Figure 7.4 shows in spite of both analysers were installed in different points, as well that GASMET gas analyser measured the gas composition in three different points, the results from both analysers are very similar. The difference at the beginning of the graph is because some issue with starting the data logger. The small difference is because each gas analyser is connected in a different point of the CFB, this difference means that with the multilevel gas sampling system is possible to acquire the small differences of the gasification or combustion depending on the place where the gas analyser is connected. This is another indication to say that the multilevel gas sampling system works correctly.

Figure 7.5 shows the CO₂ concentration from when both gas analysers were connected to the same point, i.e, at the top of the CFB. It was a combustion test conducted on 02/12/2015.

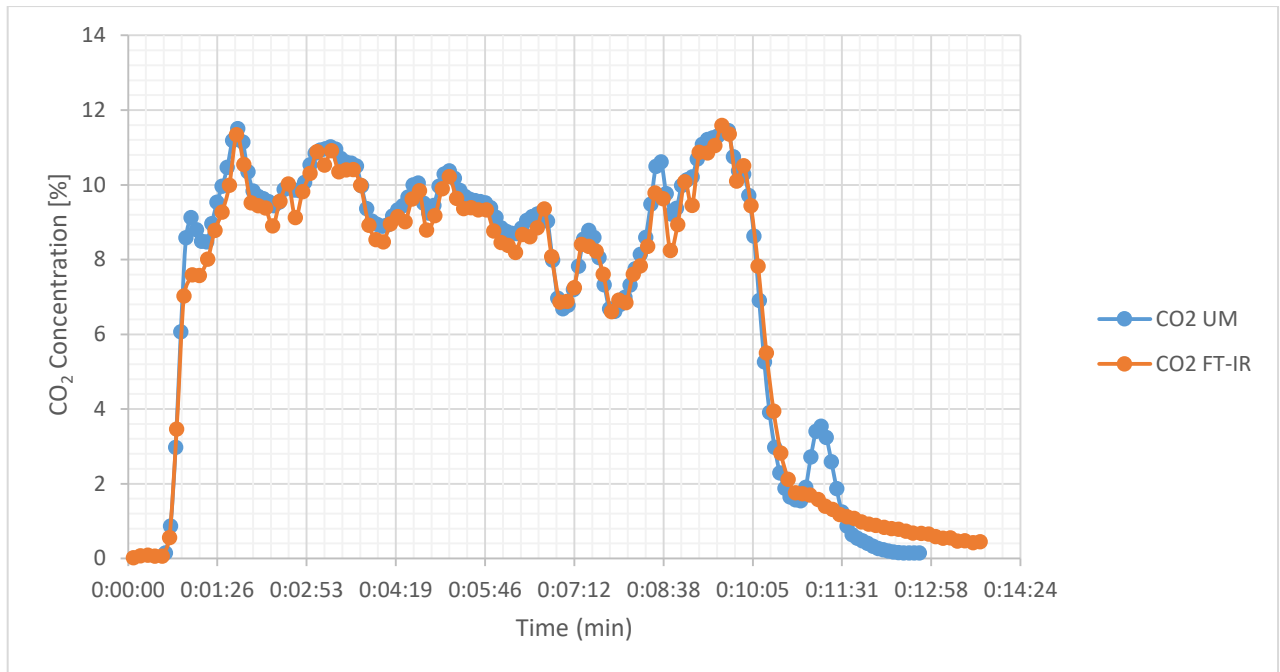


Figure 7.5 CO₂ Concentration with both analysers in a combustion test on 02/12/2015.

Figure 7.5 shows that both gas analysers measure almost the same CO₂ concentration in the flue gases. It means that when the gas analysers are connected to the same point of the reactor, they give similar results. However, when they are connected in different point, as well that one of them analyses the gas composition in three different points (multilevel gas sampling system), the concentration that they analyse is similar but there are some small differences (Figure 7.4).

7.1.3 Comparison of the Results with Older Tests

Besides of the explained in chapter 7.1.2, if the concentration of some gases of the combustion are compared not with the other gas analyser, but with the results from an older combustion test using GASMET gas analyser in the top of the reactor, it is possible to see that there are some differences as shown Figure 7.6.

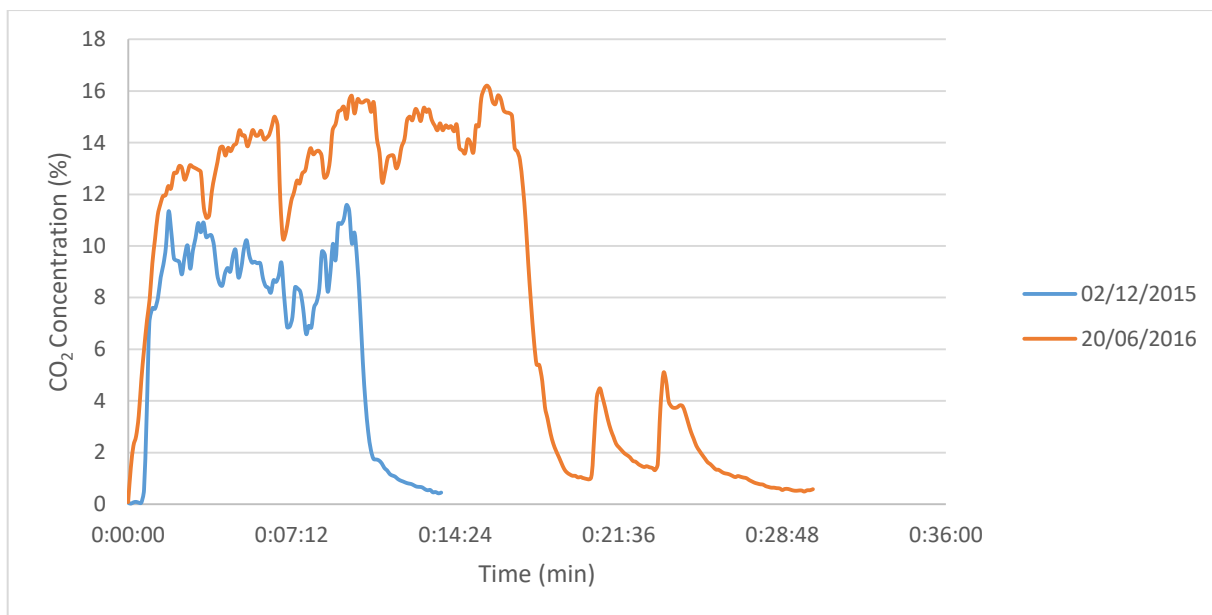


Figure 7.6 CO₂ Concentration of two combustion test, one with multilevel gas sampling system and other without it.

Figure 7.6 shows differences between the results from two combustion tests, one with (20/06/2016) and one without (02/12/2015) the multilevel gas sampling system. The results compare in an analogous way to those shown in Figure 7.4 and Figure 7.6.

7.1.4 Results from the Tar Trap with Oil Scrubbers

Once that the multilevel gas sampling system had been checked, the tar trap was checked in order to know whether it protects the system or not.

The test on 20/06/2016 was a combustion test not a gasification test. Most of the tar formed during a combustion test is oxidized, but there might be some tar in the lower levels of the reactor. The decision of conducting a combustion test instead of a gasification test was for safety reasons, as explained in chapter 7.1. At the end of the test, it was possible to see that the tar trap works, since it retained some solid substances and also some of the bed material of the reactor (sand). Figure 7.7 shows the contents of the tar trap of the three different levels after the combustion test.



Figure 7.7 Tar trap (oil scrubbers) with retained substances after one combustion test in the reactor.

In Figure 7.7, it is possible to see that the tar trap on the first level contains a lot of sand. It is because in this level the flow of the bed material is higher than in the others two levels. In the tar trap on the second level, there is no sand, but there are other substances in the oil, since the color of the oil is whiter than in the other levels. Finally, in the tar trap on the third level, there is almost nothing in the oil, since in this level it seems like there are less solid or dangerous substances.

8 Conclusions and Future Research

In conclusion, the multilevel gas sampling systems works and the tar trap retains the unwanted and dangerous substances for the gas analyser. Besides, all the electronic control with the optocoupler and LabVIEW also works for controlling the solenoid valves, and permits that the gas composition is analysed correctly in one level at the same time. In addition, the trend of the measurements in this work using the multilevel gas sampling system show the same trend as if the gas analyser would be installed on the top of the reactor. The small difference is only due to that the gas analyser is connected in other points of the reactor than before of this Master's Thesis. This permits the future studies of how the physicochemical reactions of gasification and combustions reacts in different levels of the reactor, in order to improve all the knowledge about them.

Other objectives such as protection of the gas analyser from unwanted and dangerous substances has also been reached as the tar trap works correctly. In addition, the residence time of the gas inside of the multilevel system is as short as possible, which was another objectives of this work that has been reached.

Future work could be some combustion and gasification test in order to compare the results of the gas composition in the three different levels with the results from previous test, in which the gas analyser was connected on the top of the reactor. Besides, it can be done not only with Dx-4000 GASMET gas analyser, but it can also be done with Siemens ULTRAMAT 23 gas analyser. However the only problem of connecting ULTRAMAT gas analyser to the multilevel system is that this gas analyser can only analyse CO, CO₂ and O₂, so some information is lost, although in the oxygen case, it can be compared with previous test (GASMET does not measure O₂).

On the other hand, not only the results of the gas composition can be compared with previous test, but in the same test the results from the analyser connected to the multilevel system can be compared with the other gas analyser connected on the top of the reactor. In this way, at least the CO and CO₂ can be compared among levels and with the results from the other gas analyser. It will help to know better what is happening inside of each level of the reactor.

One thing that can be done in future test or research in the reactor are for example to change the duration of reliable measurements in each level. In this work the reliable measurements are 60 seconds to GASMET analyser and 40 seconds to ULTRAMAT analyser. For example longer reliable measurements and less number of cycles per level may be done or the opposite, i.e, shorter reliable measurements and more number of cycles per level may be done. With all these options a lot of future test might be done and the results could be compared. In addition, not only the duration of the reliable data can be changed, but also the order of the levels that the gas analyser analyses. In the test on 20/06/2016 explained in chapter 7, the order of measurements was first level 3, then level 2 and then level 1, however the sampling level order can be changed for future experiments. In this way, making different test it is possible to know what is happening at the beginning, during and at the end of combustion or gasification in each different level of the reactor and compare the results of this level with what happened in the other levels, for example when the fuel starts to be fed.

For future work and research, the tar trap can also be a source of new information, since the oil after a combustion or gasification test can be analysed. With the analysis of the oil from three different levels of the reactor, it would be a good way to know more about how the formation of tar and other substances, what chemical reactions are related with the formation of these substances and how it is possible to avoid the formation of them.

Other future work-that may be done based on this Master's Thesis is to change the size of the bed material, temperatures of the reactor, type of fuel, superficial velocity of the gas, air factor, etc. Changing these parameters, new gasification or combustion test may be done to know how these parameters influence the physicochemical reactions and products produced in each level of the reactor.

Lastly, apart from other futures work and research about the reactor, other works may be done in the own multilevel gas sampling system. For example, some improvements could be done about the residence time, since if other components were used to build the steel pipes or other type of solenoid valves or scrubbers were used, the residence time could be reduced. Furthermore, other substances could be used in the tar trap instead of oil, because they might retain better the unwanted substances in the scrubbers.

In conclusion, it is possible to say that the work of this Master's Thesis is the beginning of a lot of future works and researches about gasification and combustion processes in the reactor, works with both gas analysers and tar traps and also works and researches about a lot of improvements in the own multilevel gas sampling system.

9. Appendix

9.1 Model of the Heat Transfer for the Steel Pipes

| T1 sup | T2 sup | sup ave (K) | T1 | T2 | Tave | Vol flow (m3/s) | Vol flow (l/min) | Normal conditions | | T ave surface and ambient | | | | | | | | | | | |
|------------------------------|--------|-------------|-----------|-----------|----------------|-----------------|------------------|-------------------|-------------|---------------------------|-----------------|-----------------------|--------------------------|---------|--------------------------|--------------------------|-----------------------------|--------------------------|--------------------|-----------------|----------------|
| 175 | 25 | 373 | 46 | 28 | 37 | 6,66667E-05 | 4 | 20 | 293 | 334,9 | | | | | | | | | | | |
| $C_p = a + bT + cT^2 + dT^3$ | | | | | | | | | | | | | | | | | | | | | |
| Substance | a | b | c | d | Cp (cal/mol*K) | PM (g/mol) | Cp (JKgK) | d (Kgm3) | d (Kgm3) | Composition (%) | Composition (%) | Sutherland's constant | Dynamic viscosity (Pa.s) | To (°C) | Dynamic viscosity (Pa.s) | Dynamic viscosity (Pa.s) | Thermal conductivity (W/mK) | Dynamic viscosity (Pa.s) | Cp (cal/mol*k) | p (JKgK) | |
| CO | 7,373 | -3,07E-03 | 6,66E-06 | -3,09E-09 | 6,97 | 28,00 | 1040,45 | 1,10 | 1,17 | 0 | 0,00 | 118 | 1,65E-04 | 0,00 | 1,65E-05 | 1,83E-05 | 0,02474 | 1,94E-05 | 6,98E+00 | 1041,43 | |
| CO2 | 4,728 | 1,79E-02 | -1,34E-05 | 4,10E-09 | 9,00 | 44,00 | 855,16 | 1,73 | 1,83 | 0 | 0,00 | 240 | 1,37E-04 | 0,00 | 1,37E-05 | 1,55E-05 | 0,014674 | 1,66E-05 | 9,26E+00 | 879,259 | |
| H2 | 6,483 | 2,22E-03 | -3,30E-06 | 1,83E-09 | 6,91 | 4,00 | 7217,93 | 0,16 | 0,17 | 0 | 0,00 | 72 | 8,40E-05 | 15,00 | 8,40E-06 | 8,84E-06 | 0,17258 | 9,32E-06 | 6,92E+00 | 7235,05 | |
| N2 | 7,44 | -3,24E-03 | 6,40E-06 | -2,79E-09 | 6,97 | 28,00 | 1040,15 | 1,10 | 1,17 | 79 | 76,70 | 111 | 1,66E-04 | 0,00 | 1,66E-05 | 1,84E-05 | 0,024001 | 1,95E-05 | 6,97E+00 | 1040,21 | |
| CH4 | 4,598 | 1,25E-02 | 2,86E-06 | -2,70E-09 | 8,65 | 16,00 | 2260,29 | 0,63 | 0,67 | 0 | 0,00 | 169 | 1,02E-04 | 0,00 | 1,02E-05 | 1,14E-05 | 0,03057 | 1,22E-05 | 8,99E+00 | 2347,79 | |
| H2O | 7,701 | 4,60E-04 | 2,52E-06 | -8,59E-10 | 8,06 | 18,00 | 1871,74 | 0,71 | 0,75 | 0 | 0,00 | 961 | 1,75E-02 | 0,00 | 1,75E-03 | 2,06E-03 | 0,0435 | 2,27E-03 | 8,11E+00 | 1882,25 | |
| O2 | 6,713 | -7,89E-07 | 4,17E-06 | -2,54E-09 | 7,04 | 32,00 | 919,30 | 1,26 | 1,33 | 21 | 23,30 | 125 | 2,00E-04 | 20,00 | 2,00E-05 | 2,09E-05 | 0,023 | 2,22E-05 | 7,08E+00 | 925,462 | |
| Syngas | | | | | | 6,98 | 28,84 | 1011,99 | 1,13 | 1,20 | 100 | 100,00 | | | | | 1,89502E-05 | 0,023767757 | 2,00997E-05 | 7,00E+00 | 1013,87 |
| | | | | | Tave | Tave | | Tave | | 293 K | | | | | | Tave | | Tave surface and ambient | | | |

$$\mu = \mu_o * \left(\frac{T_o + C}{T + C} \right) * \left(\frac{T}{T_o} \right)^{1.75}$$

Non-Metals=constant

$$X_i = Y_i * \frac{M_i}{M_t}$$

| | |
|------------------|-----------|
| Mass flow (Kg/s) | 8,00E-05 |
| Q (W) | 1,4577134 |

$$Q = m * C_p * (T_1 - T_2)$$

$$q' = \frac{(T_{ins} - T_{out})}{\frac{1}{2\pi r_i h_i} + \frac{\ln(r_o/r_i)}{2\pi k} + \frac{1}{2\pi r_o (h_o + h_R)}}$$

| | | | | |
|---------|------------------------------|------------|---------|--|
| m | Material | k (W/mK) | | |
| 0,03333 | Stainless Steel | 17,2333333 | Tave | Metals-> proportional with the temperature |
| n | Di (mm) | 3,75 | 0,85 | ε |
| 16 | Thickness (mm) | 1,125 | | |
| | Do (mm) | 6 | | |
| | Tins (°C) | 46 | | Developed flow |
| | Tout (°C) | 23,8 | 296,8 | L/D |
| | Area inside (m2) | 1,1045E-05 | | > |
| | Area outside (m2) | 2,8274E-05 | | |
| | Speed (m/s) | 6,38631591 | 0,05*Re | 71689861 |
| | Reynolds numbe | 1433,79722 | <2300 | Checked |
| | Re = $\frac{d * v * D}{\mu}$ | Laminar | Checked | |
| | Pr | 0,80688811 | >0,6 | |

| | | |
|------------------------------|--|-------------|
| Resistance to heat transfer | | 4,616716219 |
| Inside convection | | 3,071676211 |
| conduction | | 0,004340623 |
| Outside convection+radiation | | 1,540699385 |
| q' (W/m) | | 4,808612647 |
| Length pipe (m) | | 0,303146352 |
| Tsup (°C) | | 31,20862655 |

$$Nu_D = \left(\frac{hD}{k} \right) = 4,36$$

| | |
|--------------------|-------------|
| hins (W/m2K) | 27,63397913 |
| hout (W/m2K) | 27,09861725 |
| hrad (W/m2K) | 7,334866786 |
| Outside conditions | |
| Dynamic viscosit | 2,00997E-05 |
| density | 1,050186077 |
| velocity | 0,5 |
| Reynolds | 156,7465623 |
| Pr | 0,857396256 |

$$Nu_D = \left(\frac{hD}{k} \right)$$

| | | |
|-----------------|-------|-------|
| Re _D | C | m |
| 0,4 a 4 | 0,989 | 0,330 |
| 4 a 40 | 0,911 | 0,385 |
| 40 a 4000 | 0,683 | 0,466 |
| 4000 a 40000 | 0,193 | 0,618 |
| 40000 a 400000 | 0,027 | 0,805 |

$$Nu_D = 6,84085173$$

$$Nu_D = C Re_D^m Pr^{1/4}$$

Bibliography

- ANDRITZ, 2016. Products & services - details [WWW Document]. URL <https://www.andritz.com/products-and-services/pf-detail.htm?productid=13863> (accessed 4.11.16).
- Basu, P., 2006. Combustion and Gasification in Fluidized Beds. CRC Press.
- Berruoco, C., Recari, J., Abelló, S., Farriol, X., Montané, D., 2015. Experimental Investigation of Solid Recovered Fuel (SRF) Gasification: Effect of Temperature and Equivalence Ratio on Process Performance and Release of Minor Contaminants. *Energy Fuels* 29, 7419–7427. doi:10.1021/acs.energyfuels.5b02032
- Bridgwater, A.V., 2013. Advances in Thermochemical Biomass Conversion. Springer Science & Business Media.
- CEN/TS 15359, 2015. Solid recovered fuels - Specifications and classes.
- Fogler, H.S., 2006. Elements of Chemical Reaction Engineering. Prentice Hall PTR.
- Frankenhaeuser, M., Klarin-Henricson, A., Hakulinen, A., Frank E., M., 2008. Co-combustion of Solid Recovered Fuel and Solid Biofuels in a Combined Heat and Power Plant. *PlasticsEurope*, Seinäjoki, Finland.
- García-Labiano, F., Gayán, P., de Diego, L.F., Abad, A., Mendiara, T., Adánez, J., Nacken, M., Heidenreich, S., 2016. Tar abatement in a fixed bed catalytic filter candle during biomass gasification in a dual fluidized bed. *Appl. Catal. B Environ.* 188, 198–206. doi:10.1016/j.apcatb.2016.02.005
- GASMET, 1997a. GASMET Instruction Manual.
- GASMET, 1997b. Dx-4000 GASMET.
- Gómez-Barea, A., Leckner, B., 2010. Modeling of biomass gasification in fluidized bed. *Prog. Energy Combust. Sci.* 36, 444–509. doi:10.1016/j.pecs.2009.12.002
- Good, J., Ventress, L., Knoef, H., Zielke, U., Lyck Hansen, P., van de Kamp, W., de Wild, P., 2005. Sampling and analysis of tar and particles in biomass producer gases.
- Görner, K., 2008. Thermal Treatment of Wastes in Practise [WWW Document]. URL https://www.uni-due.de/imperia/md/content/luat/publikationen/2008-01-30_waste-seminar_helsinki_goerner.pdf (accessed 3.10.16).
- Grace, J.R., 2003. Handbook of Fluidization and Fluid Particle System.
- Heat Transmission Course Universitat Politècnica de València, 2011a. Convection.
- Heat Transmission Course Universitat Politècnica de València, 2011b. Introduction to Heat Transference.
- Hu, F.-X., Yang, G.-H., Ding, G.-Z., Li, Z., Du, K.-S., Hu, Z.-F., Tian, S.-R., 2016. Experimental study on catalytic cracking of model tar compounds in a dual layer granular bed filter. *Appl. Energy* 170, 47–57. doi:10.1016/j.apenergy.2016.02.080
- Kurkela, E., Palonen, J., Kivelä, M., Takala, H., 2003. Solid Recovered Fuel Gasification for Co-combustion in Pulverised Coal-fired Boilers - Lahti Case Study.
- Nakamura, S., Kitano, S., Yoshikawa, K., 2016. Biomass gasification process with the tar removal technologies utilizing bio-oil scrubber and char bed. *Appl. Energy* 170, 186–192. doi:10.1016/j.apenergy.2016.02.113

- Niu, M., Yan, Z., Guo, Q., Liang, Q., Yu, G., Wang, F., Yu, Z., 2008. Experimental measurement of gas concentration distribution in an impinging entrained-flow gasifier. *Fuel Process. Technol.* 89, 1060–1068. doi:10.1016/j.fuproc.2008.04.009
- Olabarria Uzquiano, M., 2013. CEN/TC 343 SOLID RECOVERED FUELS.
- Phuphuakrat, T., Namioka, T., Yoshikawa, K., 2011. Absorptive removal of biomass tar using water and oily materials. *Bioresour. Technol.* 102, 543–549. doi:10.1016/j.biortech.2010.07.073
- Reed, T., Das, A., 1988. *Handbook of Biomass Downdraft Gasifier Engine Systems*. Biomass Energy Foundation.
- Saeed, L., 2015. Waste Incineration [WWW Document]. URL https://mycourses.aalto.fi/pluginfile.php/136046/mod_resource/content/3/Waste%20Incineration_29.09.2015.pdf (accessed 3.10.16).
- Saeed, L., 2004. EXPERIMENTAL ASSESSMENT OF TWO-STAGE COMBUSTION OF HIGH PVC SOLID WASTE WITH HCl RECOVERY.
- Siedlecki, M., De Jong, W., Verkooijen, A.H.M., 2011. Fluidized Bed Gasification as a Mature And Reliable Technology for the Production of Bio-Syngas and Applied in the Production of Liquid Transportation Fuels—A Review. *Energies* 4, 389–434. doi:10.3390/en4030389
- SIEMENS, 2015. ULTRAMAT 23.
- Skagersten, J., Saeed, L., Järvinen, M., 2015. Thermal Treatment of Solid Recovered Fuel in a Pilot Scale Circulating Fluidized Bed.
- Thermodynamic Department Univeristat Politècnica de València, 2005. *Tables and Graphs of Thermodynamic*.
- Unifrax, 2009. Insulfrax S Blanket.
- Uuskallio, V., 2014. Lahti Energian jätti-investoinnin lastentaudit jatkuneet kaksi vuotta: “Vakavia prosessiin liittyviä ongelmia” [WWW Document]. ESS.fi. URL <http://www.ess.fi/uutiset/kotimaa/2014/04/28/lahti-energian-jatti-investoinnin-lastentaudit-jatkuneet-kaksi-vuotta-vakavia-prosessiin-liittyvia-ongelmia> (accessed 5.11.16).
- Williams, P.T., 2013. *Waste Treatment and Disposal*. John Wiley & Sons.
- Wolfesberger, U., Aigner, I., Hofbauer, H., 2009. Tar content and composition in producer gas of fluidized bed gasification of wood—Influence of temperature and pressure. *Environ. Prog. Sustain. Energy* 28, 372–379. doi:10.1002/ep.10387
- Yang, L.H., 2008. A Review of the Factors Influencing the Physicochemical Characteristics of Underground Coal Gasification. *Energy Sources Part Recovery Util. Environ. Eff.* 30, 1038–1049. doi:10.1080/15567030601082803